ISBN: 978-3-95450-200-4 doi:10.18429/JACoW-ICAP2018-SAPLG01

ADVANCES IN SIMULATION OF HIGH BRIGHTNESS/HIGH INTENSITY BEAMS

Ji Qiang*, LBNL, Berkeley, CA, USA

Abstract

High brightness/high intensity beams play an important role in accelerator based applications by driving x-ray free electron laser (FEL) radiation, producing spallation neutrons and neutrinos, and generating new particles in high energy colliders. In this paper, we report on recent advances in modeling the high brightness electron beam with application to the next generation FEL light sources and in modeling space-charge effects in high intensity proton accelerators.

START-TO-END SIMULATION OF MICROBUNCHING INSTABILITY EXPERIMENT IN AN FEL LINAC

The x-ray FEL provides a great tool for scientific discoveries in chemistry, physics, biology and material science. The microbunching instability seeded by shot noise and driven by collective effects (primarily space charge), can significantly degrade the quality of the electron beam before it enters the FEL undulators. Without proper control of the instability, the large final electron beam energy spread and phase space filamentation degrade the x-ray FEL performance [1–7]. The microbunching instability experiments recently carried out at the LCLS [8] provides a good opportunity to validate the computational model used in the simulation [9]. In the microbunching measurement at LCLS, the X-band transverse deflecting cavity (XTCAV) diagnostic [10] is located downstream of the undulator before the dump to measure the longitudinal phase space of the electron beam through the entire accelerator. The start-to-end beam dynamics simulations using the real number of electrons were done using a 3D parallel beam dynamics simulation framework IMPACT [11, 12]. It includes a time-dependent 3D space-charge code module IMPACT-T for injector modeling and a position-dependent 3D space-charge code module for linac and beam transport system model. The simulation starts from the generation of photo-electrons at the photocathode following the initial laser pulse distribution and the given initial thermal emittance. The electron macroparticles out of the cathode will be subject to both the external fields from a DC/RF gun and solenoid, and the space-charge/image charge fields from the Coulomb interaction of the particles among themselves. After exiting from the injector, the electron macroparticle will transport through a linear accelerator and beam transport system that includes laser heater, bunch compressors, accelerating RF cavities, harmonic linearizer, and magnetic focusing elements. Besides the 3D space-charge effects, the simulation also includes coherent synchrotron radiation (CSR) effects through a bending magnet, incoherent synchrotron radiation inside the bending magnet, RF cavity structure wakefield, and resistive wall wakefield. In the simulations, we track the beam down to the XTCAV screen and compare with the measurements. Figure 1 shows the final longitudinal phase space after the XTCAV from the experimental observation and from the simulation with laser heater turned off for the 1 kA study case.

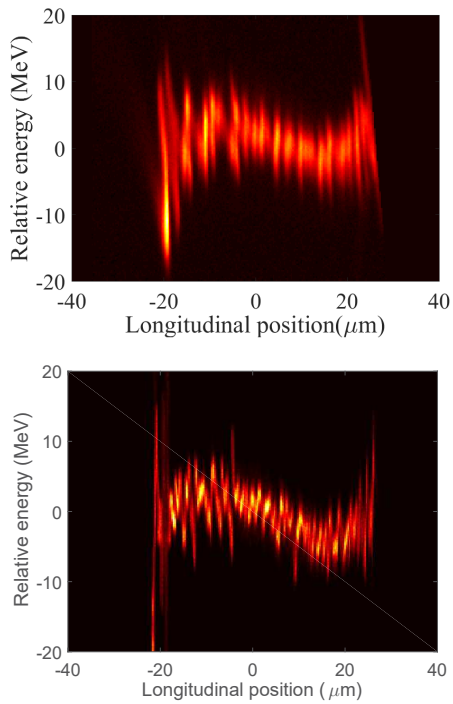

Figure 1: Measurement (top) and simulation (bottom) of the final longitudinal phase space distribution with the laser heater off. Beam current is 1 kA, with bunch charge 180 pC. The bunch head is to the right.

Here, a strong phase space fluctuation due to the microbunching instability can be seen from both the measurement and the simulation. There is no external seeded initial modulation. This large fluctuation arises from the shot-noise inside the beam and is amplified by collective effects, especially space charge effects through the accelerator.

The microbunching instability can be suppressed through Landau damping by increasing the electron beam uncorrelated energy spread before the bunch compressor using the laser heater. Figure 2 shows the final longitudinal phase space after the XTCAV from both the measurement and the simulation with extra 19 keV uncorrelated slice energy spread from the laser heater. The phase space fluctuation is significantly reduced with the use of the laser heater. This is observed in both the measurement and the simulation.

* jqiang@lbl.gov

ISBN: 978-3-95450-200-4 doi:10.18429/JACoW-ICAP2018-SAPAF01

GENETIC ALGORITHM ENHANCED BY MACHINE LEARNING IN DYNAMIC APERTURE OPTIMIZATION

Yongjun Li,* Weixing Cheng, Li Hua Yu, Robert Rainer,
Brookhaven National Laboratory, Upton, New York 11973

Abstract

With the aid of machine learning techniques, the genetic algorithm has been enhanced and applied to the multi-objective optimization problem presented by the dynamic aperture of the NSLS-II storage ring.

INTRODUCTION

Population-based optimization techniques, such as evolutionary (genetic) [1–16] and particle swarm [17–19] algorithms, have become popular in modern accelerator design. Optimization of a nonlinear lattice's dynamic aperture usually has multiple objectives, such as the area and the profile of the dynamic aperture, energy acceptance, beam lifetime [1, 3], and nonlinear driving terms (NDT) [4] etc. Dynamic aperture and energy acceptance can be evaluated through direct single-particle tracking simulations. NDTs can be extracted analytically from the one-turn-map for a given nonlinear lattice configuration [20–23]. Recent studies have found that the spread from a constant of the action obtained with the square matrix method [24–27] represents a kind of nonlinearity measure of a lattice, which can be treated as an optimization objective as well. Another optimization objective, which is deduced from the square matrix method and used in this paper, is the spread of linear action $J_{x,y}$ from a constant. The spread is numerically computed from simulated turn-by-turn data [28, 29]. Based on the number of objectives presented in this application, multi-objective genetic algorithm (MOGA) [30] is a suitable optimization tool to compromise among these objectives simultaneously.

A general model for multi-objective optimization is:

- given a set of free variables x_n within the range $x_n \in [x_n^L, x_n^U]$, $n \in [1, N]$;
- subject to some constraints $c_j(x_n) \geq 0$, $j \in [1, J]$, and $e_k(x_n) = 0$, $k \in [1, K]$;
- simultaneously minimize a set of objective functions $f_m(x_n)$, $m \in [2, M]$.

Here x_n^L, and x_n^U are the lower and the upper boundaries of the n^{th} free variables. N, J, K and M are non-negative integers. Note for simplicity, clarity, and without loss of generality, all constraints are lower bounds, and all objectives are minimized.

A genetic algorithm (GA) is a type of evolutionary algorithm. It can be used to solve both constrained and unconstrained optimization problems based on a natural selection process [30]. Each candidate has a set of free variables which it inherits from its parents and is mutated at random corresponding to a certain probability. Each candidate's free variables x_n can be regarded as an N-dimensional vector $\mathbf{x}$. Their ranges $[x_n^L, x_n^U]$ define a volume of an N-dimensional "search space". The evolution is an iterative process. The new population from each iteration is referred to as a "generation". The process generally starts with a population that is randomly generated and the fitness of the individuals is evaluated. Individuals with greater fitness are randomly selected, and their genomes are modified to form the next generation. The average fitness of each generation therefore increases with each iteration of the algorithm. The goal of multi-objective optimization (MO) is to optimize functions simultaneously. These functions are sometimes related and their objectives may conflict. In these events, trade-offs are considered among the objectives. In non-trivial MO problems the objectives conflict such that none can be improved without degrading others in value and are referred to as non-dominated or "Pareto optimal". In these cases a non-dominated sorting algorithm can be used to judge if one candidate is better than another [30]. In the absence of constraints or preferences, however, all Pareto optimal candidates are equally valid and given the same rank. If constraints are provided, the rank of each individual accounts for the constraints, and qualified candidates are guaranteed to dominate unqualified ones. Each qualified candidate has M fitness values f_m, which compose another M-dimensional "fitness space". The combination of multi-objective, non-dominated sorting with employment of the genetic algorithm forms the basis of the "MOGA" method. MOGA has some limitations in its application to modern storage ring optimization. In general, the application of MOGA on dynamic aperture optimization can be driven by either direct particle tracking, or analytical calculation of nonlinear characterization. It is time-consuming to evaluate the fitness quantitatively, as seen with the calculation of a large-scale storage ring's dynamic aperture using the symplectic integrator [31].

Although there is no a priori reason why the genetic evolution process needs external intervention, examples without it such as the evolution of biological life on earth or planetary formation in the solar system, were only possible after billions of years [32]. One reason why natural evolution is comparatively slow is that the percentage of elite candidates among the whole population is low. A brute force method for speeding up evolution is to narrow down the search ranges around good candidates found early in the evolution process. This decreases diversity, however, and could lead to a trapping in local minima. An effective intervention step would be able to significantly speed up the evolution in the desired

* Email: yli@bnl.gov

ISBN: 978-3-95450-200-4 doi:10.18429/JACoW-ICAP2018-SAPAF02

OPTIMIZATION OF HEAVY-ION SYNCHROTRONS USING NATURE-INSPIRED ALGORITHMS AND MACHINE LEARNING

S. Appel*, W. Geithner, S. Reimann, M. Sapinski, R. Singh, D. M. Vilsmeier
GSI, Darmstadt, Germany

Abstract

The application of machine learning and nature-inspired optimization methods, like for example genetic algorithms (GA) and particle swarm optimization (PSO) can be found in various scientific/technical areas. In recent years, those approaches are finding application in accelerator physics to a greater extent. In this report, nature-inspired optimization as well as the machine learning will be shortly introduced and their application to the accelerator facility at GSI/FAIR will be presented. For the heavy-ion synchrotron SIS18 at GSI, the multi-objective GA/PSO optimization resulted in a significant improvement of multi-turn injection performance and subsequent transmission for intense beams. An automated injection optimization with genetic algorithms at the CRYRING@ESR ion storage ring has been performed. The usage of machine learning for a beam diagnostic application, where reconstruction of space-charge distorted beam profiles from ionization profile monitors is performed, will also be shown. First results and the experience gained will be presented.

INTRODUCTION

FAIR—the Facility for Antiproton and Ion Research will provide antiproton and ion beams of unprecedented intensities as well as qualities to drive forefront heavy ion and antimatter research [1]. The multi-turn injection (MTI) into heavy-ion synchrotron SIS18 is one of the bottlenecks for providing unprecedented intensities. The loss-induced vacuum degradation and associated life-time reduction for intermediate charge state ions is one of the key intensity limiting factors for SIS18 [2]. Beam loss during injection can trigger the pressure bump instability. An optimized injection can relax the dynamic vacuum problem, but is also crucial to reach the synchrotron intensity limit by a large multiplication of the injected current [3].

The complexity of the FAIR facility demands a high level of automation to keep anticipated manpower requirements within acceptable levels, as shown in [4]. An example of complexity is the High Energy Beam Transport System of FAIR which forms a complex system connecting among other things seven storage rings and experiment caves and has a total length of 2350 metres [5]. An automatized machine based optimization would improve the time for optimization and control of HEBT.

In the frame of the Swedish in-kind contribution to the FAIR project the storage ring CRYRING@ESR is planned to be used for experiments with low-energy ions and antiprotons. The ring is already installed in the existing GSI target hall and commissioning has started in 2015 [6–8]. Since CRYRING@ESR has its own local injector it can be used stand-alone for testing novel technical developments like automatized configuration of beam line devices. A semi-automatized optimization has been already preformed at the CRYRING in Sweden [9]. Figure 1 shows the CRYRING@ESR and is local injector. Over the second transfer line the CRYRING@ESR can also receive beams form the experimental storage ring ESR.

* s.appel@gsi.de

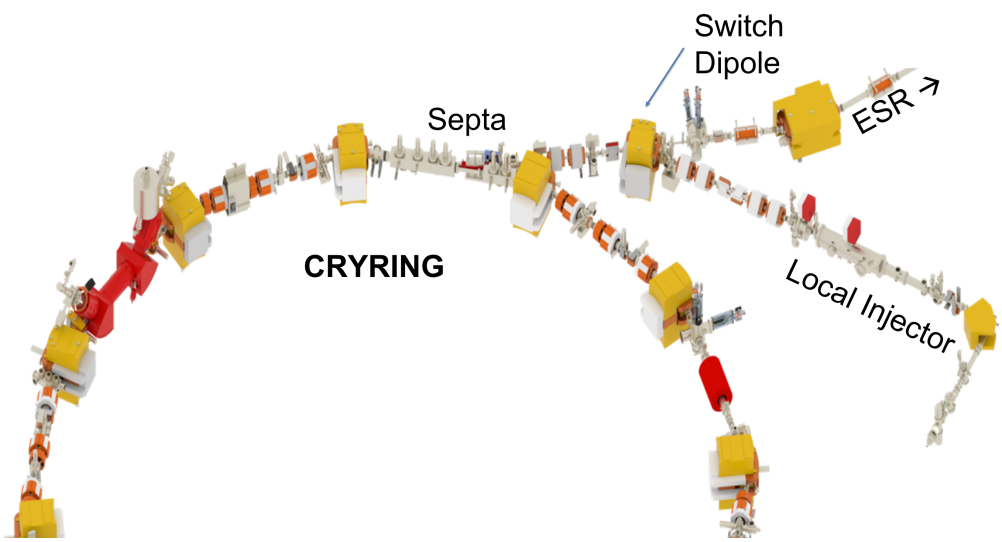

Figure 1: CRYRING@ESR injection from the local injector has been online optimized with an evolutionary algorithm.

ISBN: 978-3-95450-200-4 doi:10.18429/JACoW-ICAP2018-SAPAF03

COMPARISON OF MODEL-BASED AND HEURISTIC OPTIMIZATION ALGORITHMS APPLIED TO PHOTOINJECTORS USING LIBENSEMBLE

N. Neveu*, L. Spentzouris, Illinois Institute of Technology, Chicago, USA
J. Larson, S. Hudson, Argonne National Laboratory, Lemont, USA

Abstract

Genetic algorithms are commonly used in the accelerator community and often require significant computational resources and manual adjustment of hyperparameters. Model-based methods can be significantly more efficient in their use of computational resources, but are often labeled as unreliable for the nonlinear or nonsmooth problems that can be found in accelerator physics. We investigate the behavior of both approaches using a photoinjector operated in the space-charge-dominated regime. All model-based optimization runs were coordinated and managed by `libEnsemble`, a Python library at Argonne National Laboratory.

ARGONNE WAKEFIELD ACCELERATOR FACILITY INTRODUCTION

The Argonne Wakefield Accelerator (AWA) facility houses two photoinjector beamlines. Ongoing research efforts at the AWA includes emittance exchange photocathode studies and two-beam acceleration experiments [1], the latter of which motivates this work. Figure 1 shows the layout of the AWA bunker during two-beam accelerator experiments. The high-charge beamline, often referred to as the drive beam, is being modeled in this work.

CODE AND RESOURCES

The particle-in-cell code `OPAL` [2] is used to simulate the high charge beam line at the AWA. `OPAL` is an open-source parallel code with two version, `OPAL-t` and `OPAL-cycl`. The former was used for this work, the latter version is used for modeling cyclotrons. `OPAL` can also simulate 3D-space charge, 1D coherent synchrotron radiation, and wakefield effects. Note that the optimization methods being compared in this study are applicable to any beam-dynamics code—Parmela [3], ASTRA [4], GPT [5], all of which have been used by AWA group members—not just `OPAL-t`.

All simulations were run on the Bebop cluster maintained by the Laboratory Computing Resource Center [6] at Argonne National Laboratory. Bebop machine consist of 664 Broadwell nodes, and 352 Knights Landing (KNL) nodes. The simulations presented here were performed on KNL nodes, due to short queue times and readily available resources.

* nneveu@hawk.iit.edu

OPTIMIZATION METHODS

Heuristic Method: Genetic Algorithm

Genetic Algorithms (GA) are a popular choice for optimizing simulations in the accelerator physics community. They have been used with success on several types of accelerator physics problems that address challenges facing both linear and circular machines [7]. It is not disputed that in these solutions were found with benefit to many facilities. However, it is also well-known that GAs are computationally intensive. They can require hundreds of thousands of core hours depending on the problem being solved. Performing optimization with fewer calls to the simulation would not only save time, but would also enable facilities to accomplish more design work without access to large core hour allocations.

Model Based Methods: APOSMM + BOBYQA

Model-based derivative free methods are increasingly popular in mathematics and other scientific domains, but have not been widely used in the accelerator physics community. This may be due to the assumption that these methods may become within local minima within a bounded search space. In a sense, this is true if the algorithm is always started with the same initial conditions and weights. However, if the algorithm is started multiple times with various initial conditions, this behavior may be mitigated.

In order to achieve a multistart approach, the asynchronously parallel optimization solver for finding multiple minima (APOSMM) [8] was used. This algorithm maintains a history of all previously evaluated points, and uses this information when deciding starting points for local optimization runs. APOSMM also allows concurrent local optimization runs while honoring the amount of resources available. For details on how local optimization points are determined, see [8, Section 3].

In this paper, we use the bounded optimization by quadratic approximation (BOBYQA) [9] local optimization method. After a set of simulation evaluations are finish, the beam parameters (i.e. objectives) at the desired location are fed to BOBYQA. The algorithm then builds and minimizes a quadratic model of the objectives in order to pick the next point to evaluate.

Both APOSMM and BOBYQA implementations used are open source, freely available, and written in Python.

ISBN: 978-3-95450-200-4 doi:10.18429/JACoW-ICAP2018-SAPAF04

SINGLE OBJECTIVE GENETIC OPTIMIZATION OF AN 85% EFFICIENT KLYSTRON*

A. J. Jensen†, J. Petillo, Leidos, 01821 Billerica, USA
M. Read, L. Ives, Calabazas Creek Research, 94404 San Mateo, USA
J. Neilson, SLAC National Accelerator Laboratory, 94025 Menlo Park, USA

Abstract

Overall efficiency is a critical priority for the next generation of particle accelerators as they push to higher and higher energies. In a large machine, even a small increase in efficiency of any subsystem or component can lead to a significant operational cost savings. The Core Oscillation Method (COM) and Bunch-Align-Compress (BAC) method have recently emerged as a means to greatly increase the efficiency of the klystron RF source for particle accelerators. The COM and BAC methods both work by uniquely tuning klystron cavity frequencies such that more particles from the anti-bunch are swept into the bunch before power is extracted from the beam. The single objective genetic algorithm from Sandia National Laboratory's Dakota optimization library is used to optimize both COM and BAC based klystron designs to achieve 85% efficiency. The COM and BAC methods are discussed. Use of the Dakota optimization algorithm library from Sandia National Laboratory is discussed. Scalability of the optimization approach to High Performance Computing (HPC) is discussed. The optimization approach and optimization results are presented.

INTRODUCTION

Klystrons have been the primary RF source for accelerators for as long as they have been used. There are multiple reasons for this. They have high gain, low phase noise, moderately high efficiency, and a low $/Watt cost. The primary deficiency of klystrons however is their moderate electronic efficiency, for which the empirical relation [1] is:

$$\eta_{max} = 78 - 16\,\mu K, \qquad (1)$$

where K is the beam perveance ($I_o\,V^{-3/2}$) provides a realistic estimate. Achieving high efficiency (>70%) in a high power klystron requires either relativistic beam voltages or a combination of many lower voltage beams, which significantly increases complexity and cost. Efficiencies of commercial klystrons are typically 40-60%, a range that has seen little change for several decades.

Somewhat surprisingly however, given the technology maturation one would expect for a device invented more than sixty years ago, a new design method for klystrons has been recently proposed (Guzilov 2014 [2]). The author of this work refers to this new technique as the "BAC" method and shows a path for obtaining significantly higher efficiencies than obtained in current klystrons. A complimentary method, "COM" [3], is also investigated as a means for increasing efficiency.

Using the COM and BAC techniques we use modern optimization techniques to design a klystron with the goal of exceeding 85% efficiency. The klystron is designed to operate at 1.3 GHz and provide 100 kW of output power.

SIMULATION SOFTWARE AND TOOLS

Several simulation and optimization tools were used. The key programs used are outlined here.

Dakota Optimization Library

Dakota [4] is a powerful optimization library developed by Sandia National Laboratory. The library consists of many algorithms including the Single Objective Genetic Algorithm (SOGA) and the Asynchronous Pattern Search (APS). All optimizations in this paper used the SOGA for global optimization or the APS for local optimization. Dakota is typically run from the command line but we ran Dakota using the Galaxy Simulation Builder framework.

Galaxy Simulation Builder

Galaxy Simulation Builder (GSB) [5] is a framework developed by the Air Force Research Laboratory (AFRL) for building simulation pipelines and optimizations. The software was used exclusively for the klystron optimizations presented here. The optimizations can be performed without the use of GSB, but the GSB framework facilitates the process of running Dakota. GSB also streamlines the process of executing large optimizations using High Performance Computing (HPC) supercomputers. Setting up optimizations on Dakota and running optimizations on supercomputers is more time consuming without using GSB as an interface.

The GSB GUI is shown in Figure 1. The GUI works based on a drag-and-drop approach to building modules that wrap the command line interface of different simulation tools.

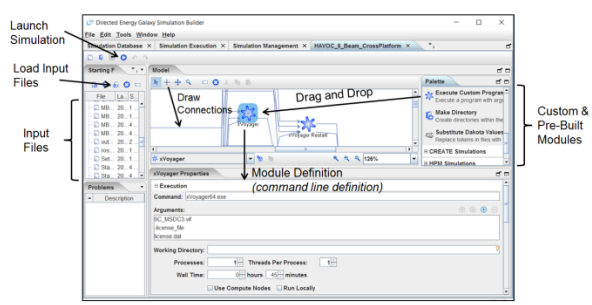

Figure 1: Galaxy Simulation Builder GUI.

* Work done under subcontract to CCR, funded by the U.S. Department of Energy through SBIR Grant, number DE-SC0017789.
† jensenaj@leidos.com

ISBN: 978-3-95450-200-4 doi:10.18429/JACoW-ICAP2018-SAPAG03

MODE-ANALYSIS METHODS FOR THE STUDY OF COLLECTIVE INSTABILITIES IN ELECTRON-STORAGE RINGS*

M. Venturini†, LBNL, 94720 Berkeley, CA, USA

Abstract

We review recent progress on the application of mode analysis to the study of collective instabilities in electron storage rings with Higher Harmonic RF Cavities (HHCs). The focus is on transverse instabilities in the presence of a dominant resistive-wall impedance, a problem of particular relevance to the new generation of diffraction-limited light sources. The secular equation is solved after applying a regularizing transformation, a key step to obtain numerically accurate solutions. We provide a demonstration that with vanishing chromaticity and in the absence of radiation damping the beam motion is always unstable. This is in contrast to the classical Transverse-Mode-Coupling Instability (TMCI) without HHCs, which is known to exhibit a well defined instability threshold.

INTRODUCTION

A narrow vacuum chamber to accommodate strong magnets or high-performance Insertion Devices (ID) and use of bunch-lengthening Higher-Harmonic Cavities (HHCs) to reduce intrabeam scattering are two distinctive features of the new generation of storage-ring light sources. This paper concerns itself with the HHC effect on the transverse collective instabilities induced by the Resistive Wall (RW) impedance, which in the new machines is a major, if not the largely dominant, source of transverse impedance due to the small chamber aperture.

HHCs achieve bunch lengthening by introducing an amplitude dependence in the synchrotron oscillation frequency and therefore altering the linear character of the longitudinal motion. The resulting frequency spread is commonly associated with the expectation of a beneficial impact on the beam stability, as alluded by the often-encountered 'Landau cavities' designation. The reality, however, is more nuanced. While HHCs have the potential to reduce or eliminate certain instabilities through the Landau damping mechanism, whether they actually do depends on a number of other factors. In fact, the presence of HHCs can under some circumstances degrade beam stability. This is known although not widely acknowledged for longitudinal multi-bunch instabilities [1–3]. The main point to be made here is that such a degradation can be realized in the transverse plane as well. This paper illustrates the main results reported in [4], to which we refer for the more technical details.

The focus is on developing a mode-analysis theory in the presence of HHCs applicable to single-bunch instabilities at vanishing chromaticities. We base the analysis on the familiar DC-conductivity, RW impedance model for a vacuum chamber with uniform circular cross section of radius b, length L, and conductivity σ_c (cgs units):

$$Z_y(k) = \frac{\mathrm{sign}(k) - i}{\sqrt{|k|}} \frac{L}{b^3} \sqrt{\frac{2}{\pi c \sigma_c}}, \qquad (1)$$

with wake-function $W_y(z) = -2L\sqrt{c}/\left(\pi b^3 \sqrt{\sigma_c |z|}\right)$, for $z \leq 0$ (and vanishing otherwise).

THE CLASSICAL TMCI (NO HHCS)

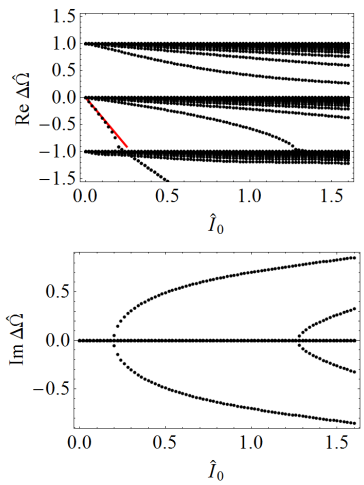

Figure 1: Classical TMCI in the absence of HHCs: real (top) and imaginary (bottom) parts of the mode complex-number frequency shift $\Delta\hat{\Omega} = (\Omega - \omega_y)/\omega_{s0}$ over a bunch-current range. The red line in the top picture is the tuneshift for the rigid dipole mode as given by Eq. (7).

In the absence of HHCs the longitudinal motion is linear and at zero chomaticities the beam is susceptible to the Transverse-Mode Coupling Instability (TMCI). The characteristic signature of the instability is the convergence of the dipole ($m = 0$) and head-tail ($m = -1$) azimuthal-mode oscillation frequencies at the critical bunch current [5]. The starting point for the analysis is the linearized Vlasov equation for the perturbation

$$g_1(r, \varphi; t) = e^{-i\Omega t} \sum_{m=-\infty}^{\infty} R_m(r; \Omega) e^{im\varphi}, \qquad (2)$$

written as a superposition of azimuthal modes with radial functions R_m and depending on the longitudinal-motion amplitude/angle coordinates (r, φ). The perturbation g_1 has a physical interpretation as the transverse (say vertical) offset of the electrons contained in the infinitesimal

* Work supported by the US Department of Energy Contract No. DE-AC02-05CH11231.
† mventurini@lbl.gov

ISBN: 978-3-95450-200-4 doi:10.18429/JACoW-ICAP2018-SAPAG04

HOM-MITIGATION FOR FUTURE SPS 33-CELL 200 MHz ACCELERATING STRUCTURES

P. Kramer[1]*, C. Vollinger, CERN, Geneva, Switzerland
[1]also at Institute of High Frequency Technology (IHF), RWTH Aachen University, Germany

Abstract

The CERN SPS 200 MHz travelling wave (TW) accelerating structures pose an intensity limitation for the planned High Luminosity (HL-) LHC upgrade. Higher-order modes (HOMs) around 630 MHz have been identified as one of the main sources of longitudinal multi-bunch instabilities. Improved mitigation of these HOMs with respect to today's HOM-damping scheme is therefore an essential part of the LHC injectors upgrade (LIU) project.

The basic principles of HOM-couplers in cavities and today's damping scheme are reviewed, before illustrating the numerous requirements an improved damping scheme for the future 33-cell structures must fulfil. These are, amongst others, the mitigation of HOMs situated in the lower part of the structure where there are no access ports for extraction, a sufficient overall damping performance and an acceptable influence on the fundamental accelerating passband (FPB). Different approaches tackling these challenges are investigated and their performance, advantages and pitfalls are evaluated by ACE3P and CST electromagnetic (EM) field solver suites.

INTRODUCTION

The Super Proton Synchrotron (SPS) at CERN relies on a 200 MHz multi-cell travelling-wave structure (TWS) for particle acceleration.

Beam dynamic simulations showed that to achieve stable beams for future HL-LHC intensities an additional mitigation by a further factor three of already heavily damped HOMs around 630 MHz is necessary in these structures [1]. A general overview of the SPS accelerating structure and the corresponding longitudinal and transverse HOM damping schemes in use today were presented in [2, 3]. For beam loading reasons, shorter 33-cell structures will be employed after the LIU upgrade together with the 44-cell structures in use today. The longitudinal damping scheme deployed today on 44- and 55-cell structures is insufficient for the HOMs around 630 MHz with future beam intensities. This equally applies if this damping scheme is used on the 33-cell structures (shown as black HOM-couplers in Fig. 1).

* patrick.kramer@cern.ch

As outlined in [3], these couplers were optimized on a single 11-cell section featuring HOMs with an integer multiple of a $\pi/11$ phase advance per cell. One such spare section is shown in Fig. 2. On 33-cells, HOMs with phase advances

Figure 2: 11-cell section of the accelerating TWS.

that are not allowed on 11-cells exist and the performance of the HOM-coupler on these modes has to be verified.

To achieve the required additional damping by a factor three of the HOMs around 630 MHz this contribution describes the systematic improvement of the existing damping scheme. The resulting beam impedance is thereby calculated by time domain wakefield simulations. Due to the importance of the damping upgrade for the future operation of the SPS, confirmation of the results by two different solver types was desired. The finite-difference wakefield solver of the CST suite [4] and the finite-element time domain solver (T3P) of the ACE3P [5] suite were used for this purpose.

The first section of this work details the model set-up and the simulation settings used for the two solvers. The HOM-mitigation strategy then comprises the following steps. First, additional couplers are placed in cells with strong electric field of the most dangerous modes present in the 33-cell configuration. These modes feature a high geometry factor R/Q. As a second step, the HOM-coupler is optimized to reach close-to-critical coupling to the HOMs in the relevant frequency range. Sufficient damping can however not be achieved merely by adding HOM-couplers in the available access ports at the top of each cell (Fig. 2). This is due to the fact that the top/ bottom symmetry of the structure is violated and as a result the EM fields of some modes are partially pushed towards the lower half of the cavity where no dedicated access ports are available for HOM-damping (for more details see [3] and compare Fig. 8a later in the text). One particular example for this effect is the high-Q $17\pi/33$ mode. Several means of damping modes in the lower half

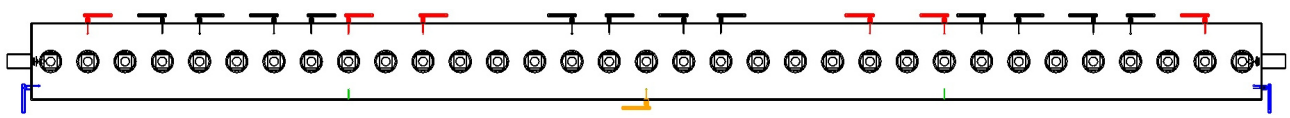

Figure 1: Several HOM-mitigation options shown together in a 3-section model. Black: existing longitudinal damping scheme. Red: additional couplers. Blue: end-plate couplers. Orange: VPP coupler. Green: mitigation by resonant posts.

ISBN: 978-3-95450-200-4 doi:10.18429/JACoW-ICAP2018-SUPAF04

SYMPLECTIC AND SELF-CONSISTENT ALGORITHMS FOR PARTICLE ACCELERATOR SIMULATION

Thomas Planche*, Paul M. Jung, TRIUMF, Vancouver, Canada

Abstract

This paper is a review of algorithms, applicable to particle accelerator simulation, which share the following two characteristics: (1) they preserve to machine precision the symplectic geometry of the particle dynamics, and (2) they track the evolution of the self-field consistently with the evolution of the charge distribution. This review includes, but is not limited to, algorithms using a particle-in-cell discretization scheme. At the end of this review we discuss to possibility to derived algorithms from an electrostatic Hamiltonian.

INTRODUCTION

The conventional approach to simulating charged particle dynamics is to start from equations of motion, such as Newton's law and Poisson's equation, and solve them approximately using some standard ordinary or partial differential equation solver. The truncation errors often lead to non-physical artifacts, such as the non-conservation of phase space volume, or the violation of conservation laws resulting from symmetries of the system (Noether's theorem). By contrast, symplectic integrators produce exactly stationary solutions to an approximate action. Solutions are exact to machine precision. Approximations are made up front, when choosing the approximate Lagrangian or Hamiltonian, and the corresponding approximate discrete action. Once the physical description of the system is chosen, there is no more arbitrariness in the arcane of the algorithm.

In accelerator physics, symplectic integrators are primarily used to study long-term stability of orbits in storage rings [1]. But their properties, the first of which is the lack of arbitrariness after the choice of physics, make them desirable for the study of all conservative processes in particle accelerators.

Self-consistent algorithms are, on the other hand, essential to study betatron resonances, and by extension dynamical aperture, in the presence of space-charge forces [2].

NOTATIONS

Throughout this paper a bold character always denotes a vector, a vector field, or a matrix. As is the convention in classical field theory, we use a dot to denote a *partial* derivative with respect to time t. All formulas are given in SI units, and we use c, ϵ_0, and μ_0 to denote respectively: the speed of light, the vacuum permittivity, and permeability.

* tplanche@triumf.ca

FROM A SINGLE-PARTICLE HAMILTONIAN

A first class of symplectic and self-consistent algorithms may be derived from a single-particle Hamiltonian. For the sake of demonstration we consider a set of (macro-)particles whose dynamics is governed by the following Hamiltonian:

$$H(\mathbf{x},\mathbf{P};t) = \frac{\mathbf{P}^2}{2m} + q\phi(\mathbf{x}) + q\psi(\mathbf{x}), \tag{1}$$

where m is the mass of the particle, q is its charge, $\mathbf{x}$ and $\mathbf{P}$ are its coordinate vector and associated canonically conjugated momentum. The space-charge force derives from the self-potential ϕ. The external focusing forces derive from the scalar potential ψ. Since this Hamiltonian has no explicit dependence on the independent variable t, and is the sum of terms depending on either position or momentum alone, the particle motion can be numerically integrated using a concatenation of jolt maps [3]:

$$\left(I - \frac{\Delta t}{2} : \frac{\mathbf{P}^2}{2m} :\right)(I - \Delta t\, q : \phi + \psi :)\left(I - \frac{\Delta t}{2} : \frac{\mathbf{P}^2}{2m} :\right). \tag{2}$$

This approximate map, accurate to second order in Δt, is symplectic if ϕ and ψ are functions of class C^2. This is shown by proving that the Jacobian matrix of the map is symplectic [4]. Higher order integrators may be derived from this second order one using Yoshida's method [5].

With this approach the numerical method for solving the equation of motion for the self-potential – namely Poisson's equation – is not obtained from a least action principle. This leads to a certain level of arbitrariness in the way the self-potential is to be computed.

FROM A DISCRETIZED LAGRANGIAN

Let us now consider methods based on variational integrators derived from a Lagrangian. We will see that with these methods all the dymanics – the evolution of the particle distribution as well as the evolution of the self-field – are obtained from Hamilton's principle of stationary action.

Low's Lagrangian

To illustrate this approach we start from the Lagrangian for non-relativistic collisionless plasma proposed by Low [6]. In the electrostatic limit, where the self-field derives solely from a scalar potential, it writes:

$$\begin{aligned} L(\mathbf{x},\dot{\mathbf{x}},\phi;t) = & \\ & \int f(\mathbf{x}_0,\dot{\mathbf{x}}_0) L_P(\mathbf{x}(\mathbf{x}_0,\dot{\mathbf{x}}_0,t),\dot{\mathbf{x}}(\mathbf{x}_0,\dot{\mathbf{x}}_0,t);t)\,\mathrm{d}\mathbf{x}_0\mathrm{d}\dot{\mathbf{x}}_0 \\ & + \frac{\epsilon_0}{2}\int |\nabla\phi(\bar{\mathbf{x}},t)|^2 \mathrm{d}\bar{\mathbf{x}}, \end{aligned} \tag{3}$$

ISBN: 978-3-95450-200-4 doi:10.18429/JACoW-ICAP2018-SUPAF05

POLARIZED PROTON BEAMS FROM LASER-INDUCED PLASMAS

A. Hützen[1], M. Büscher*[1], I. Engin
Peter Grünberg Institut (PGI-6), Forschungszentrum Jülich,
Wilhelm-Johnen-Str. 1, 52425 Jülich, Germany

J. Thomas, A. Pukhov
Institut für Theoretische Physik I, Heinrich-Heine-Universität Düsseldorf,
Universitätsstr. 1, 40225 Düsseldorf, Germany

J. Böker, R. Gebel, A. Lehrach[2]
Institut für Kernphysik (IKP-4), Forschungszentrum Jülich,
Wilhelm-Johnen-Str. 1, 52425 Jülich, Germany

R. Engels
Institut für Kernphysik (IKP-2), Forschungszentrum Jülich,
Wilhelm-Johnen-Str. 1, 52425 Jülich, Germany

T. P. Rakitzis[3], D. Sofikitis[3]
Department of Physics, University of Crete, 71003 Heraklion-Crete, Greece

[1]also at Institut für Laser- und Plasmaphysik, Heinrich-Heine-Universität Düsseldorf,
Universitätsstr. 1, 40225 Düsseldorf, Germany
[2]also at JARA-FAME und III. Physikalisches Institut B, RWTH Aachen,
Otto-Blumenthal-Str., 52074 Aachen, Germany
[3]also at Institute of Electronic Structure and Laser, Foundation for Research and Technology-Hellas,
71110 Heraklion-Crete, Greece

Abstract

We report on the concept of an innovative laser-driven plasma accelerator for polarized proton (or deuteron) beams with a kinetic energy up to several GeV. In order to modell the motion of the particle spins in the plasmas, these have been implemented as an additional degree of freedom into the Particle-in-Cell simulation code VLPL. Our first simulations for nuclear polarized Hydrogen targets show that, for typical cases, the spin directions remain invariant during the acceleration process. For the experimental realization, a polarized HCl gas-jet target is under construction where the degree of proton polarization is determined with a Lamb-shift polarimeter. The final experiments, aiming at the first observation of a polarized particle beam from laser-generated plasmas, will be carried out at the 10 PW laser system SULF at SIOM/Shanghai.

INTRODUCTION

The field of laser-induced relativistic plasmas and, in particular, of laser-driven particle acceleration, has undergone impressive progress in recent years. Despite many advances in the understanding of fundamental physical phenomena, one unexplored issue is how the particle (in particular hadron) spins are influenced by the huge magnetic fields inherently present in the plasmas [1–4].

Several mechanisms can potentially lead to a sizesable degree of polarization of laser-accelerated particle beams: first, a genuine polarization build-up from an unpolarized target by the laser-plasma fields themselves and, second, polarization preservation of pre-aligned spins during the acceleration despite of these fields. The work of our group aims at the first scenario using a novel dynamically polarized Hydrogen target.

Two effects are currently discussed to build up a nuclear polarization in the plasma: either the polarization is generated due to a spin-flip according to the Sokolov-Ternov effect, induced by the magnetic fields of the incoming laser pulse. Besides that, the spatial separation of spin states by the magnetic-field gradient, *i.e.* the Stern-Gerlach effect, may result in the generation of polarization for different beam trajectories [5].

In addition to these two mechanisms, all particle spins precess around the laser or plasma magnetic fields as characterized by the Thomas-Bargmann-Michel-Telegdi (T-BMT) equation describing the spin motion in arbitrary electric and magnetic fields in the relativistic regime.

The first and up to now only experiment measuring the polarization of laser-accelerated protons has been performed at the ARCturus laser facility at Heinrich-Heine University Düsseldorf [2]. Figure 1 schematically depicts the setup: for the measurements a 100-TW class Ti:Sa laser system with a typical pulse duration of 25 fs and a repetition rate of 10 Hz

* m.buescher@fz-juelich.de

ISBN: 978-3-95450-200-4 doi:10.18429/JACoW-ICAP2018-SUPAF06

SIMULATIONS OF COHERENT ELECTRON COOLING WITH FREE ELECTRON LASER AMPLIFIER AND PLASMA-CASCADE MICRO-BUNCHING AMPLIFIER

J. Ma[1], G. Wang[1], V. N. Litvinenko[1,2]
[1] Brookhaven National Laboratory, Upton, New York 11973, USA
[2] Stony Brook University, Stony Brook, New York 11794, USA

Abstract

SPACE is a parallel, relativistic 3D electromagnetic Particle-in-Cell (PIC) code used for simulations of beam dynamics and interactions. An electrostatic module has been developed with the implementation of Adaptive Particle-in-Cloud method. Simulations performed by SPACE are capable of various beam distribution, different types of boundary conditions and flexible beam line, as well as sufficient data processing routines for data analysis and visualization. Code SPACE has been used in the simulation studies of coherent electron cooling experiment based on two types of amplifiers, the free electron laser (FEL) amplifier and the plasma-cascade micro-bunching amplifier.

COHERENT ELECTRON COOLING

Coherent electron cooling (CeC) [1, 2, 3] is a novel and promising technique for rapidly cooling high-intensity, high-energy hadron beams. A general CeC scheme consists of three sections: modulator, amplifier and kicker. In the modulator, the ion beam co-propagates with electron beam and each ion imprints a density wake on the electron distribution through Coulomb force. In the amplifier, the density modulation induced by ions is amplified by orders. In the kicker, the electron beam with amplified signal interacts with ion beam, giving coherent energy kick to ions towards their central energy, which consequently leads to cooling of the ion beam.

Figure 1 [3] shows the schematic of CeC using high gain free electron laser (FEL) as the amplifier, which is related with the CeC experiment in the Relativistic Heavy Ion Collider (RHIC) at the Brookhaven National Laboratory (BNL).

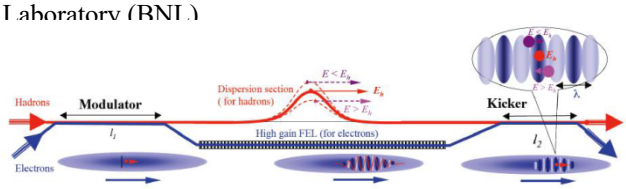

Figure 1: Schematic of coherent electron cooler based on high gain free electron laser.

Figure 2 [4] illustrates the layout of a CeC with a plasma-cascade amplifier (PCA). In the PCA, we use solenoids to control the transverse size of electron beam and make use of the exponential instability of longitudinal plasma oscillations to amplify the initial modulation. A CeC with a PCA does not require bending of ion beam.

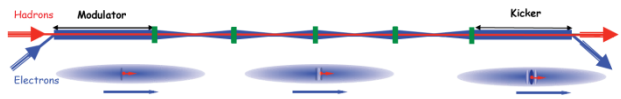

Figure 2: Layout of coherent electron cooler with a plasma-cascade amplifier.

SIMULATION TOOL

Our main simulation tool is code SPACE [5]. SPACE is a parallel, relativistic, 3D electromagnetic Particle-in-Cell (PIC) code developed for the simulations of relativistic particle beams, beam-plasma interaction, and plasma chemistry. Benchmark test has been performed for SPACE with several accelerator physics codes including MAD-X, ELEGANT and Impact-T, and a good agreement has been achieved. SPACE has been used for the study of plasma dynamics in a dense gas filled RF cavity [6] and the study of mitigation effect by beam induced plasma [7].

Electrostatic module contained in code SPACE has been mainly used in our study, as the particle interaction is essentially electrostatic in the co-moving frame. This code module includes two different approaches. The first one is the traditional PIC method for the Poisson-Vlasov equation, which uses uniform Cartesian mesh, linear charge deposition scheme and fast Fourier transform (FFT) solver. This approach is precise and effiective for particles with uniform distribution and computational domain with pure periodic boundary condition. The second approach is a new adaptive Particle-in-Cloud (AP-Cloud) method [8]. This method, based on real particle distribution, generates an adaptively chosen set of computational particles as the mesh, and uses the weighed least squares method for approximation of differential and integral operators. AP-Cloud method is beneficial for particles with non-uniform distribution and computational domain with irregular geometry and mixed type of boundary conditions, such as open boundary condition in the transverse directions and periodic in the longitudinal direction. Both approaches have passed series of verification tests and have been compared in our study. AP-Cloud method produced higher accuracy for electron beam with Gaussian distribution and computational domain with mixed boundary conditions, which are used in CeC simulations, so we have used AP-Cloud method in this study.

SPACE contains various data processing routines and provides sufficient output for data analysis and

ISBN: 978-3-95450-200-4 doi:10.18429/JACoW-ICAP2018-SUPAF07

HIGH-FIDELITY THREE-DIMENSIONAL SIMULATIONS OF THERMIONIC ENERGY CONVERTERS*

N. M. Cook†, J. P. Edelen, C. C. Hall, M. Keilman, P. Moeller, R. Nagler
RadiaSoft LLC, Boulder, CO, USA
J.-L. Vay, Lawrence Berkeley National Laboratory, Berkeley, CA, USA

Abstract

Thermionic energy converters (TEC) are a class of thermoelectric devices, which promise improvements to the efficiency and cost of both small- and large-scale electricity generation. A TEC is comprised of a narrowly-separated thermionic emitter and an anode. Simple structures are often space-charge limited as operating temperatures produce currents exceeding the Child-Langmuir limit. We present results from 3D simulations of these devices using the particle-in-cell code Warp, developed at Lawrence Berkeley National Lab. We demonstrate improvements to the Warp code permitting high fidelity simulations of complex device geometries. These improvements include modeling of non-conformal geometries using mesh refinement and cut-cells with a dielectric solver. We also consider self-consistent effects to model Schottky emission near the space-charge limit for arrays of shaped emitters. The efficiency of these devices is computed by modeling distinct loss channels, including kinetic losses, radiative losses, and dielectric charging. We demonstrate many of these features within an open-source, browser-based interface for running 3D electrostatic simulations with Warp, including design and analysis tools, as well as streamlined submission to HPC centers.

INTRODUCTION

Thermionic energy converters (TECs) generate electrical power from external heat sources using thermionic emission. By driving electrons across a narrow vacuum gap connected to an external load, electric power is created. For modest gap distances however, the thermionic current quickly exceeds the Child-Langmuir limit, reducing the peak achievable device power. To overcome space charge limitations an accelerating grid is used to compensate the negative potential generated by the beam space charge. The efficiency of such a device is theoretically limited only by the difference in temperature between the hot emitter and cold collector. However, the presence of a grid, along with realistic material properties of the device, serve to reduce their efficiency. Sophisticated simulations are needed to properly capture these dynamics.

Previous efforts to address these needs led to the development of an efficiency model and self-consistent simulation procedure for evaluating TEC designs [1]. In this paper we provide a brief review of this model and its implementation using the Warp particle-in-cell framework [2]. We then illustrate the value of this model in optimizing devices using a simple case study in grid placement and transparency. Lastly, we discuss the improvements being made to the electrostatic solver within the Warp to further improve vacuum nano-electronic device modeling.

* This material is based upon work supported by the U.S. Department of Energy, Office of Science, Office of Advanced Scientific Computing Research under Award Number DE-SC0017162.
† ncook@radiasoft.net

EFFICIENCY MODEL

Energy conversion in a TEC is limited by a set of discrete loss channels, including kinetic, thermal, radiative, and resistive losses. Proper evaluation necessitates the tracking and quantification of each loss channel. For the Warp simulations discussed in these studies, we've adopted a model that is well-established in literature [3] and has been applied in recent experimental studies [4].

The model identifies four main loss mechanism of power from the TEC system: power carried by electrons leaving the emitter P_{ec}, net radiative power from the emitter P_R, conductive heat loss in the attached circuit P_{ew}, and finally power lost from holding the voltage on the grid P_{grid}. We note that the simulations assume periodic boundaries, and so the current and corresponding power quantities are normalized by area. The conversion efficiency of the device is the ratio of the net electrical power generated divided by the net thermal power exhausted. If the electrical power that is generated from circuit load is P_{load}, the efficiency η is:

$$\eta = \frac{P_{load} - P_{grid}}{P_{ec} + P_R + P_{ew}} \ . \tag{1}$$

The net power transmitted from emitter to collector is:

$$P_{ec} = J_e \left(\phi_e + 2k_B T_e\right) - J_c \left(\phi_e + 2k_B T_c\right) \ . \tag{2}$$

Here, J_e, the current leaving the emitter, is known exactly from the simulation. The second term accounts for return current back to the emitter. The emitter and collector work functions are ϕ_e and ϕ_c. The collector is assumed to be held at a low temperature ($T_c < 500°$ K), thus we analytically compute the return current J_c.

The radiative heat loss is based on an analytic calculation for infinite parallel plates with some shielding from the grid. This is calculated as:

$$P_R = \epsilon \sigma_{sb} \left(T_e^4 - T_c^4\right) \ , \tag{3}$$

where ϵ is an effective emissivity, σ_{sb} is the Stefan-Boltzmann constant, and T_e and T_c are the emitter and collector temperature respectively.

ISBN: 978-3-95450-200-4 doi:10.18429/JACoW-ICAP2018-SUPAF08

PARTICLE-IN-CELL SIMULATION OF A BUNCHED ELECTRONS BEAM ACCELERATION IN A TE_{113} CYLINDRICAL CAVITY AFFECTED BY A STATIC INHOMOGENEOUS MAGNETIC FIELD*

E. A. Orozco†, Universidad Industrial de Santander, A.A. 678 Bucaramanga, Colombia
V. E. Vergara, J. D. González, J. R. Beltrán,
Universidad del Magdalena, A.A.731 Santa Marta, Colombia

Abstract

The results of the relativistic full electromagnetic Particle-in-cell (PIC) simulation of a bunched electrons beam accelerated in a TE_{113} cylindrical cavity in the presence of a static inhomogeneous magnetic field are presented. This type of acceleration is known as Spatial AutoResonance Acceleration (SARA). The magnetic field profile is such that it keeps the electrons beam in the acceleration regime along their trajectories. Numerical experiments of bunched electrons beam with the concentrations in the range 10^8–10^9 cm^{-3} in a linear TE_{113} cylindrical microwave field of a frequency of 2.45 GHz and an amplitude of 15 kV/cm show that it is possible accelerate the bunched electrons up to energies of 250 keV without serious defocalization effect. A comparison between the data obtained from the full electromagnetic PIC simulations and the results derived from the relativistic Newton-Lorentz equation in a single particle approximation is carried out. This acceleration scheme can be used as a basis to produce hard x-ray.

INTRODUCTION

The last decades, particle accelerators based on the electron cyclotron resonance (ECR) phenomenon has been extensively studied. Different technological applications based on this phenomenon has been proposed [1–5]. There are different ways to maintain the ECR condition, which use: (i) Transversal electromagnetic (TEM) waves in a homogeneous magnetostatic field [6,7], (ii) Transversal electric (TE) waves in waveguides placed on inhhomogeneous magnetostatic field [8, 9], (iii) TE standing electromagnetic waves in cavities affected by a homogeneous magnetic field growing slowly in time, known as GYRAC [10, 11] or (iv) TE standing electromagnetic waves in cavities affected by an inhomogeneous magnetostatic field, known as SARA [12–16]; among others [17]. In the SARA concept the magnetostatic field is fitted along the resonant cavity axis to keep the ECR acceleration regime as the electrons move in helical trajectories. The SARA concept has been studied both analytically and numerically in cylindrical TE_{11p} cavities [12–15] as well as in a TE_{112} rectangular cavities [16]. An X ray source based on the SARA concept has been certificated [18].

In the present paper, the influence of the self-consistent field on the space autoresonance acceleration (SARA) of bunched electrons beams in the linear TE_{113} cylindrical cavity is analized, by using a full electromagnetic relativistic particle-in-cell code. In our numerical scheme, the simulation is carried out in two stages:

1. Calculation of the TE_{113} steady-state microwave field before injecting the electrons bunched

2. Self-consistent simulation of the bunched electrons beams in the SARA acceleration.

The cylindrical TE_{113} cavity, whose radius and length are 4.54 cm and 30 cm respectively, is excited by a 2.45 GHz source. In our numerical model, to excite the TE_{113} microwave field of 15 kV/cm tension, an input power of 728 kW is injected into the cavity through a TE_{10} waveguide. The electron's bunched, whose concentrations are in the range 10^8–10^9 cm^{-3}, are described in the framework of the Vlasov-Maxwell equation; which is solved numerically through the particle-in-cell (PIC) method [19].

The obtained results show that it is possible accelerate bunched electrons up to energies of 260 keV without serious defocalization effect. A comparison between the data obtained from the full electromagnetic PIC simulations and the results derived from the relativistic Newton-Lorentz equation in a single particle approximation [15] is carried out. This acceleration scheme can be used as a basis to produce hard x-ray.

THEORETICAL FORMALISM AND NUMERICAL METHOD

Physical Scheme and Theoretical Formalism

The electron acceleration in the autoresonance regime by a standing transversal electric microwave field in an inhomogeneous magnetostatic field, known as *Spatial AutoResonance Acceleration (SARA)*, can be realized in the physical system shown in Fig. 1.

The cylindrical cavity 1 is placed inside the current coil set 2 that produces an azimuthally symmetric magnetostatic field whose value at the end where is the electron gun 5 is the corresponding to obtain classical resonance. The magnetostatic field profile has a relation with the used TE_{11p} ($p = 1, 2, 3, \ldots$) mode 4, which is excited through the microwave port 3. The electrons gun 5 injects electrons by one end of the cavity 1 along the magnetostatic field axis, taken as z axis. The right-hand polarized electric field component of the microwave field accelerates the electrons by electron

* Work supported by Universidad Industrial de Santander (Colombia) and Universidad del Magdalena (Colombia)
† eaorozco@uis.edu.co

ISBN: 978-3-95450-200-4 doi:10.18429/JACoW-ICAP2018-SUPAF09

SPARSE GRID PARTICLE-IN-CELL SCHEME FOR NOISE REDUCTION IN BEAM SIMULATIONS

L. F. Ricketson*, Lawrence Livermore National Laboratory, Livermore, CA, USA
A. J. Cerfon, Courant Institute of Mathematical Sciences, New York University, New York, NY, USA

Abstract

We demonstrate that the sparse grid combination technique, a scheme originally designed for grid based solvers of high-dimensional partial differential equations, can be effectively applied to reduce the noise of Particle-in-Cell (PIC) simulations. This is because the sparse grids used in the combination technique have large cells relative to a comparable regular grid, which, for a fixed overall number of particles, increases the number of particles per cell, and thus improves statistical resolution. In other words, sparse grids can accelerate not only the computation of the electromagnetic fields, but also the particle operations, which typically dominate the computation and storage requirements.

INTRODUCTION

In charged beams in particle accelerators, the Coulomb collision frequency is much smaller than the other frequencies of interest, even at the highest achievable beam intensities. A kinetic description of the beam is therefore required, in which one solves for the beam distribution function giving the number of particles in an infinitesimal six-dimensional phase space volume. Because of the high dimensionality of the phase space volume, intense beam simulations are very computationally intensive; even a modest grid resolution for each of the six dimensions pushes the limits of today's largest supercomputers.

To circumvent this difficulty, particle based approaches to the problem have been widely adopted, usually in the form of the Particle-in-Cell (PIC) algorithm [1]. The PIC method has the advantages of being conceptually intuitive, being well-suited for massive parallelization, and only requiring discretization of configuration space. Detailed PIC simulations of intense charged beams are routinely run and relied upon to explain experimental results and to design new accelerators [2, 3]. Even so, the accuracy of these PIC simulations remains limited due to the probabilistic nature of the PIC scheme, which requires a large number of particles to be simulated in order to reduce statistical noise. We will indeed show in this article that the slow decay of this noise with the number of simulated particles implies that for a given target accuracy, standard PIC simulations may even be more computationally intensive than grid based simulations.

In this work, we present a new algorithm which addresses this unsatisfying state of affairs by reducing the noise in PIC simulations. The algorithm is based on the sparse grid combination technique, a method originally intended to address the poor scaling of grid based PDE solvers with dimension [4]. We will explain how to apply the combination technique in a PIC setting, and demonstrate its promise by using our algorithm to solve standard problems in plasma and beam physics. The structure of the article is as follows. In the first Section, we compare the asymptotic run time complexity of a standard grid based kinetic solver and a standard PIC solver, and arrive at the conclusion that noise reduction strategies need to be implemented for the PIC approach to be desirable from a complexity point of view. In the second Section, we briefly present the sparse grid combination technique in the simple yet enlightening context of linear interpolation. The combination technique is the central idea motivating our new scheme. In the third Section, we explain how the combination technique can indeed be favorably applied in the context of PIC solvers, and numerically demonstrate the significant reduction in noise from doing so in the fourth Section. The fifth Section focuses on the limitations of our new sparse PIC scheme in its current, somewhat naive implementation, and highlights directions for further improvement. We provide a brief summary of our work in the last Section.

THE CURSE OF DIMENSIONALITY VS THE CURSE OF NOISE

It is well known that grid-based solvers for the kinetic equations describing beam evolution scale badly with the dimensionality of the problem. The computational complexity κ of a grid-based code can be expressed, in the best case scenario, as

$$\kappa \sim \frac{h^{-d}}{\Delta t},$$

where h is the grid size, Δt is the time step, and d is the dimension of the problem. If we consider a typical solver which would be second-order accurate in space and time, the numerical error ε scales like h^2 and Δt^2, so numerical error ε and run-time complexity κ can be related through the scaling

$$\kappa \sim \varepsilon^{-\frac{d+1}{2}}.$$

The exponential dependence of κ on d is a major reason why continuum kinetic simulations are computationally intensive. It is often referred to as the *curse of dimensionality*.

Particle based algorithms such as the PIC algorithm address the curse of dimensionality by approximating the distribution function in terms of macro-particles which evolve in configuration space, which is at most three-dimensional. If N_p is the number of particles used in the simulation, we can write

$$\kappa \sim \frac{dN_p}{\Delta t}$$

* ricketson1@llnl.gov

ISBN: 978-3-95450-200-4 doi:10.18429/JACoW-ICAP2018-SUPAF10

RECONSTRUCTION OF PARTICLE DISTRIBUTIONS AT RFQ EXIT AT SNS BEAM TEST FACILITY*

Z. Zhang†, S. Cousineau[1], Department of Physics and Astronomy, University of Tennessee, Knoxville, USA
A. Aleksandrov, Oak Ridge National Laboratory, Oak Ridge, USA
[1] also at Oak Ridge National Laboratory, Oak Ridge, USA

Abstract

Fluctuations of beam parameters and uncertainties of quadrupole gradients during measurements have effects on the reconstruction of initial particle distributions. To evaluate these effects, the concept of a distribution discrepancy is proposed. Results suggest effects of fluctuations of beam parameters are small, while uncertainties of quadrupole gradients are the main factors that affect the reconstructed distributions. By comparing the measured distributions with distributions produced by tracking the reconstructed initial distributions, it is proved that the real or quasi-real (closest to real) initial distribution can be obtained as long as the minimum distribution discrepancy is found.

INTRODUCTION

The Beam Test Facility (BTF) at SNS consists of a 65 kV H- ion source, a 2.5 MeV RFQ, a beam line with advanced transverse and longitudinal beam diagnostic devices and a 6kW beam dump (as shown in Fig. 1). One of the main goals of the BTF is to provide a platform for conducting R&D for novel accelerator physics and technological concepts related to high intensity hadron beam generation, acceleration, manipulation and measurement [1]. Of particular importance is to conduct the first direct 6D phase space measurement of a hadron beam [2] which will be used to high intensity beam halo study [3].

Reconstruction of particle distributions from 6D phase space measurement is not trivial. Therefore, reconstruction of a 2D distribution without considering coupling between horizontal, vertical and longitudinal planes can be carried out as the first step, which can help validate the approach of reconstruction of particle distributions and obtaining of the real initial distribution which may be affected by beam parameters and quadrupole gradients, gaining experiences for the eventual reconstruction of 6D phase space particle distributions.

There are usually two methods to reconstruct the initial particle distributions by PIC simulation codes, one is fitting the RMS beam sizes of the measured distributions, the other is a tomography-like technique [4]. At SNS, a more direct method based on emittance data in both transverse directions and the backward tracking ability of PyORBIT is used [5,6], and a dedicated PIC back-tracking simulation code based on PyORBIT has been developed. The simulation code can transform measured particle distributions into bunches for backward tracking, create backward lattice to track the bunch from measurement location to entrance of the lattice. In the work presented here, the lattice is the section of the BTF from the RFQ exit to the first slit (Slit 1) which is used to measure the transverse particle distributions. There are four quadrupoles (Q1, Q2 Q3 and Q4) in the lattice, which can be seen in Fig. 1. This paper mainly focuses on the investigation of influences of beam parameters and quadrupole gradients on the reconstructed particle distributions and how to obtain the real initial distributions.

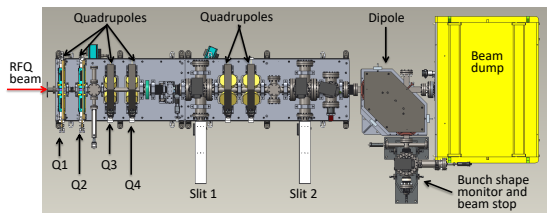

Figure 1: Layout of beam test facility at SNS.

VALIDATION OF BACK-TRACKING SIMULATION CODE

The back-tracking simulation code needs to be verified that it can accurately backward track a distribution before it is applied to the distribution reconstruction.

First, an ideal Gaussian distribution is used to validate the back-tracking code. An ideal Gaussian distribution is generated at the RFQ exit and tracked to the slit 1 by the forward-tracking code. Then the back-tracking code tracks the distribution at slit 1 backward to the RFQ exit with the same quadrupole settings, and the final distribution is compared with the initial distribution. Specifically, corresponding particle coordinates are compared between the two distributions, and the maximum particle coordinates discrepancy in phase space is used as a measure of comparison. The parameters of the initial distributions are α_x =−1.99, β_x = 20 mm/mrad, ε_x = 0.16 mm·mrad, α_y =−1.99, β_y = 20 mm/mrad, ε_y = 0.16 mm·mrad, respectively, and the particle number is ten thousand.

Figure 2 displays the initial Gaussian distributions (black) and the distributions produced by back tracking (red). It illustrates the two distributions are coinciding completely in both x-plane and y-plane. Detailed comparison results show that the maximum particle coordinates discrepancies in x and y planes are (5.65×10^{-5} mm, 5.05×10^{-4} mrad), (5.0×10^{-5} mm, 5.0×10^{-4} mrad) for 0 mA and (6.37×10^{-5} mm, 8.21×10^{-4} mrad), (5.31×10^{-5} mm, 8.6×10^{-4} mrad) for 50 mA, which prove that

* Work supported by NSF Accelerator Science grant 1535312
† email address: zzhang87@utk.edu

ISBN: 978-3-95450-200-4 doi:10.18429/JACoW-ICAP2018-SUPAG01

SPACE CHARGE AND TRANSVERSE INSTABILITIES AT THE CERN SPS AND LHC

E. Métral†, D. Amorim, G. Arduini, H. Bartosik, H. Burkhardt, E. Benedetto, K. Li, A. Oeftiger, D. Quatraro, G. Rumolo, B. Salvant, C. Zannini, CERN, Geneva, Switzerland

Abstract

At the CERN accelerator complex, it seems that only the highest energy machine in the sequence, the LHC, with space charge (SC) parameter close to one, sees the predicted beneficial effect of SC on transverse coherent instabilities. In the other circular machines of the LHC injector chain (PSB, PS and SPS), where the SC parameter is much bigger than one, SC does not seem to play a major (stabilising) role, and it is maybe the opposite in the SPS. All the measurements and simulations performed so far in both the SPS and LHC will be reviewed and analysed in detail.

INTRODUCTION

In the PSB, transverse instabilities (which still need to be fully characterized) are observed without damper during the ramp, where space charge could potentially play a role but no important change of instability onset was observed along the cycle when changing the bunch length (and shape) for constant intensity.

In the PS, a Head-Tail (HT) instability with six nodes is predicted at injection without space charge and observed with natural chromaticities and in the absence of Landau octupoles, linear coupling and damper.

In the SPS, a fast vertical single-bunch instability is observed at injection above a certain threshold (depending on the slip factor), with a travelling-wave pattern along the bunch. Several features are close to the ones from the predicted Transverse Mode-Coupling Instability (TMCI) between modes - 2 and - 3 without SC (for Q' ~ 0).

Finally, in the LHC, the predicted HT instability with one node for a chromaticity of about five units, with neither Landau octupoles nor damper, is observed only above a certain energy, as confirmed by simulations with space charge. Furthermore, the intensity threshold for the TMCI at injection for a chromaticity close to zero (which has not been measured yet as it is much higher than the current LHC intensities) is predicted to be significantly increased by space charge according to simulations.

Considering the case of a TMCI with zero chromaticity, a two-particle approach would conclude that both SC and/or a reactive transverse damper (ReaD) would affect TMCI in a similar way and could suppress it (see Fig. 1).

Using a two-mode approach (instead of the previous two-particle approach), a similar result would be obtained in the "short-bunch" regime (i.e. TMCI between modes 0 and – 1, such as in the LHC) as both a ReaD and SC are expected to be beneficial: the ReaD would shift the mode 0 up and SC would shift the mode – 1 down, but in both cases the coupling would therefore occur at higher intensities. However, the situation is more involved for the "long-bunch" regime (i.e. TMCI between higher-order modes, such as in the SPS). As the ReaD modifies only the (main) mode 0 and not the others (where the mode-coupling occurs), it is expected to have no effect for the main mode-coupling (as confirmed in Fig. 2, using the Vlasov solver GALACTIC [3]). As concerns SC, it modifies all the modes except 0, and the result is still in discussion and the subject of this paper, which is structured as follows: the first section is devoted to the many SPS studies, while the LHC results will be discussed in the second section before concluding and discussing the next steps.

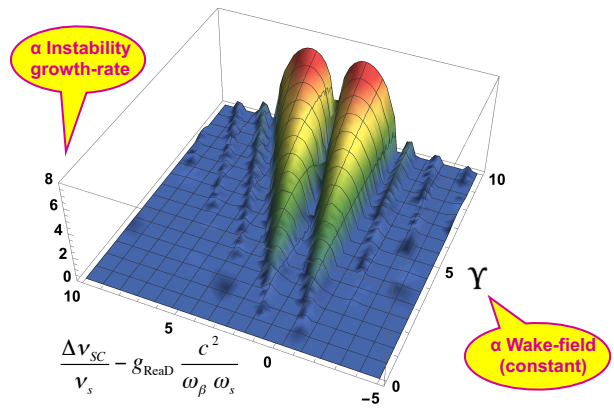

Figure 1: Two-particle approach for the TMCI following Ref. [1] but adding a reactive transverse damper (ReaD). This combines the results from Ref. [1] (with SC only) and Ref. [2] (with reactive damper only).

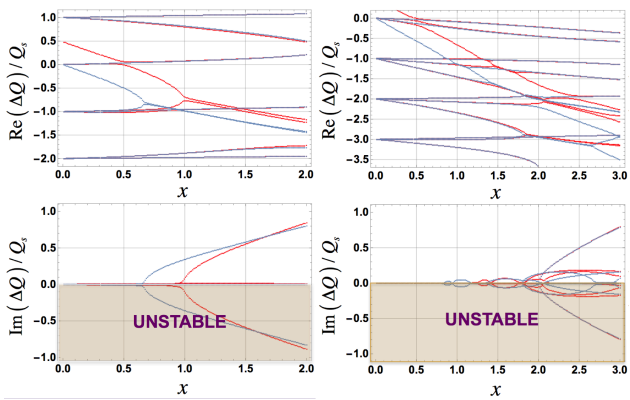

Figure 2: Usual TMCI plots for the LHC (left) and SPS (right) assuming a Broad-Band resonator impedance (with Q' = 0), without / with ReaD (50 turns) in blue / red [3].

† Elias.Metral@cern.ch

ISBN: 978-3-95450-200-4 doi:10.18429/JACoW-ICAP2018-SUPAG03

CHALLENGES IN EXTRACTING PSEUDO-MULTIPOLES FROM MAGNETIC MEASUREMENTS

S. Russenschuck, G. Caiafa, L. Fiscarelli, M. Liebsch, C. Petrone, P. Rogacki
CERN, Geneva, Switzerland

Abstract

Extracting the coefficients of Fourier-Bessel series, known as pseudo-multipoles or generalized gradients, from magnetic measurements of accelerator magnets involves technical and mathematical challenges. First, a novel design of a short, rotating-coil magnetometer is required that does not intercept any axial field component of the magnet. Moreover, displacing short magnetometers, step-by-step along the magnet axis, yields a convolution of the local multipole field errors and the sensitivity (test function) of the induction coil. The deconvolution must then content with the low signal-to-noise ratio of the measurands, which are integrated voltages corresponding to spatial flux distributions. Finally, the compensation schemes, as implemented on long coils used for measuring the integrated field harmonics, cannot be applied to short magnetometers. All this requires careful design of experiment to derive the optimal length of the induction coil, the step size of the scan, and the highest order of pseudo-multipoles in the field reconstruction. This paper presents the theory of the measurement method, the data acquisition and deconvolution, and the design and production of a saddle-shaped, rotating-coil magnetometer.

INTRODUCTION

The magnetic measurement section within the magnet group of CERN's technology department is responsible for the qualification of all superconducting and normal conducting magnets in CERN's accelerator complex. To supplement the long rotating-coil magnetometers and stretched-wire systems (the section's workhorses for magnetic measurements) we have recently developed moving induction-coil arrays, axial and transversal rotating-coil scanners [1], and induction-coil transducers for solenoidal magnets. Applications of these tools require, however, a sophisticated post-processing step based on the regularity conditions of electromagnetic fields. To this end, the magnet bores can be considered as trivial domains, i.e., simply connected and source-free with piecewise smooth, closed and consistently oriented boundaries. Calculating the transversal field harmonics as a function of the coordinate in the magnet's axial direction, for example, by using the numerical field calculation program ROXIE [2], or measuring these harmonics with a very short, rotating-coil scanner, allows the extraction of the coefficients of Fourier-Bessel series, known as pseudo-multipoles [3] or generalized gradients [4].

However, the raw measurement data from the field transducers are induced voltages that are integrated using a digital integrator, triggered by an angular encoder. Developing these signals into Fourier series results in convoluted functions of the spacial flux distribution, because strictly speaking, point-like measurements of the magnetic flux density are not possible.[1] Before such signals can be used as boundary data for harmonic analysis or boundary-element methods (BEM), a deconvolution is required.

A careful design of experiment is required, considering a low signal-to-noise ratio of the measurand, the sensitivity of the induction coil with respect to transversal harmonics, the step-size of the longitudinal scan, and the compensation schemes for the main-field component. In this paper we present the design and production of the transversal-field scanner and the challenges in applying the pseudo-multipole theory to measurement data.

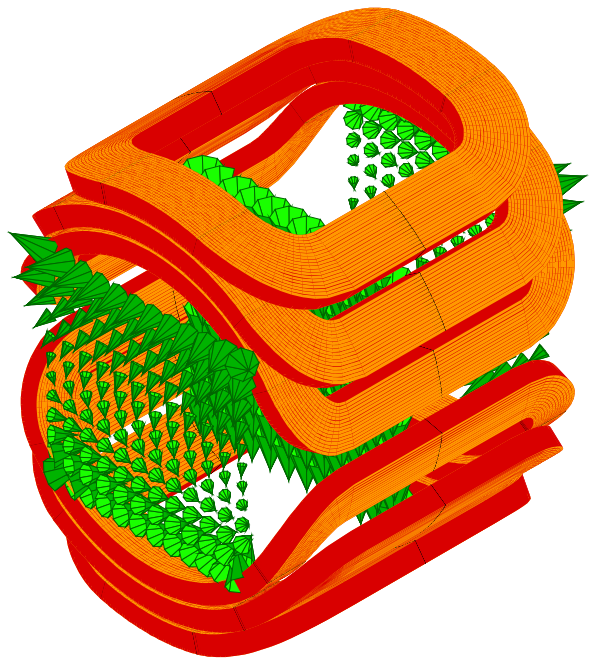

Figure 1: Representation of the magnetic flux density in 3 different planes of an orbit corrector for the ELENA project. Notice the large z-component in the end fields. Computed with the CERN field computation program ROXIE [2].

PSEUDO MULTIPOLES

The local field distribution in short magnets, such as the one shown in Fig. 1, cannot be expressed by the usual field harmonics (Fourier series) for the integrated fields because they do not constitute a complete orthogonal basis of the

[1] Transversal Hall sensors come close but their active area (the Hall plate) typically has a diameter of 2-3 mm.

ISBN: 978-3-95450-200-4 doi:10.18429/JACoW-ICAP2018-SUPAG05

MUON BACKGROUND STUDIES FOR BEAM DUMP OPERATION OF THE K12 BEAM LINE AT CERN

M. Rosenthal*, D. Banerjee, J. Bernhard, M. Brugger, N. Charitonidis, M. van Dijk, B. Döbrich, L. Gatignon, A. Gerbershagen, E. Montbarbon, B. Rae
European Organization for Nuclear Research (CERN), 1211 Geneva 23, Switzerland
T. Spadaro
Istituto Nazionale di Fisica Nucleare, Laboratori Nazionali di Frascati (INFN/LFN), Frascati, Italy

Abstract

In the scope of the Physics Beyond Colliders study at CERN a future operation of the NA62 experiment in beam dump mode is discussed, enabling the search for dark sector particles, e.g. heavy neutral leptons, dark photons and axions. For this purpose, the 400 GeV/c primary proton beam, extracted from the SPS, will be dumped on a massive dump collimator located in the front end of the K12 beam line. Muons originating from interactions and decays form a potential background for this kind of experiment. To reduce this background, magnetic sweeping within the beam line is employed. In this contribution, the muon production and transport has been investigated with the simulation framework G4beamline. The high computational expense of the muon production has been reduced by implementing sampling methods and parametrizations to estimate the amount of high-energy muons and efficiently study optimizations of the magnetic field configuration. These methods have been benchmarked with measured data, showing a good qualitative agreement. Finally, first studies to reduce the muon background by adapting the magnetic field configuration are presented, promising a potential background reduction by a factor four.

INTRODUCTION

The North Area at the Super Proton Synchrotron (SPS) at CERN has a long history of fixed target experiments and R&D studies. Extracted from the SPS, a 400 GeV/c proton beam is directed via transfer lines to two experimental halls (EHN1, EHN2) and an underground cavern (ECN3) located at the CERN Prévessin site. In ECN3, a high-intensity secondary hadron beam, that has been created at a beryllium target, is transported via the K12 beam line towards the NA62 experiment [1]. This experiment aims to measure the branching ratio of the very rare decay $K^+ \rightarrow \pi^+ \nu\bar{\nu}$. First results of this operation have been presented recently [2]. Besides the main measurement program, a future proposal for NA62 suggests the search for dark sector particles such as heavy neutral leptons, dark photons and axions in "dedicated dump runs" [3]. For this purpose, the beryllium target will be removed and the primary proton beam will be dumped on a 3.2 m long massive dump collimator (TAX) in order to create the hypothetical dark sector particles. The decay of these particles into Standard Model particles, e.g. muons in the final state, might be observable by the NA62 experiment. The implementation of this proposal is studied by the the Conventional Beams Working Group (CBWG) within the Physics Beyond Colliders (PBC) framework. Muons directly produced in the primary interactions within the TAX pose an crucial background for this kind of experiment, e.g. through random spatiotemporal track combinations of muons and antimuons. Studies to understand the trajectories of this muon background are essential to further optimize the magnetic sweeping of the K12 beam line, when operated in beam dump mode. To investigate and reduce this muon background, the optimisation of the magnetic sweeping along the K12 beam line is performed. Monte Carlo studies based on the program G4beamline [4] have been combined with analytical parametrisations of the muon distributions to reduce the computational demands. In this contribution, benchmarking results with recorded data as well as first results from the optimization studies are shown.

THE K12 BEAM LINE MODEL

The simulation of production and transport of the muon background is computationally highly expensive and requires the precise knowledge of the magnetic field maps in the entire K12 beam line. A G4beamline model, including a simplified model of the NA62 experiment, has been developed to investigate the particle production, transport and decay of the particles in the beam line. It is illustrated in Fig. 1. The 400 GeV/c protons with a nominal intensity of 3×10^{12} protons per burst impinge on a 400 mm-long beryllium target (T10), which corresponds to about one nuclear

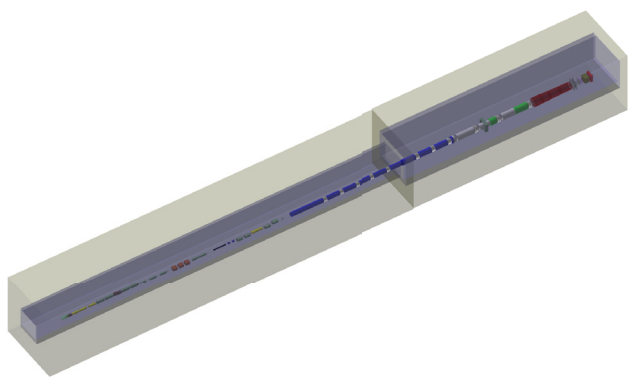

Figure 1: The G4Beamline model of the K12 beam line and NA62 experiment.

* marcel.rosenthal@cern.ch

ISBN: 978-3-95450-200-4 doi:10.18429/JACoW-ICAP2018-SUPAG06

SIMULATION CHALLENGES FOR eRHIC BEAM-BEAM STUDY*

Yun Luo, BNL, Upton, NY, USA
Yue Hao, FRIB, East Lansing, MI, USA
Ji Qiang, LBNL, Berkeley, CA, USA
Yves Raymond Roblin, JLab, Newport News, VA, USA

Abstract

The 2015 Nuclear Science Advisory Committee Long Rang Plan identified the need for an electron-ion collider (EIC) facility as a gluon microscope with capabilities beyond those of any existing accelerator complex. To reach the required high energy, high luminosity, and high polarization, the eRHIC design, based on the existing heavy ion and polarized proton collider RHIC, adopts a very small β-function at the interaction points, a high collision repetition rate, and a novel hadron cooling scheme. A full crossing angle of 22 mrad and crab cavities for both electron and proton rings are required. In this article, we will present the high priority R&D items related to the beam-beam interaction studies for the current eRHIC design, the simulation challenges, and our plans and methods to address them.

INTRODUCTION

The key EIC machine parameters identified in the 2015 Long Range Plan [1] are: 1) polarized (70%) electrons, protons, and light nuclei, 2) ion beams from deuterons to the heaviest stable nuclei, 3) variable center of mass energies ~20–100 GeV, upgradable to ~140 GeV, 4) high collision luminosity $\sim 10^{33}$–10^{34} cm^{-2}sec^{-1}, and possibly have more than one interaction region. To reach such a high luminosity, both designs of eRHIC at Brookhaven National Laboratory (BNL) and JLEIC at Thomas Jefferson National Accelerator Facility (JLab) aimed to increasing the bunch intensities, reducing the beam sizes at the interaction points (IPs), and increasing the collision frequency, while keeping achievable maximum beam-beam parameters for involved beams [2, 3].

The relative priorities of R&D activities for a next generation EIC were published in the 2016 NP Community EIC Accelerator R&D panel report [4]. The panel evaluated the R&D items needed for each of the current EIC design concepts under considerations by the community. Beam-beam interaction have been identified as one of the most important challenges needed to be addressed to reduce the overall design risk.

We join the expertise from BNL, JLAB, Lawrence Berkeley National Laboratory (LBNL), and Michigan State University (MSU) to address 4 challenging items related to the EIC beam-beam interaction in the two EIC ring-ring designs, namely, 1) beam dynamics study and numerical simulation of crabbed collision with crab cavities, 2) quantitative understanding of the damping decrement to the beam-beam performance, 3) impacts on protons with electron bunch swap-out in eRHIC ring-ring design, and 4) impacts on beam dynamics with gear-changing beam-beam interaction in JLEIC design.

To address the above critical items related to EIC beam-beam interaction, we propose new beam-beam simulation algorithms and methods to the existing strong-strong beam-beam simulation codes, together with a deep physics understanding of the involved beam dynamics. At the completion of this proposal, we should have a clear understanding of the beam-beam interaction in the next generation EIC designs and be able to provide robust counter-measures to possible beam-beam interaction related beam lifetime reduction, beam emittance growth, beam instabilities, and luminosity degradation. This work would significantly mitigate the technical risks associated with the EIC accelerator designs.

In this article, we will only focus on the simulation challenges related to the eRHIC beam-beam study, or the first three R&D items listed above. They are the common challenges to the eRHIC and JLEIC designs. JLEIC design also have another challenge: impacts on beam dynamics with gear-changing beam-beam interaction, which will not be discussed here.

eRHIC DESIGN PARAMETERS

For the present eRHIC design, the maximum beam-beam parameters for the electron and proton beams are $\xi_e = 0.1$ and $\xi_p = 0.015$, respectively. The choice of the beam-beam parameter of $\xi_e = 0.1$ for the electron beam is based on the successful operational experience of KEKB, where it was achieved with a transverse radiation damping time of 4000 turns. The choice of the beam-beam parameter for the proton ring is based on the successful operational experience of RHIC polarized proton runs, where a beam-beam parameter of $\xi_p = 0.015$ was routinely achieved.

To avoid long-range collisions, a crossing-angle collision scheme is adopted. For the present design, the proton and electron beams collide with a total horizontal crossing angle of 22 mrad. Such a crossing angle scheme is also required by the experiment to avoid separator dipoles in or near the detector, thus minimizing the background in the interaction region (IR). To compensate the luminosity loss by the crossing angle collision, crab cavities are to be used to tilt the proton and electron bunches such that they collide head-on at the IP. Table 1 shows key beam-beam interaction related parameters of the current eRHIC design. Without cooling, the design luminosity is 4.4×10^{33}cm^{-2}s^{-1}. With cooling in the proton ring, it is 1.05×10^{34}cm^{-2}s^{-1}.

* Work supported by Brookhaven Science Associates, LLC under Contract No. DE-AC02-98CH10886 with the U.S. Department of Energy.

ISBN: 978-3-95450-200-4 doi:10.18429/JACoW-ICAP2018-SUPAG09

BEAM DYNAMICS SIMULATIONS OF MEDICAL CYCLOTRONS AND BEAM TRANSFER LINES AT IBA

J. Van de Walle†, E. Forton, V. Nuttens, W. Kleeven, J. Mandrillon, E. Van der Kraaij,
Ion Beam Applications, 1347 Louvain-la-Neuve, Belgium

Abstract

At the Belgian company Ion Beam Applications (IBA), several in-house developed computational tools are used to simulate beam dynamics from a range of proton and electron accelerators. The main beam dynamics simulation tool is the "Advanced Orbit Code" (AOC), which integrates the equations of motion in any 2D or 3D magnetic field map with superimposed time variable or fixed electric fields. CLORIBA is the in-house closed orbit code for cyclotrons, which provides the tunes and isochronicity conditions for the isochronous cyclotrons. A tool developed especially for the super conducting synchro-cyclotron (S2C2) is the phase space motion code, which tracks energy, RF phase and orbit centre coordinates in the synchro-cyclotron. The calculation tools are described briefly and some examples are given of their applicability on the IBA accelerators.

INTRODUCTION

The computational tools at IBA are oriented towards three main categories of accelerators. The first types are isochronous cyclotrons, which operate at a fixed RF frequency. The three most common isochronous cyclotrons are the 18 MeV proton cyclotron called the Cyclone® KIUBE, used for production of radioactive F-18 [1], the 70 MeV proton cyclotron called the Cyclone® 70, mainly used for production of radiopharmaceuticals other than F-18 (for ex. Sr-82) and the 230 MeV proton cyclotron the Cyclone® 230. The latter is used in proton therapy systems. The second type of accelerator is the superconducting synchro cyclotron (the S2C2) [2], which is so far the only superconducting cyclotron at IBA and operates at a variable RF frequency (from 90 to 60 MHz). This accelerator delivers a pulsed (1 kHz) 230 MeV protons beam with pulse lengths of 10 μs. The last type of accelerator which will be covered is the rhodotron electron accelerator, which is a special arrangement of magnets around an accelerating cavity. This accelerator typically delivers a 10 MeV electron beam [3].

CALCULATION TOOLS

The main beam tracking code used at IBA is the "Advanced Orbit Code" (AOC) [4]. This code was originally developed by W. Kleeven and solves the equations of motion for a range of particles (protons, electrons, etc...) relevant to IBA accelerators. The independent integration variable is the RF phase advance (τ), which is related to time in the following way:

$$\tau = \omega_0 \int_0^t f(t')\,dt',$$

where ω_0 is the angular RF frequency and $f(t')$ is an arbitrary function of time. For isochronous cyclotrons $f(t')$=1. The differential equations are solved with a 4th order Runge Kutta integrator with variable step size. As input AOC can handle 2 or 3D static magnetic field maps, 3D potential maps on which a RF frequency is applied and static electric potential maps. In case of a 2D static magnetic field map, the magnetic field can be expanded around the median plane up to 3rd order. AOC is mainly used in studies related to extracted beam emittances, resonance studies and to optimize magnetic designs.

At IBA an in-house closed orbit code called CLORIBA was developed. This code is available in both C++ and python (pyCLORIBA). The code uses the established algorithm developed by Gordon [5] to determine the tunes and phase slip.

A last computational code is called "phase space motion" and was developed especially for the S2C2. This code tracks the energy, RF phase, orbit centre coordinates and the vertical beam motion of protons in a synchro-cyclotron. It uses a 4th order Runge-Kutta integrator with adaptive step size and takes as input the harmonic components of the magnetic field map, the frequency sweeps as a function of time and the voltage profile as a function of time.

The utilization of these three calculation tools will be illustrated in the following paragraphs.

ISOCHRONOUS CYCLOTRONS

Closed Orbit Program

The first step after the mechanical and electrical assembly of an isochronous cyclotron is a magnetic mapping to ensure the isochronicity of the magnetic field, so that a constant RF frequency can be applied and the beam is accelerated up to full energy without beam losses. These measured 2D maps serve as input to CLORIBA. A python script was developed which calculates the tune curves, the phase slip and the needed magnetic shimming which needs to be performed to make the cyclotron isochronous. An example 2D magnetic map from the Cyclone® KIUBE with the closed orbits on top of it is shown in Figure 1. The yellow regions in the centre of the poles are the regions where the "pole insertions" are placed. These are removable pieces of iron which can easily be machined to obtain isochronicity of the machine. The amount of machining of these pole pieces is directly calculated in pyCLORIBA based on the closed orbit analysis and magnetic perturbation maps calculated with the OPERA3D software.

ISBN: 978-3-95450-200-4 doi:10.18429/JACoW-ICAP2018-SUPAG10

DESIGN STUDY OF A FAST KICKER MAGNET APPLIED TO THE BEAMLINE OF A PROTON THERAPY FACILITY

Wenjie Han†, Xu Liu, Bin Qin
Institute of Applied Electromagnetic Engineering
Huazhong University of Science and Technology, Wuhan 430074, Hubei, China

Abstract

A proton therapy facility based on an isochronous superconducting cyclotron is under development in HUST (Huazhong University of Science and Technology). A fast kicker magnet will be installed in the upstream of the degrader to perform the beam switch function by kicking the proton beam to the downstream beam stop. The rising and falling time of the kicker is about 100 μs, and the maximum repetition rate is 500 Hz. This paper introduces simulation and optimization of the eddy current and dynamic magnetic field of the fast kicker, by using FEM code OPERA-3D. For kicker materials, laminated steel and soft ferrite are compared and the MnZn ferrite is chosen. Designing considerations includes the eddy current effect, field hysteresis, and mechanical structure of the kicker will also be introduced.

INTRODUCTION

HUST proton therapy facility (HUST-PTF) is based on an isochronous superconducting cyclotron and spot scanning technique. Two 360-degree rotation gantry treatment-rooms and one fixed beamline treatment station will be constructed at first stage. A detail description of the facility parameters can be found in Ref. [1]. During the treatment process of the pencil beam spot scanning, the proton beam is applied to the patient for only a few milliseconds, and then kicked away. After repositioning and/or readjustment of the beam energy, the beam is directed back to the patient [2]. A fast kicker magnet will be installed in the upstream of the degrader, to perform the 'beam off' function by kicking the proton beam to the downstream beam stop.

This paper mainly compares two material schemes for the kicker magnet yoke and analyses the eddy current and field hysteresis effect of kicker magnets. The design of mechanical structure is also introduced.

PHYSICAL SPECIFICATIONS

The kicker magnet system is one of the key components of spot scanning technique. The layout of the kicker system is shown in Fig 1. In HUST-PTF, vertical kicker scheme is adopted. The main parameters of the kicker magnet are listed in Table 1. The kicker magnet is located at 1.24 m before the degrader. There is a quadrupole (Q3) between the kicker magnet and the degrader, whose defocusing direction is the same to the kicker deflected direct

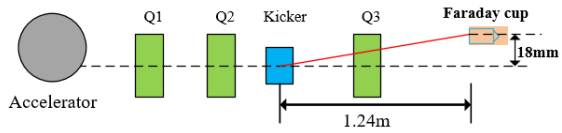

Figure 1: Layout of kicker system.

ion. The proton beam is deflected by the kicker magnet, then passing through a drift, the quadrupole between the kicker magnet and the degrader will further bend the proton beam to a Faraday cup (FC). According to the simulation of beam trajectory, the gap and pole width of kicker magnet is determined, the distance from beam stop to the center of the kicker magnet is about 1.24 m. The minimum integral field is 0.0252 T·m, deflecting the 250 MeV proton beam an angle about 10.36 mrad. The beam offset at the FC is about 18 mm (7 mm for the beam size, 3 mm for the thickness of FC, 8 mm for the radius of FC). As for the power supply, the kicker magnet is excited by pulse current with a maximum repetition frequency of 500 Hz and a rising/falling time of 100 μs. The current ramping speed is up to 5040 kA/s and the magnetic field ramping speed is up to 1010 T/s.

Table 1: Parameters of the Kicker Magnet

Name	Parameter
Deflection angle	10.36 mrad
Magnet gap	50 mm
Integral field	0.0252 T·m
Magnet length	200 mm
Number of coil turn	4 Turns/pole
Field strength	0.101 T
Good field region	±30 mm (vertical) ±14 mm (horizontal)
Coil Induction	44 μH
Max repetition Frequency	500 Hz
Rise/fall time	100 μs

MAGNET DESIGN

Kicker magnet applied to HUST-PTF is a window frame type magnet with two bedstead coils. To insure the required rapid change of the magnetic field, eddy currents in the core must be evaluated. Soft ferrite or laminated silicon sheets can be chosen as the material of the magnet cores.

* Work supported by The National Key Research and Development Program of China, with grant No.2016YFC0105305, and Natural Science Foundation of China with grant No. 11375068
† email address: hanwenjie@hust.edu.cn

ISBN: 978-3-95450-200-4 doi:10.18429/JACoW-ICAP2018-SUPLG01

COMPUTATIONAL ACCELERATOR PHYSICS: ON THE ROAD TO EXASCALE

R. D. Ryne*, Lawrence Berkeley National Laboratory, Berkeley, California 94720, USA

Abstract

The first conference in what would become the ICAP series was held in 1988. At that time the most powerful computer in the world was a Cray YMP with 8 processors and a peak performance of 2 gigaflops. Today the fastest computer in the world has more than 2 million cores and a theoretical peak performance of nearly 200 petaflops. Compared to 1988, performance has increased by a factor of 100 million, accompanied by huge advances in memory, networking, big data management and analytics. By the time of the next ICAP in 2021 we will be at the dawn of the Exascale era. In this talk I will describe the advances in Computational Accelerator Physics that brought us to this point and describe what to expect in regard to High Performance Computing in the future. This writeup as based on my presentation at ICAP'18 along with some additional comments that I did not include originally due to time constraints.

INTRODUCTION AND BRIEF HISTORY

The first conference in what would become the Computational Accelerator Physics series was held 30 years ago in San Diego, California in January 1988. At the time I was 28 years old. The meeting was called the Conference on Linear Accelerator and Beam Optics Codes [1]. I think there are three of us here now who were present for that meeting: Martin Berz, Herman Wollnik, and me. I'll describe the ICAP conference series in a moment, but first want to briefly address the the origins of the field of Computational Accelerator Physics. This summary is based on the paper, "Oh Camelot! A memoir of the MURA years," by F.T. Cole [2].

As is well known, Lawrence invented the first cyclotron in 1930 inspired by the work of Rolf Wideroe on resonance acceleration. In 1940 Donald Kerst built the first betatron, a 2 MeV electron machine. Soon after WWII Edwin McMillan was at Los Alamos waiting to return to Berkeley. According to Cole, McMillan told him that, in a single evening, he worked out the concepts for the sychrocyclotron and the synchrotron. Independently in the Soviet Union Vladimir Veksler did the same. Two proton synchrotrons were built in the early 1950's to go beyond a GeV, the Cosmotron at Brookhaven and the Bevatron at Berkeley.

Along with progress in circular accelerators there were also developments in linear accelerators. Luis Alvarez developed the first proton linac at Berkeley in 1948. Also, developments in radar during WWII led to high frequency, GHz power sources that Hanson and Panofsky used to develop electron linacs at Stanford.

A revolution in accelerator physics took place in 1952 with the invention of strong focusing by Courant, Snyder, and Livingston. As it turns out, Nick Christopholis had actually filed for a patent on strong focusing in 1950 and it was eventually granted in 1954. John Blewitt (BNL) applied alternating-gradient focusing to high intensity linacs. Also, the concept of Fixed Field Alternating Gradient (FFAG) was invented independently by multiple researchers, including Symon in 1954.

Strong focusing provided a totally new approach to high energy accelerators. A new lab, CERN, was founded after the war. Thanks to Lew Kowarski CERN acquired its first electronic computer in 1958. The CERN PS was commissioned in the Fall of 1959. The 30 GeV AGS at BNL began operation in 1960.

THE BEGINNING OF COMPUTATIONAL ACCELERATOR PHYSICS

So far I've described some key developments in accelerator physics through the 1950's. The 1950's also brings us to the first digital computations for accelerator modeling. While there was plenty of activity in the field, I would particularly like to mention the work of L. Jackson Laslett. Laslett was a pioneer in using digital computers for orbit calculations and for calculating electromagnetic fields. There are records of Laslett performing his simulations on a computer known as the ILLIAC I, a computer comprised of 2800 vacuum tubes. While working for the Midwestern Universities Research Association Laslett observed and analyzed sensitive dependence on initial conditions – what we now call chaos. He did this in the mid 1950's. His studies actually predate the work of Edward Lorenz who discovered chaos in weather simulations and whose 1962 paper launched chaos theory. Of course mathematicians going back to Poincare had predicted dynamical behavior that we now describe as chaotic dynamics.

I would also like to mention another important event of the 1950's involving scientific computing that included someone who would later become heavily involved in Computational Accelerator Physics. That event was the simulation of the Fermi-Pasta-Ulam (FPU) problem, and the person involved was Mary (Tsingou) Menzel [3]. Mary was the programmer for the FPU problem on the MANIAC computer at Los Alamos National Laboratory (LANL). I met her in the 1980's. By then she was a member of the Accelerator Technology Division at LANL and I was a graduate student who spent my summers there. I remember Mary telling me there were cans of water on top of the computer for cooling!

Along with computational developments, there were also key theoretical developments in the 1950s. Most notably, Kolmogorov published his original paper in 1954, which set the stage for the KAM Theorem. A key consequence,

* rdryne@lbl.gov

ISBN: 978-3-95450-200-4 doi:10.18429/JACoW-ICAP2018-MOPLG01

CHALLENGES IN SIMULATING BEAM DYNAMICS OF DIELECTRIC LASER ACCELERATION

U. Niedermayer[1,2*],
A. Adelmann[7], R. Aßmann[4], S. Bettoni[7], D. S. Black[2], O. Boine-Frankenheim[1], P. N. Broaddus[2], R. L. Byer[2], M. Calvi[7], H. Cankaya[4,11,15], A. Ceballos[2], D. Cesar[10], B. Cowan[9], M. Dehler[7], H. Deng[2], U. Dorda[4], T. Egenolf[1], R. J. England[3], M. Fakhari[4], A. Fallahi[11], S. Fan[2], E. Ferrari[5,7], F. Frei[7], T. Feurer[12], J. Harris[2], I. Hartl[4], D. Hauenstein[7], B. Hermann[7,12], N. Hiller[7], T. Hirano[2], P. Hommelhoff[6], Y.-C.Huang[13], Z. Huang[2], T. W. Hughes[2], J. Illmer[6], R. Ischebeck[7], Y. Jiang[2], F. Kärtner[4,11,15], W. Kuropka[4,15], T. Langenstein[2], Y. J. Lee[8], K. Leedle[2], F. Lemery[4], A. Li[6], C. Lombosi[7], B. Marchetti[4], F. Mayet[4,15], Y. Miao[2], A. Mittelbach[6], P. Musumeci[10], B. Naranjo[10], A. Pigott[2], E. Prat[7], M. Qi[8], S.Reiche[7], L. Rivkin[5,7], J. Rosenzweig[10], N. Sapra[2], N. Schönenberger[6], X. Shen[10], R. Shiloh[6], E.Skär[1], E. Simakov[14], O. Solgaard[2], L. Su[2], A. Tafel[6], S. Tan[2], J. Vuckovic[2], H. Xuan[4,15], K. Yang[2], P. Yousefi[6], Z. Zhao[2], J. Zhu[4]
[1] Technische Universität Darmstadt, 64289 Darmstadt, Germany
[2] Stanford University, Stanford, CA 94305, USA
[3] SLAC National Accelerator Laboratory, Menlo Park, CA 94025
[4] Deutsches Elektronen-Synchrotron, D-22607 Hamburg, Germany
[5] École Polytechnique Fédérale de Lausanne, CH-1015 Lausanne, Switzerland
[6] Friedrich-Alexander Universität Erlangen-Nürnberg, 91058 Erlangen, Germany
[7] Paul Scherrer Institut CH-5232 Villigen, Switzerland
[8] Purdue University, West Lafayette, IN 47907, USA
[9] Tech-X Corporation, Boulder, CO 80303, USA
[10] University of California, Los Angeles, CA 90095, USA
[11] Center for Free-Electron Laser Science, 22607 Hamburg, Germany
[12] Universität Bern, Switzerland
[13] Nat. Tsing Hua University, Taiwan
[14] Los Alamos National Laboratory, USA
[15] Universität Hamburg, 22761 Hamburg, Germany

Abstract

Dielectric Laser Acceleration (DLA) achieves the highest gradients among structure-based electron accelerators. The use of dielectrics increases the breakdown field limit, and thus the achievable gradient, by a factor of at least 10 in comparison to metals. Experimental demonstrations of DLA in 2013 led to the Accelerator on a Chip International Program (ACHIP), funded by the Gordon and Betty Moore Foundation. In ACHIP, our main goal is to build an accelerator on a silicon chip, which can accelerate electrons from below 100 keV to above 1 MeV with a gradient of at least 100 MeV/m. For stable acceleration on the chip, magnet-only focusing techniques are insufficient to compensate the strong acceleration defocusing. Thus spatial harmonic and Alternating Phase Focusing (APF) laser-based focusing techniques have been developed. We have also developed the simplified symplectic tracking code DLAtrack6D, which makes use of the periodicity and applies only one kick per DLA cell, which is calculated by the Fourier coefficient of the synchronous spatial harmonic. Due to coupling, the Fourier coefficients of neighboring cells are not entirely independent and a field flatness optimization (similarly as in multi-cell cavities) needs to be performed. The simulation of the entire accelerator on a chip by a Particle In Cell (PIC) code is possible, but impractical for optimization purposes. Finally, we have also outlined the treatment of wake field effects in attosecond bunches in the grating within DLAtrack6D, where the wake function is computed by an external solver.

INTRODUCTION

The Accelerator on a Chip International Program (ACHIP) [1], funded by the Gordon and Betty Moore Foundation in the period between 2015 and 2020, aims to explore Dielectric Laser Acceleration (DLA). This nascent acceleration scheme provides the highest gradients among structure-based (non-plasma, non-vacuum, etc.) electron accelerators and thus allows reduction of the size of high energy electron accelerators significantly. The principle of DLA relies on the inverse Smith-Purcell (or the inverse Cerenkov effect) and was first proposed in 1962 [2, 3]. In 2013, the accel-

* niedermayer@temf.tu-darmstadt.de

ISBN: 978-3-95450-200-4 doi:10.18429/JACoW-ICAP2018-MOPLG03

SPIN DYNAMICS IN MODERN ELECTRON STORAGE RINGS: COMPUTATIONAL AND THEORETICAL ASPECTS

Klaus Heinemann*, Oleksii Beznosov, James A. Ellison, UNM, Albuquerque, NM, USA
Desmond P. Barber[1], DESY, Hamburg, Germany
Daniel Appelö, University of Colorado, Boulder, CO, USA
[1] also at UNM, Albuquerque, NM, USA

INTRODUCTION

In this presentation we describe some numerical and analytical results from our work on the spin polarization in high energy electron storage rings aimed towards the proposed Future Circular Collider (FCC-ee) and the proposed Circular Electron Positron Collider (CEPC). Photon emission in synchrotron radiation imparts a stochastic element ("noise") into particle motion and there are also damping effects. However, instead of considering single particles it is often convenient to model the stochastic photon emission as a Gaussian white noise process and to then study the evolution of the particle density in phase space with a Fokker-Planck equation.

The noise in trajectories together with the spin-orbit coupling embodied in the Thomas-BMT equation of spin precession [1], can cause spin diffusion and thus depolarization. On the other hand photon emission can lead to a build up of polarization via spin flip. This is the Sokolov-Ternov process [2]. The attainable polarization is the outcome of the balance of the two effects.

So far, analytical estimates of the attainable polarization have been based on the so-called *Derbenev-Kondratenko formulas* [3, 4]. In analogy with studies of the trajectories of single particles, that approach leans towards the study of single spins and relies in part on plausible assumptions grounded in deep physical intuition. However, just as with particle motion it would be convenient to have a treatment of the Fokker-Planck (F-P) kind and thereby minimize the reliance on assumptions. But the polarization at a point in phase space cannot be handled in that way since polarization is not a density. Nevertheless a density is available, namely the density in phase space of the spin angular momentum and with this there is a generalization of the F-P equation which we call the Bloch equation. We use that name to reflect the analogy with equations for magnetization in condensed matter [5]. In fact the Bloch equation works with the so-called *polarization density*. This is proportional to the spin angular momentum density per particle in phase space. With this we can calculate the polarization vector of the bunch.

Thus we study the initial value problem of what we call the full Bloch equation (FBE). The FBE takes into account non spin-flip and spin-flip effects due to synchrotron radiation including the spin-diffusion effects and the Sokolov-Ternov effect with its Baier-Katkov generalization. The FBE was introduced by Derbenev and Kondratenko in 1975 [6] as a generalization to the whole phase space (with its noisy trajectories) of the Baier-Katkov-Strakhovenko (BKS) equation which just describes the evolution of polarization by spin flip along a single trajectory [7]. The FBE is a system of three F-P equations coupled by a Thomas-BMT term and the BKS terms but uncoupled within the F-P terms. By neglecting the spin flip terms in the FBE we obtain what we call the reduced Bloch equation (RBE). The RBE approximation is sufficient for computing the physically interesting depolarization time and it shares the terms with the FBE that are challenging to discretize. Thus, here we only consider the discretization of the RBE.

Our approach has three parts. First we approximate the RBE analytically using the method of averaging, resulting in an average RBE which allows us to use large time steps. The minimum length of the time interval of interest is of the order of the orbital damping times. Secondly, the phase space coordinates of the average RBE come in $d = \{1, 2, 3\}$ pairs of polar-radial coordinates that we discretize using a Fourier-Chebyshev pseudospectral approach. The averaging decouples the parabolic and mode coupling terms allowing for a parallel implementation with only local communication. Thirdly, we further exploit the decoupling by evolving the resulting system of ODEs by an implicit-explicit (ARK) method. Parabolic operators are treated implicitly and can be inverted rapidly due to the decoupling. If each of the d angle variables is discretized on a grid of M grid points and if each of the d radial variables is discretized on a grid of N grid points then the total number of operations for each time step scales, to leading order, as $O(N^{dq}M^d)$ where $1 \leq q \leq 3$, depending on the algorithms used for the linear solve. For Gaussian elimination $q = 3$. Details and more results have been presented in this meeting by O.Beznosov, see [8].

The main issues for very high energy rings like the FCC-ee and CEPC are: (i) Can one get polarization, (ii) what are the theoretical limits of the polarization? We believe that the FBE offers a more complete starting point for very high energy rings than the Derbenev-Kondratenko formulas. See [9] for a recent review of polarization history and phenomenology.

RBE IN LAB FRAME

In a semiclassical probabilistic description of an electron bunch the spin-orbit dynamics is described by the *spin*-1/2 *Wigner function* (also called the *Stratonovich function*) ρ

* Corresponding author: heineman@math.unm.edu

ISBN: 978-3-95450-200-4 doi:10.18429/JACoW-ICAP2018-MOPAF02

REALISTIC MODELING OF THE MUON $g-2$ EXPERIMENT BEAMLINES AT FERMILAB*

D. A. Tarazona†, M. Berz, K. Makino, Michigan State University, East Lansing, MI, USA
D. Stratakis, M. J. Syphers[1], Fermi National Accelerator Laboratory, Batavia, IL, USA
[1]also at Northern Illinois University, DeKalb, IL, USA

Abstract

The main goal of the Muon $g-2$ Experiment at Fermilab (E989) is to measure the muon anomalous magnetic moment (a_μ, also dubbed as the "anomaly") to unprecedented precision. This new measurement will allow to test the completeness of the Standard Model (SM) and to validate other theoretical models beyond the SM. Simulations of the beamlines from the pion production target to the entrance of the $g-2$ Storage Ring (SR) using COSY INFINITY [1] contribute to the understanding and characterization of the muon beam production in relation to the statistical and systematic uncertainties of the E989 measurement. The effect of nonlinearites from fringe fields and high-order contributions on the beam delivery system performance are considered, as well as interactions with the beamline elements apertures, particle decay channels, spin dynamics, and beamline misalignments.

INTRODUCTION

The most recent measurement of a_μ at the Brookhaven National Laboratory Muon $g-2$ Experiment (E821) yielded an experimental relative uncertainty of 0.54 ppm, which differs from current SM predictions by about 3.7σ [2]. In contrast to E821, the goal of E989 is to deliver a measurement of the anomaly to a precision of 0.14 ppm or less to reach $> 5\sigma$ discrepancy with the SM and therefore strongly establish evidence for new physics.

For that purpose, the number of recorded muon decays in the $g-2$ storage ring at E989 is required to increase by a factor of 20 with respect to E821. The Fermilab Muon Campus E989 beam delivery system (BDS), which is a set of 1 km-long beamlines between the pion-production target and the entrance of the storage ring downstream, is designed to meet the statistical goal and deliver $(0.5\text{–}1.0)\times10^5$ muons to the storage ring per 10^{12} protons interacting with the pion-production target.

On the other hand, the relative statistical uncertainty in the experimental a_μ is inversely proportional to the muon beam polarization (see [2], Eq. (16.6)). Thus, it is worth to study the effect of nonlinearities and perform spin dynamics simulations. In addition, due to the momentum acceptance of about ±0.5% of the storage ring it is of interest to numerically evaluate the dynamical properties of the muon beam as it is delivered to the muon storage ring.

Motivated by the reasons exposed above, we have developed a model of the E989 beamlines to reproduce numerical simulations of the muon beam's statistical performance and dynamical behavior including spin using COSY INFINITY. This program prepares detailed high-order transfer maps calculated with an 8th order Runge-Kutta integrator and Differential-Algebraic (DA) methods to solve the beam optics Ordinary Differential Equations (ODEs) and perform beam tracking. In particular, we present results from tracking of secondary protons, pions, daughter muons from pion decay, and muons produced right at the entrance of the E989 beamlines downstream the pion-production target. Nonlinear effects due to standard fringe fields, up to 4th-order beam dynamics, spin dynamics, beam collimation, and misalignments of the multiple BDS beamline elements are considered.

The paper begins with a brief description of the Muon Campus E989 beam delivery system. Then details of the beam dynamics simulations throughout the E989 beamlines from the production target to the storage ring entrance and beam performance results considering nonlinear effects are discussed.

E989 BEAM DELIVERY SYSTEM (BDS)

The main purpose of the E989 beamlines considered in simulations, depicted in Figure 1, is to deliver a clean muon beam with momentum $p_0 = 3094\,\text{MeV}/c$ to the storage ring. Batches of four bunches made of 10^{12} protons each are directed to an Inconel-600 "pion-production" target located at the AP0 target hall, from which positive secondary particles emerge. 30 cm downstream the target, a 232 T/m magnetic gradient produced by a lithium lens focuses the secondaries. Thereafter, a pulsed magnet with a field of 0.53 T selects $3.115\,\text{GeV}/c$ ±10% positive particles and bends them 3° towards the 50 m long M2 line, which consists of matching quadrupoles followed by eight more quadrupoles and a dipole that horizontally bends the beam 3° to match with the M3 line (230 m long).

The M3 line is made of FODO cells that maintain small beta functions to provide continuity of pions and daughter muons from pion decay. By the end of M3, the secondary beam is mainly composed of protons that do not interact with the target, pions that need more time to decay, and muons. In order for such beam to become a clean muon beam, the M3 line is aligned with the injection leg of the Delivery Ring (DR) for which horizontal bends deviate the beam to the right by about 18° at $s \sim 160$ m away from the target (s represents the longitudinal distance). At the end of M3, a series of magnets involving a C-magnet, a pulsed magnetic

* Fermilab report: FERMILAB-CONF-18-620-APC.
† Email: tarazona@msu.edu. ORCID: 0000-0002-7823-7986.

ISBN: 978-3-95450-200-4 doi:10.18429/JACoW-ICAP2018-MOPAF03

POLARIZATION LIFETIME IN AN ELECTRON STORAGE RING, AN ERGODIC APPROACH IN eRHIC EIC*

F. Méot, BNL C-AD, Upton, NY, USA

Abstract

Electron polarization in a storage ring is subject to two long-term effects: Sokolov-Ternov polarization and depolarization by diffusion. Over a long time scale this leads to an equilibrium state and, simulation-wise, can be highly CPU time and memory consuming. Simulations aimed at determining optimal ring storage energy in an electron-ion collider use to track thousand particle bunches, for a long time—yet still short compared to depolarization time scales, due to HPC limitations. Based on considerations of ergodicity of electron bunch dynamics in the presence of synchrotron radiation, tracking a single particle instead is investigated. This allows substantial saving in teh required HPC volume, "CPU-time × Memory-allocation". The concept is illustrated with polarization lifetime and equilibrium polarization simulations at the eRHIC electron-ion collider.

INTRODUCTION

The eRHIC installation is briefly described in Fig. 1 [1]. The 18 GeV eRHIC electron storage lattice used in the present spin polarization simulations has been provided by S. Tepikian [1], optical parameter values relevant to the present simulations will be introduced in due place. The eRHIC lattice includes a double non-planar rotator system (Fig. 2) at the interaction point (IP), comprised of strong solenoids and series of bends, which allows to locally move the stable spin precession direction $\vec{n}_0$, from vertical in the arcs to longitudinal at the IP. In a defect-free ring, this region of off-vertical $\vec{n}_0$ is a major contribution to spin diffusion.

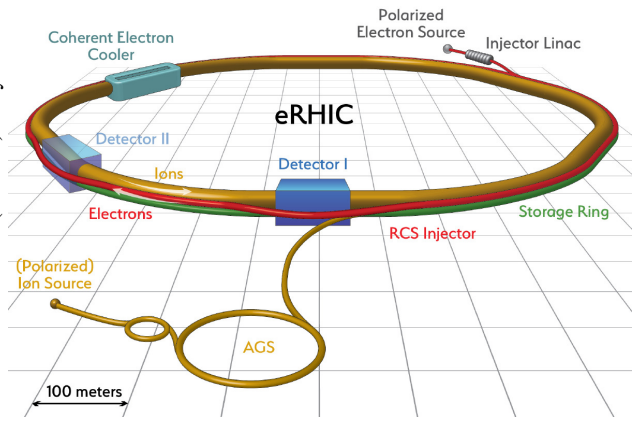

Figure 1: The eRHIC electron-ion collider complex, an 18 GeV–255 Gev/nucleon electron-ion collider installation.

Bunches are injected in the storage ring with alternately up and down polarization, and replaced every 6 min in order to ensure an average polarization of 70% over the hundreds of bunches stored [1]. A proper lattice should maintain bunch depolarization below 20% (absolute) over the 6 min storage. The evolution of the polarization, from $P_0 = \pm 0.85$ at injection to P_{eq} at equilibrium (an asymptotic quantity to be determined), satisfies

$$P(t) = P_{eq}(1 - e^{-t/\tau_{eq}}) + P_0 e^{-t/\tau_{eq}}. \quad (1)$$

This results from (i) synchrotron-radiation (SR) self-polarization and (ii) polarization loss by diffusion, with time constant τ_D, such that

$$1/\tau_{eq} = 1/\tau_{SP} + 1/\tau_D \quad (2)$$

Sokolov-Ternov (ST) self polarization in a flat ring has a time constant $\tau_{ST[sec.]} \approx 99\rho^2_{[m]}R_{[m]}/E^5_{[GeV]}$ [2], about 30 min at eRHIC at 18 GeV, 10 hrs at 10 GeV, with asymptotic value $P_{ST} = 92.4\%$; the asymptotic self-polarization is taken instead $P_{SP} = 90\%$ here to account for the non-planar spin rotator, and with time constant τ_{SP}, such that [2]

$$P_{eq} = P_{SP} \times \tau_{eq}/\tau_{SP}. \quad (3)$$

The goal in tracking spin motion is (i) to validate a ring design, including preservation of polarization under the effect of defects, corrections, etc. and (ii) to determine an optimal working point $a\gamma_{ref}$ ($a = 1.15965 \times 10^{-3}$ is the electron anomalous magnetic moment).

In the following, a method based on single-particle tracking is discussed. First, basic aspects of the stochasticity of particle and spin motions are recalled. Then tracking outcomes are displayed and the single-particle method is discussed.

The numerical simulations discussed in this paper have strongly benefited from NERSC means and environment [3].

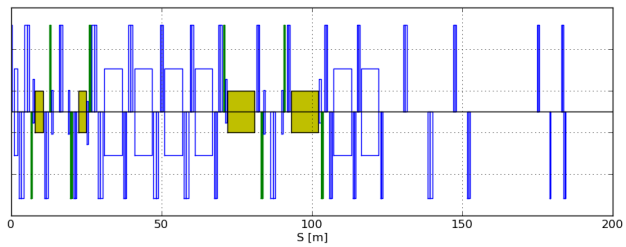

Figure 2: Half of the spin rotator system at eRHIC (the system is symmetric with respect to the IP, at the origin here). In green: solenoids.

STOCHASTIC MOTION

The dynamical system of a high energy stored electron bunch at equilibrium is ergodic: over a long time interval, trajectories in the system cover all parts of the 6D phase space.

* Work supported by Brookhaven Science Associates, LLC under Contract No. DE-AC02-98CH10886 with the U.S. Department of Energy

ISBN: 978-3-95450-200-4 doi:10.18429/JACoW-ICAP2018-MOPAF04

SPIN DYNAMICS IN MODERN ELECTRON STORAGE RINGS: COMPUTATIONAL ASPECTS

Oleksii Beznosov*, James A. Ellison, Klaus A. Heinemann, UNM, Albuquerque, NM, USA
Desmond P. Barber[1], DESY, Hamburg, Germany
Daniel Appelö, University of Colorado, Boulder, CO, USA
[1] also at UNM, Albuquerque, NM, USA

INTRODUCTION

In [1] we report on our spin/polarization project for understanding the possibility of polarization for the next generation of the high energy particle (HEP) accelerators, e.g., the Future Circular Collider (FCC) and Circular Electron Positron Collider (CEPC). The physics background and the basic model to compute the polarization is discussed there. The starting point is what we call the full Bloch equation (FBE) in the Lab frame. This model includes synchrotron radiation and the concomitant depolarization from the radiation caused by damping and diffusion as well as Sokolov-Ternov spin-flip polarization effects and its Baier-Katkov generalization. Ignoring spin flip we obtain the reduced Bloch equation (RBE) which we believe contains the most difficult part of the FBE to integrate numerically. We then introduce the 3 degree of freedom (DOF) reduced Bloch equation (RBE) in the beam frame in the first section below. We further discuss the general computational issues and give an estimates for what can be done with current computational techniques. For $d = \{1, 2, 3\}$ DOF the polarization density has $(2d + 1)$ independent variables. For simplicity, suppose that each of the space-like variables has been discretized on a grid with N grid-points, then the computational cost of each time step will scale no better than $O(N^{2d})$. The presence of parabolic terms in the governing equations necessitates implicit time stepping and thus solutions of linear systems of equations. For a fully coupled 3 DOF problem this will bring the per time step cost to $O(N^{6q})$, with $1 \leq q \leq 3$, depending on the algorithms used for the linear solve. However, only algorithms with $q \approx 1$ are feasible (for Gaussian elimination $q = 3$). Fortunately, as we outline below, the structure of the averaged equations (e.g the parabolic terms are uncoupled from mode coupling terms) allows the efficient parallel implementation. Further, we exploit the decoupling by evolving the resulting ODE system with the additive Runge-Kutta (ARK) method. Described in [2] ARK methods are high order semi-implicit methods that are constructed from a set of consistent Runge-Kutta (RK) methods. In the RBE the parabolic part of the equation is treated with a diagonally implicit RK method (DIRK) and the hyperbolic mode coupling part is treated with an explicit RK (ERK) method which does not require a linear solve. The ODE system in time can be evolved independently for each Fourier mode resulting in a computational cost for each timestep that scales as $O(N^{3q})$ per mode.

We first summarize the 3 DOF problem and 2 DOF problem from [1]. Then we describe the new algorithm on the example of 1 DOF model with parameters taken from the Hadron-Electron Ring Accelerator (HERA). Using that the RBE in 1 DOF can be solved exactly we demonstrate the accuracy of the algorithm by compering the exact polarization to the polarization measured by integrating the numerical solution in space. Further, we present the results showing that achieved accuracy of the algorithm for the polarization density after 1500 turns for varying discretization parameters which allows us to conclude that the algorithm is feasible for the accurate simulation of the 3 DOF model.

* Corresponding author: obeznosov@unm.edu

RBE IN 3 DEGREES OF FREEDOM

Consider the system of Langevin equations for the orbital phase space variable $Y \in \mathbb{R}^6$ and the spin variable $\vec{S}$ in the beam frame given by

$$Y' = \mathcal{A}(\theta)Y + \sqrt{\varepsilon}\sqrt{\omega(\theta)}e_6\xi(\theta), \tag{1}$$

$$\vec{S}' = \Omega_Y(\theta, Y)\vec{S}. \tag{2}$$

Here θ is the accelerator azimuth and ξ is a version of the white noise process and $e_6 = (0, 0, 0, 0, 0, 1)^T$. Also $\mathcal{A}(\theta)$ is a 6×6 matrix encapsulating radiationless motion and the deterministic effects of synchrotron radiation (see, e.g., [3, eq. 5.3]). Moreover $\Omega_Y(\theta, Y)$ in the Thomas-BMT term is a skew-symmetric 3×3 matrix linear in Y and $\omega(\theta)$ is real valued. Note also that $\mathcal{A}(\theta)$, $\Omega_Y(\theta, y)$ and $\omega(\theta)$ are 2π-periodic in θ.

The RBE for the polarization density $\vec{\eta}_Y$ is

$$\partial_\theta \vec{\eta}_Y = (L_Y + L_{Y,TBMT})\vec{\eta}_Y, \tag{3}$$

where

$$L_Y = \overbrace{-\sum_{j=1}^{6} \partial_{y_j}\left(\mathcal{A}(\theta)y\right)_j}^{\text{Drift}} + \overbrace{\frac{1}{2}\omega_Y(\theta)\partial_{y_6}^2}^{\text{Diffusion}},$$

$$L_{Y,TBMT}\vec{\eta}_Y = \underbrace{\Omega_Y(\theta, y)\vec{\eta}_Y}_{\text{Spin}}.$$

Our ultimate aim is to understand the solutions of (3). The main quantity of interest is the polarization of the bunch

$$\vec{P}(\theta) = \int \vec{\eta}_Y(\theta, y)dy.$$

However, as noted in the introduction, numerical discretization of (3) will have the an enormous computational cost. To simplify the problem we first use the method of averaging.

ISBN: 978-3-95450-200-4 doi:10.18429/JACoW-ICAP2018-MOPAF05

APPROACHES TO OPTIMIZING SPIN TRANSMISSION IN LATTICE DESIGN

V. H. Ranjbar*, BNL, Upton, USA

Abstract

We present our experiences in optimizing the proposed Rapid Cycling Synchrotron (RCS) injector for the eRHIC Storage ring and the RHIC 2017 lattice. We have developed a Python code to drive lattice calculations in MADX [1] which are then used to calculate spin resonances using the DEPOL algorithm [2]. This approach has been used to minimize intrinsic spin resonances during the RCS acceleration cycle while controlling lattice parameters such as dispersion and beta functions. This approach has also been used to construct localized imperfection bumps using a spin response matrix and the singular valued decomposition (SVD) algorithm. It has also been used to reduce interfering intrinsic spin resonances during the RHIC acceleration ramp.

INTRODUCTION

The design of lattices to transport beam with minimal polarization loss requires special attention to the potential sources of depolarizing spin resonances. In the past accelerators where usually optimized initially without consideration of their spin effects. Later careful spin matching and harmonic bumps were applied to reduce the effects of the various spin resonances. These were usually performed by using simple analytical estimates which were then verified using more exact numerical calculations using codes like DEPOL [2]. However the process was slow and decoupled from the optics calculations since for small perturbations the optic changes were assumed to be small. Later the use of full and partial snakes reduced the need to worry as much about the strength of the spin resonances.

However experience with the full snakes in RHIC and partial snakes in the AGS have shown that optimizing the underlying spin resonances can still have an important impact on the performance of the lattice even with snakes. For example the overlap of minor spin resonances during strong spin resonances crossings has been shown to reduce polarization transmission on the RHIC ramp [3].

Also in the design of a future high energy polarized electron injector for the proposed eRHIC facility, snakes are not a viable option due to the large orbit excursion and radiative effects they induce in lighter particles. So a new design has been developed which exploits high periodicity to avoid spin depolarizing resonances [4]. This new design required optimizing for both the beam dynamics and polarization transmission.

We have developed a Python code which we call SOptim [5], to perform these types of optimizations. It uses MADX [1] as an optics calculator and performs its own DEPOL calculations across a specified range of spin resonances. It then varies the magnet strengths, usually quadrupoles, or vertical corrector magnets to achieve a desired spin resonance structure and optics.

* vranjbar@bnl.gov

SOptim CODE STRUCTURE

The core of the code is a function which takes the name of a MADX sequence file, a string containing the names of the magnets to be varied, and a vector of associated magnet strengths. These are read together with the anomalous G factor, emittance and a switch to indicate if an intrinsic or imperfection spin resonance calculations are to be performed.

This function then feeds the sequence and new magnet strengths to MADX and takes back the optics and orbit information which is then used to perform a native spin resonance calculation following the DEPOL algorithm. These are done for a currently hard coded range of spin resonance energies.

The function returns an array of spin resonance strengths, twiss parameters, dispersion values and a flag indicating if the twiss calculation failed or not, as well as a MADX readable string containing the magnet settings used. This string is saved once the optimization is completed so that it can be easily included in future MADX calculations.

The values for the spin resonances and optics values are then combined with various weights to produce an overall penalty function. This penalty function is then iterated upon using Scipy's [6] minimize function which is part of its optimize library. The minimize function can use a variety of optimizers and takes bounds for the magnet settings.

Alternatively it is possible to construct spin response matrix which relates the spin resonance strengths to the magnet settings. One can invert this using a pseudo inverse to either suppress of generate spin resonance 'bumps'.

RHIC LATTICE OPTIMIZATION

Studies of polarization transport with two orthogonal snakes during the RHIC acceleration ramp revealed the importance of interfering spin resonances [3]. For example during the crossing of the strongest intrinsic spin resonance at $G\gamma = 422.685$ it was found that the weak spin resonance located at $G\gamma = 423.325$ plays an important role in determining the total polarization transmission. As is shown in Figs. 1 and 2 it was shown that minimizing this can improve the total spin transmission. We used the SOptim code to reduce these neighboring resonances. The results from spin-orbit 6D tracking are shown in Fig. 3, where the polarization transmission versus emittance is greatly expanded. Similar optimization was applied around the three major spin resonances at $G\gamma = 422.685, 382.325$, and 260.685 for both the Blue and Yellow RHIC rings.

ISBN: 978-3-95450-200-4 doi:10.18429/JACoW-ICAP2018-MOPAG01

PLASMA WAKEFIELD START TO END ACCELERATION SIMULATIONS FROM PHOTOCATHODE TO FEL WITH SIMULATED DENSITY PROFILES*

A. Marocchino†, E. Brentegani, A. Biagioni, E. Chiadroni, M. Ferrario,
A. Giribono, F. Filippi, R. Pompili, C. Vaccarezza, INFN-LNF, Frascati, Italy
A. Cianchi, University of Rome Tor Vergata, Rome, Italy
A. Bacci, A. R. Rossi INFN Milano, Milano, Italy
V. Petrillo, Università di Milano, Milano, Italy

Abstract

Plasma Wakefield acceleration is a promising new acceleration technique that profits by a charged bunch, e.g. an electron bunch, to break the neutrality of a plasma channel to produce a wake where a trailing bunch (or witness) is eventually accelerated. The quest to achieve extreme gradient conserving high brightness has prompted to a variety of new approaches and techniques. Most of the proposed schemes are however limited to the only plasma channel, assuming in the vast majority of cases, ideal scenarios (e.g. ideal bi-gaussian bunches and uniform density plasma channels). Realistic start-to-end simulations, from the photo-cathode to FEL via a high gradient, emittance and energy spread preserving plasma section, are mandatory for paving the way towards plasma-based user facilities.

INTRODUCTION

Plasma-based accelerators (PBAs) represent, today, a new frontier for the development of compact advanced radiation sources and next generation linear colliders. High brightness electron beams are the future goal of such kind of accelerators, a new technology that is envisioned to compete with the RF technology. Since the very first conception [1] great effort (with equivalent progress) has been placed [2–8] to demonstrate the acceleration of electron beams with gradients of the order of several tens of GV/m, produced either by a laser drive (LWFA) or with a particle driven (PWFA). In PWFA the high gradient wakefield is induced by a high-energy charged particle beam (referred to as driver bunch) travelling through a pre-ionised plasma. The background electrons by shielding the charge breakup produced by the driver induce an accelerating field. The second bunch (referred to as trailing bunch or witness) placed on the right phase is so accelerated by the induced electric field [9–11].

The aforementioned publications indicate that either LWFA and PWFA are capable to produce strong accelerating gradients, but do not address the issue of beam acceleration with quality retention. In other words, the capability for a PWFA scheme to accelerate a trailing bunch with an acceptable quality for any scientific applications, such a Free Electron Laser (FEL) or a future particle-particle collider, or even for medical applications is still an open question.

The work presented in this proceeding tries to address the problem of quality bunch transport numerically for a PWFA scheme. The scheme proposed leverages on the well establish RF know-how to produce and manipulate the bunches to match the strict plasma matching requirements, so that, once injected into the plasma the trailing bunch is boosted to the desired energy. The scheme can thus be decoupled into two parts. A first stage aims in generating two electron bunches (the driver and the trailing bunch) with a given time-separation so that once injected into the plasma they will be at right phase to maximize acceleration. The generation, distance positioning and acceleration is achieved using the COMB [12] technique and an RF in the X-band regime, for a final particle energy of 500 MeV. The plasma with a 10^{16} cm^{-3} number density is confined by a millimeter diameter capillary and ionized with plasma discharges, accelerates the particles from 500 MeV to 1 GeV in about 30 cm. The particle extracted from the plasma accelerating section are then injecting into a FEL. The evolution of the beam, from the photo-injector to the FEL via the plasma cell, is performed with a *single* simulation by concatenating several codes used to addressed the different physics occurring in the different accelerating section. We refer to this single simulation as a *start-to-end* simulation. This work is part of EuPRAXIA [13, 14] (European Plasma Research Accelerator with eXcellence In Applications) European project whose final goal is to use PBA to seed a FEL for physical and biological applications. Specifically EuPRAXIA@SPARC_LAB [14] is the envisioned EuPRAXIA European Italian-located facility operating at 1–5 GeV for FEL experiments.

SECTION I: INJECTOR

A comb-like configuration for the electron beam is used to generate simultaneously a 200 pC driver followed by a 30 pC trailing bunch. The comb-like operation foresees the generation of two or more bunches within the same RF accelerating bucket through the so-called laser-comb technique [12, 15] consisting in a train of laser time-spaced pulses illuminating the photo-cathode. The witness arrives earlier than the driver on the photo-cathode and then they are reversed in time at the end of the velocity bunching process, during

* Work supported by European Union Horizon 2020 research and innovation program, Grant Agreement No. 653782 (EuPRAXIA)
† alberto.marocchino@lnf.infn.it

ISBN: 978-3-95450-200-4 doi:10.18429/JACoW-ICAP2018-MOPAG02

EFFICIENT MODELING OF LASER WAKEFIELD ACCELERATION THROUGH THE PIC CODE SMILEI IN CILEX PROJECT

Francesco Massimo*, Arnaud Beck, Imen Zemzemi, Arnd Specka
Laboratoire Leprince-Ringuet, 91128 Palaiseau, France
Julien Derouillat, Maison de la Simulation, 91191 Gif-sur-Yvette, France
Mickael Grech, Frédéric Pérez,
Laboratoire d'Utilisation des Lasers Intenses, 91128 Palaiseau Cedex, France

Abstract

The design of plasma acceleration facilities requires considerable simulation effort for each part of the machine, from the plasma injector and/or accelerator stage(s), to the beam transport stage, from which the accelerated beams will be brought to the users or possibly to another plasma stage. The urgent issues and challenges in simulation of multi-stage acceleration with the Apollon laser of CILEX facility will be addressed. To simulate the beam injection in the second plasma stage, additional physical models have been introduced and tested in the open source Particle in Cell collaborative code Smilei. The efficient initialisation of arbitrary relativistic particle beam distributions through a Python interface allowing code coupling and the self consistent initialisation of their electromagnetic fields will be presented. The comparison between a full PIC simulation and a simulation with a recently developed envelope model, which allows to drastically reduce the computational time, will be also shown for a test case of laser wakefield acceleration of an externally injected electron beam.

INTRODUCTION

Laser Wakefield Acceleration (LWFA) is a promising technique to accelerate particles with gradients order of magnitudes higher than those of metallic accelerating cavities [1–3]. A high intensity laser pulse propagating in a plasma and of length of the order of the plasma wavelength can create a cavity empty of electrons in its wake. In this "bubble", the generated high gradient wakefields are suitable for electron focusing and acceleration. The realization of the PetaWatt laser Apollon in the CILEX (Centre Interdisciplinaire Lumière EXtrême) facility [4] in France will pave the way to innovative LWFA experiments. The use of a second plasma stage of LWFA in the weakly nonlinear regime is considered, implying both experimental and modelization challenges. In this work we present new features in the Particle-in-Cell (PIC) code Smilei [5] to address the simulation challenges of the project.

The length of the first plasma stage, acting as an electron injector in nonlinear regimes, is of the order of millimeters. The length of this second stage will instead need to be at least of the order of the centimeters in order to accelerate particles at high energies with the less intense fields generated in weakly nonlinear regimes. The standard PIC technique [6] would be unfeasible for the much longer distances to simulate required by the second plasma stage. A solution to considerably reduce the computation time consists in using an envelope model for the laser pulse [7, 8]. In this approach one only needs to sample the envelope spatio-temporal scales, of the order of the plasma wavelength λ_p and frequency $\omega_p = 2\pi c/\lambda_p = c/k_p$ instead of the laser wavelength λ_0 and frequency $\omega_0 = 2\pi c/\lambda_0$. Doing so allows for a coarser, and cheaper, resolution while retaining all the relevant physics. The use of cylindrical symmetry in an envelope model, like in [9] would be unsuited for CILEX, since even a cylindrically symmetric beams exiting from the first plasma stage would be influenced by the intrinsic asymmetry in the focusing elements of the conventional transport line towards the second plasma stage. Thus, we developed a 3D completely parallelized envelope model for the laser-plasma dynamics, first implemented in the PIC code ALaDyn [10] and described in detail in [8]. In this paper, we briefly recall the envelope model's equations and the initialization of arbitrary beam phase distributions with their self-consistent electromagnetic fields, as initial conditions for a simulation (following the procedure described in [11, 12]). Both these features have been implemented in Smilei. After showing the results of two validation tests of the envelope model against analytical theory, we show an application of these two features in a Smilei simulation of a second plasma stage of LWFA.

ENVELOPE MODEL

The hypothesis of the envelope model, i.e. a shape of the laser pulse vector potential $\mathbf{A}$ given by a slowly varying complex envelope $\tilde{\mathbf{A}}$ modulated by oscillations at the laser frequency $\omega_0 = k_0 c$ can be expressed as

$$A(\mathbf{x}, t) = \mathrm{Re}[\tilde{A}\, e^{ik_0(x-ct)}]. \tag{1}$$

The laser pulse is supposed to propagate in the positive x direction. Following [8], the envelope hypothesis can be inserted in D'Alembert's Equation for the laser vector potential, obtaining the envelope equation in laboratory coordinates, solved in [8] and in Smilei:

$$\nabla\tilde{A} + 2ik_0\left(\partial_x\tilde{A} + \frac{1}{c}\partial_t\tilde{A}\right) - \frac{1}{c^2}\partial_t^2\tilde{A} = \chi\tilde{A}, \tag{2}$$

where χ is the plasma susceptibility, which takes into account the envelope modification due to the presence of the

* massimo@llr.in2p3.fr

ISBN: 978-3-95450-200-4 doi:10.18429/JACoW-ICAP2018-TUPAF01

UPGRADE OF MAD-X FOR HL-LHC PROJECT AND FCC STUDIES

L. Deniau*, A. Latina, T. Persson, I. Shreyber, P. Skowronski,
H. Burkhardt, R. De Maria, M. Giovannozzi, J.M. Jowett, F. Schmidt, CERN, Meyrin, Switzerland
T. Gläßle, HIT, Heidelberg, Germany

Abstract

The design efforts for the High Luminosity upgrade project of the Large Hadron Collider (HL-LHC) and for the FCC-ee studies required significant extensions of the MAD-X code, widely used for designing and simulating particle accelerators. The modelling of synchrotron radiation effects has recently been reviewed, improved, and tested on the lattices of ESRF, LEP, and CLIC Final Focus System. The results were cross checked with several codes, such as AT, PLACET, Geant4, and MAD8. The implementation of space charge has been deeply restructured into a fully modular design. The linear coupling calculation has been completely reviewed and improved to ensure its robustness in the presence of strong coupling effects as is the case for some HL-LHC studies. The slicing module has been generalized to allow for generating thick slices of bending magnets, quadrupoles and solenoids. The `SBEND` element has been extended to take into account not only the bending angle, but also the integrated dipole strength. Patches have been added to the list of supported elements. Finally, the PTC program inside MAD-X has been extended to provide the tracking of resonance driving terms along lattices, as well as an AC dipole element.

INTRODUCTION

MAD-X is a code to simulate beam dynamics and design beam optics, which was released in 2002. Although it has been tailored to the needs of the LHC, it still remains the most used tool for optics design inside and outside CERN. In order to extend the MAD-X capabilities to better satisfy the users' needs, in particular for the HL-LHC project and the FCC study, several new features have been implemented. An example of such a new feature is the synchrotron radiation, which has a negligible effect on the beam dynamics in the LHC, but plays a major role for the FCC-ee future collider. An element to rotate the coordinate system along the x- and y-direction has also recently been added.

Moreover, to be ready for future studies, several parts of the code and the underlying physics have been reviewed or improved. In this paper we present the clean up of space-charge code as well as of the review of the linear coupling.

An important extension to MAD-X is the Polymorphic Tracking Code (PTC) by E. Forest [1]. In this paper, some of the recently added features, including the possibility to obtain the Resonance Driving Terms (RDT) in the `PTC_TWISS` table will be presented and discussed.

* laurent.deniau@cern.ch

SYNCHROTRON RADIATION EFFECTS

The effects of synchrotron radiation were originally implemented in MAD8 for the needs of the high-energy e^+e^- collider ring LEP at CERN [2]. This implementation was ported to MAD-X and has recently been reviewed and improved. Note that the review of the implementation of synchrotron radiation emission as a quantum phenomenon revealed the presence of a bug in MAD-X versions earlier than 5.04.01. The bug was corrected and the new implementation tested in several cases.

Synchrotron radiation emission is included in the modules `TWISS`, `TRACK`, and `EMIT` at four different levels:

1. No radiation, corresponding to the usual Hamiltonian dynamics.
2. Deterministic radiation, in which all particles radiate the same energy as a single particle on the closed-orbit (`TWISS` and `TRACK`). This gives a Hamiltonian system with the correct tunes and closed orbit, including the "stable phase angle" and "energy sawtooth" in electron rings.
3. Deterministic radiation with full dependence on canonical coordinates to generate radiation damping naturally (`EMIT`, `TRACK`). Since this method exposes the full dissipative structure of the non-linear phase space dynamics, it is the preferred method for dynamic aperture calculations in high-energy lepton rings [3].
4. Tracking with individual stochastic photon emissions, to provide quantum excitation and particle distributions (`TRACK`) and equilibrium emittances from first principles. Both the probability of photon emission, i.e. an instantaneous Poisson distribution, and the generation of the random photon-energy distribution depend on the *local* magnetic field and canonical coordinates of the particle.

The MAD-X implementation has been benchmarked against MAD8 using a conversion of the LEP-optics database to the MAD-X format. Rather than attempting to reproduce old results dating from the LEP times, this conversion allowed to run equivalent simulations with MAD8 and MAD-X so that results could be compared in detail. Quantities such as radiation damping rates, equilibrium emittances, energy sawtooth, and the Bassetti component [4] of the horizontal closed orbit $x_c - D_x p_{tc}$, where x_c is the position coordinate of the closed orbit, and p_{tc} is the momentum deviation of the closed orbit, are in excellent agreement between the two codes, confirming that the physics implemented in MAD8 has been preserved in MAD-X.

In addition, MAD-X was tested against other established codes capable of dealing with particle tracking in presence

ISBN: 978-3-95450-200-4 doi:10.18429/JACoW-ICAP2018-TUPAF02

SixTrack PROJECT: STATUS, RUNTIME ENVIRONMENT, AND NEW DEVELOPMENTS*

R. De Maria†, J. Andersson, V. K. Berglyd Olsen, L. Field, M. Giovannozzi, P. D. Hermes, N. Høimyr, S. Kostoglou, G. Iadarola, E. Mcintosh, A. Mereghetti, J. Molson, D. Pellegrini, T. Persson, M. Schwinzerl, CERN, Geneva, Switzerland
E. H. Maclean, CERN, Geneva, Switzerland and University of Malta, Msida, Malta
K. N. Sjobak, CERN, Geneva, Switzerland and University of Oslo, Oslo, Norway
I. Zacharov, EPFL, Lausanne, Switzerland
S. Singh, IIT Madras, India‡

Abstract

SixTrack is a single-particle tracking code for high-energy circular accelerators routinely used at CERN for the Large Hadron Collider (LHC), its luminosity upgrade (HL-LHC), the Future Circular Collider (FCC), and the Super Proton Synchrotron (SPS) simulations. The code is based on a 6D symplectic tracking engine, which is optimised for long-term tracking simulations and delivers fully reproducible results on several platforms. It also includes multiple scattering engines for beam-matter interaction studies, as well as facilities to run integrated simulations with FLUKA and GEANT4. These features differentiate SixTrack from general-purpose, optics-design software like MAD-X. The code recently underwent a major restructuring to merge advanced features into a single branch, such as multiple ion species, interface with external codes, and high-performance input/output (XRootD, HDF5). This restructuring also removed a large number of build flags, instead enabling/disabling the functionality at run-time. In the process, the code was moved from Fortran 77 to Fortran 2018 standard, also allowing and achieving a better modularization. Physics models (beam-beam effects, RF-multipoles, current carrying wires, solenoid, and electron lenses) and methods (symplecticity check) have also been reviewed and refined to offer more accurate results. The SixDesk runtime environment allows the user to manage the large batches of simulations required for accurate predictions of the dynamic aperture. SixDesk supports CERN LSF and HTCondor batch systems, as well as the BOINC infrastructure in the framework of the LHC@Home volunteering computing project. SixTrackLib is a new library aimed at providing a portable and flexible tracking engine for single- and multi-particle problems using the models and formalism of SixTrack. The tracking routines are implemented in a parametrized C code that is specialised to run vectorized in CPUs and GPUs, by using SIMD intrinsics, OpenCL 1.2, and CUDA technologies. This contribution presents the status of the code and an outlook on future developments of SixTrack, SixDesk, and SixTrackLib.

* Research supported by the HL-LHC project
† riccardo.de.maria@cern.ch
‡ Work supported by Google Summer of Code 2018

INTRODUCTION

SixTrack [1,2] is a 6D single-particle symplectic tracking code able to compute the trajectories of individual relativistic charged particles in circular accelerators for studying dynamic aperture (DA) or evaluating the performance of beam-intercepting devices like collimators [3]. It can compute linear and non-linear optics functions, time-dependent effects, and extract indicators of chaos from tracking data. SixTrack implements scattering routines and aperture calculations to compute "loss maps", i.e., leakage from collimators as a function of longitudinal position along the ring, and collimation efficiency [4].

Different from a general-purpose code like MAD-X [5,6], SixTrack is optimised for speed and numerical reproducibility. It can be also linked with the BOINC library to use the volunteering computing project LHC@Home [7]. SixTrack studies, such as estimation of dynamic aperture of large storage rings like the Large Hadron Collider (LHC) or the Future Circular Collider (FCC), require massive computing resources, since they consist of scans over large parameter spaces for probing non-linear beam dynamics over long periods.

The SixDesk runtime environment manages SixTrack simulations from input generation, job queue management (using HTCondor or LSF in the CERN BATCH service and customised software in CERN Boinc server), to collecting and post-processing results.

SixTrackLib is a new library built from scratch in C with the main aim of offering a portable tracking engine for other codes and offloading SixTrack simulation to GPUs.

This paper summarises the main existing features of SixTrack, SixDesk and SixTrackLib and provide detail about the main development lines.

MAIN FEATURES

SixTrack tracks an ensemble of particles defined by a set of coordinates through several beam-line elements, using symplectic maps [8–10], or scattering elements.

Coordinates

The set of coordinates is larger than the minimum needed to describe the motion. Additional variables are used to store energy-related quantities used in the tracking maps

ISBN: 978-3-95450-200-4 doi:10.18429/JACoW-ICAP2018-TUPAF06

SIMULATIONS OF LONGITUDINAL BEAM STABILISATION IN THE CERN SPS WITH BLonD

J. Repond*[1], K. Iliakis, M. Schwarz, E. Shaposhnikova
CERN, Geneva, Switzerland
[1]also at École Polytechnique Fédérale de Lausanne, Switzerland

Abstract

The Super Proton Synchrotron (SPS) at CERN, the Large Hadron Collider (LHC) injector, will be pushed to its limits for the production of the High Luminosity LHC proton beam while beam quality and stability in the longitudinal plane are influenced by many effects. Particle simulation codes are an essential tool to study the beam instabilities. BLonD, developed at CERN, is a 2D particle-tracking simulation code, modelling the longitudinal phase space motion of single and multi-bunch beams in multi-harmonic RF systems. Computation of collective effects due to the machine impedance and space charge is done on a multi-turn basis. Various beam and cavity control loops of the RF system are implemented (phase, frequency and synchro-loops, and one-turn delay feedback) as well as RF phase noise injection used for controlled emittance blow-up. The longitudinal beam stability simulations during long SPS acceleration cycle (~20 s) include a variety of effects (beam loading, particle losses, controlled blow-up, double RF system operation, low-level RF control, injected bunch distribution, etc.). Simulations for the large number of bunches in the nominal LHC batch (288) use the longitudinal SPS impedance model containing broad and narrow-band resonances between 50 MHz and 4 GHz. This paper presents a study of beam stabilisation in the double harmonic RF system of the SPS system with results substantiated, where possible, by beam measurements.

INTRODUCTION

The High-Luminosity Large Hadron Collider (HL-LHC) project [1] is the next milestone at CERN for the LHC and its experiments. The linac and the three synchrotrons in the injector chain will be upgraded to enable the production of HL-LHC proton beam with a bunch intensity N_b twice that of the current setup, as specified by the LHC Injector Upgrade (LIU) project [2].

The LIU target for the SPS, the LHC injector, is to produce four batches of 72 bunches spaced by 25 ns with an intensity of 2.4×10^{11} particles per bunch (ppb), each batch separated by 225–250 ns. Large particle losses, increasing with intensity, are observed at the SPS flat bottom [3] and multi-bunch longitudinal instabilities limit the ability to increase the bunch intensity [4]. The maximum bunch length allowed for the extraction to the LHC injection is fixed at 1.9 ns with an average value along the batches of 1.65 ns.

To reach the LIU target, major upgrades are necessary. The SPS RF system will have more cavities, more power available and a better control of the beam loading through the low-level RF control loops (LLRF). Moreover, the longitudinal beam-coupling impedance of the machine will be reduced, but the baseline improvements may be insufficient to ensure beam stability at HL-LHC intensities [4]. Further impedance reduction would be useful but is limited by technical and budget considerations. Therefore, different ways of enhancing beam stability also have been investigated.

Currently, to provide a good quality beam to the LHC, a second RF system operating at 800 MHz supports the main 200 MHz RF system of the SPS. It increases the synchrotron frequency spread inside the bunch and provides more effective Landau damping of beam instabilities [5]. The longitudinal beam dynamics of the bunch train in the SPS is, in general, too complex to be treated with analytical estimations for instability growth rates in a single RF system. The double RF system and the large number of contributors to the impedance make particle tracking simulations a powerful tool in the analysis of instability mechanisms. Moreover, beam measurements in conditions close to those after LIU upgrade cannot be achieved since the present RF system is limited in power for LIU beam intensities. Predictions of future performance and longitudinal instability thresholds rely mainly on numerical simulations.

The particle tracking simulation code BLonD (Beam LONgitudinal Dynamics) [6] was used to study effects of the second RF system on beam stability and results are substantiated with beam measurements where available. In the first part of the paper we present the simulation code and the features of the SPS simulations. Then, the effects of the 800 MHz RF system on beam stability at flat top are investigated. Very promising results have been obtained in simulation at highest energy but they cannot be applied at flat bottom as explained in the third part of the publication. Finally, the goal was to find an optimum RF program for the 800 MHz RF system during the full acceleration cycle to enhance beam stability, and results are presented in the last part.

FEATURES OF PARTICLE TRACKING SIMULATIONS IN THE SPS WITH BLOND

Developed at CERN, BLonD is a 2D particle tracking simulation code, modelling the longitudinal phase space motion of single and multi-bunch beams in multi-harmonic RF systems [6]. The particle motion is tracked through a sequence of longitudinal energy kicks and drifts. The equations of longitudinal motion are discretised in time on a turn-by-turn basis with a time step equal to the revolution

* joel.repond@cern.ch

ISBN: 978-3-95450-200-4 doi:10.18429/JACoW-ICAP2018-TUPAF08

A FULL FIELD-MAP MODELING OF CORNELL-BNL CBETA 4-PASS ENERGY RECOVERY LINAC*

F. Méot†, N. Tsoupas, S. Brooks, D. Trbojevic, BNL C-AD, Upton, NY, USA
J. Crittenden, Cornell University (CLASSE), Ithaca, NY, USA

Abstract

The Cornell-BNL Electron Test Accelerator (CBETA), a four-pass, 150 MeV energy recovery linac (ERL), is now in construction at Cornell. Commissioning will commence in March 2019. A particularity of CBETA is that a single channel loop recirculates the four energies (42, 78, 114 and 150 MeV). The return loop arcs are based on fixed-field alternating gradient (FFAG) optics. The loop is comprised of 107 quadrupole-doublet cells, built using Halbach permanent magnet technology. Spreader and combiner sections (4 independent beam lines each) connect the 36 MeV linac to the FFAG arcs. We introduce here to a start-to-end simulation of the 4-pass ERL, entirely, and exclusively, based on the use of magnetic field maps to model the magnets.

INTRODUCTION

The Cornell-BNL Electron Test Accelerator (CBETA), a four-pass, 150 MeV energy recovery linac (ERL), is now in construction at Cornell. A particularity of CBETA is in its single channel loop recirculating four energies, 42, 78, 114 and 150 MeV, four-pass up, four-pass down. The return loop arcs (FA-TA and TB-FB sections, Fig. 1) are based on fixed-field alternating gradient (FFAG) optics. The loop is comprised of 107 quadrupole-doublet cells, built using Halbach permanent magnet technology. Spreader (SX) and combiner (RX) sections (4 independent beam lines each) connect the 36 MeV linac to the FFAG arcs. This paper introduces to a start-to-end simulation of the 4-pass ERL, entirely, and exclusively, based on the use of magnetic field maps to model the magnets, now under development in view of the commissioning of CBETA which will commence in March 2019.

The OPERA field maps of the return loop Halbach magnets are produced at BNL. The OPERA field maps of most of the spreader and combiner line conventional electro-magnets are produced at Cornell.

Why Use Field Maps?

There is a variety of reasons for that:

- All necessary material is available or will soon be: the return loop Halbach magnet field maps have been produced during the design [1], the spreader and combiner section conventional magnet field maps (dipoles and quadrupoles) are under production. Thus, as it yields highest simulation accuracy, why not just do it? And, in passing, forget about questionable mapping approximations.
- FFAG experience dictates to do so: as early as in the 1950s, Frank Cole wrote on the virtues of the use of field maps and Runge-Kutta ray-tracing in designing and operating the MURA scaling FFAG rings [3]:
  "[...] digital computation to explore nonlinear problems in spiral-sector orbits. This was not done by mapping in the usual sense of the term, but by step-by step integration of the equations of motion, using the fourth-order Runge-Kutta method. It was a marvelous productive year for the [MURA] group.";
  Kyushu University and KURRI 150 MeV scaling FFAG proton rings (amongst others in Japan) were designed, and are operated, using 3D OPERA field maps of the cell dipoles [4]; the RACCAM spiral FFAG dipole constructed and measured in 2009 was designed and optimized, successfully, based on field map simulations [5–7]; the optics of the EMMA linear FFAG ring accelerator at Daresbury (CBETA arc cell is similar to EMMA's) was studied using OPERA field maps of its QF-QD cell magnets [8].
- Using field maps yields closest-to-real-life modeling of the Halbach doublets return loop, over the all 8 passes (4 accelerated, 4 decelerated).

Now, the method must be validated. This will be discussed here and includes showing the feasibility of

- using separate field maps, especially of the QF and BD focusing quadrupole and combined function defocusing dipole in the return loop,
- including field overlapping between neighboring magnets, all along the return loop,
- and accounting for iron yoke corrector magnets superimposed on the Halbach magnets.

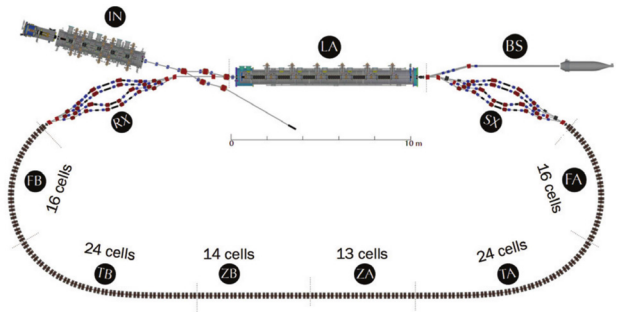

Figure 1: CBETA 150 MeV ERL [2]. The linac is 36 MeV, four different energies circulate concurrently in the single-channel return loop: 42, 78, 114 and 150 MeV (hence, 4 spreader (SX) and recombiner lines (RX), at linac downstream and upstream ends, respectively).

* Work supported by Brookhaven Science Associates, LLC under Contract No. DE-AC02-98CH10886 with the U.S. Department of Energy
† fmeot@bnl.gov

ISBN: 978-3-95450-200-4 doi:10.18429/JACoW-ICAP2018-TUPAF09

MULTI PASS ENERGY RECOVERY LINAC DESIGN WITH A SINGLE FIXED FIELD MAGNET RETURN LINE*

D. Trbojevic†, J. Scott Berg, Stephen Brooks, Francois Meot, Nicholaos Tsoupas
BNL, Upton, NY, USA
William Lou, Cornell University (CLASSE), Ithaca, NY, USA

Abstract

We present a new approach of the Energy Recovery Linac Design for the future projects: PERLE (Powerful Energy Recovery Linac for Experiments), LHeC/FCCeH and eRHIC. The concept uses superconducting linacs and a single fixed field beam line with multiple energy passes of electron beams. This represents an update to the existing CBETA (Cornell University Brookhaven National Laboratory ERL Test Accelerator) where the superconducting linac uses a single fixed field magnet beam line with four energy passes during acceleration and four passes during the energy recovery. To match the single fixed field beam line to the linac the CBETA uses the spreaders and combiners on both sides of the linac, while the new concept eliminates them. The arc cells from the single fixed field beam line are connected to the linac with adiabatic transition arcs wher cells increase in length. The orbits of different energies merge into a single orbit through the interleaved linac within the straight sections as in the CBETA project. The betatron functions from the arcs are matched to the linac. The time of flight of different electron energies is corrected for the central orbits by additional correction magnet controlled induced beam oscillations.

INTRODUCTION

The Energy Recovery Linacs (ERLs) and Recirculating Linacs (RAL) are considered to be a part of the future Electron Ion Colliders in several world programs: LHeC (CERN) [1], FCC eh [2], eRHIC(BNL) [3], ELIC (Jefferson Lab) [4] and EIC@HIAF (China) [5]. A proposal presented in this report describes a solution of ERL where the electron beam is brought back to the linac with a single large energy acceptance beam line using a concept of linear fixed field alternating (FFA) gradient. The concept of the FFA beam transport with large momentum acceptance is not a novelty. There are three experimentally confirmed proof-of-principles: EMMA-Electron Model for Many Applications [6], ATF (Accelerator Test Facility) [7] experiment with 12 FFA cells, and Fractional Arc Test of the Cornell University-Brookhaven National Laboratory ERL Test Accelerator-CBETA [8]. A comparison of these three examples are compiled and shown by Stephen Brooks [9] in Fig. 1 and in Table 1.

We present a new concept of the ERLs where the large momentum acceptance linear FFA magnet beam lines bring the electron beam back to the superconducting linac without spreaders and combiners. In multiple passes through the ERLs the acceleration of electrons generated by the linac is too fast to consider any return beam line by using fast cycling magnets. With the large momentum acceptance linear FFA gradient magnets this can be achieved. The first test of the concept will be achieved in 2019 by the ERL CBETA at Cornell University. There are many advantages and simplifications: 1) the replacement of multiple returning beam lines with a single beam line reduces the cost and complications; 2) established technology of the Halbach type permanent magnets used at CBETA project will confirm the reduction of cost and simplification of the beam lines; the magnet aperture remains to be very small while transporting multiple energy beams. In the present study the superconducting linac is made of 5-6 cavity cells, each separated with small permanent FFA triplets. The same type of triplet cells con-

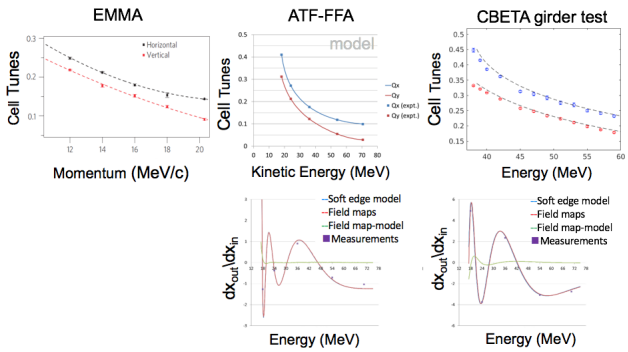

Figure 1: Comparisons on tune dependence on Energy in the three FFA examples.

Table 1: EMMA-ATF-CBETA Comparisons

Parameter	EMMA	ATF-FFA	CBETA girder	CBETA Future
Energy (MeV)	10–20	18–71	37.5–59	41–150
Mom. ratio	1.953	3.837	1.553	3.572
ρ of curv. (m)	2.637	2.014	5.0879	5.0879
Avrg. dip. (T)	0.026	0.118	0.0983	0.0983
Total angle (°)	360.0	40.0	20.0	280.0
Oper. mode	ring	Tr. line	Tr. Line	ERL
Acceleration?	YES	none	none	linac
Lattice	Doublet	~FODO	Doublet	Doublet
Cell Length (m)	0.395	0.234	0.444	0.444
Cell per turn	42	54	72	107.5
Length (m)	16.57	1.406	1.776	47.73

* Work supported by Work performed under Contract Number DE-AC02-98CH10886
† dejan@bnl.gov

ISBN: 978-3-95450-200-4 doi:10.18429/JACoW-ICAP2018-TUPAF10

EXPERIENCE WITH CBETA ONLINE MODELING TOOLS

C. Gulliford, D. Sagan, A. Bartnik, J. Dobbins, Cornell University, Ithaca, NY, USA
J. S. Berg, BNL, Upton, Long Island, New York, USA,
Antonett Nunez-delPrado, Department of Physics, University of Central Florida

Abstract

The Cornell-Brookhaven CBETA machine is a four pass Energy Recovery Linac (ERL) with a Non-scaling Fixed-Field Alternating gradient (NS-FFA) arc. For online modeling of single particle dynamics in CBETA, a customized version of the Tao program, which is based upon the Bmad toolkit, has been developed. This online program, called CBETA-V, is interfaced to CBETA's EPICS control system. This paper describes the online modeling system and initial experience during machine running.

INTRODUCTION

The Cornell-Brookhaven Energy recovery linac Test Accelerator (CBETA) [1], currently under construction at Cornell University, is a 4-pass, 150 MeV Energy Recovery Linac (ERL), utilizing a Non-Scaling Fixed Field Alternating-gradient (NS-FFA) permanent magnet return loop. CBETA is a joint collaboration of Brookhaven National Laboratory (BNL) and the Cornell Laboratory for Accelerator based Sciences and Education (CLASSE).

The CBETA project builds on the significant advancements in high-brightness photoelectron sources and Superconducting RF (SRF) technology developed at Cornell [2–5], as well as the FFA magnet and lattice design expertise from BNL. One aim of CBETA is to establish the operation of a multi-turn SRF based ERL utilizing a compact FFA return loop with large energy acceptance (a factor of roughly 3.6 in energy), and thus demonstrate the feasibility of one possible cost-reduction technology under consideration for the eRHIC Electron-Ion Collider (EIC) currently being designed at BNL. The CBETA project involves the study and measurement of many critical phenomena relevant to proposed EIC machine designs: the Beam-Breakup (BBU) instability, halo-development and collimation, growth in energy spread from Coherent Synchrotron Radiation (CSR), and CSR micro bunching. The CBETA project should provide valuable insight for both the EIC and ERL communities [1].

As part of the CBETA commissioning sequence, a combined test of the elements of all of the critical subsystems required for the CBETA project was done in the spring of 2018. This "Fractional Arc Test" (FAT) involved the injector, the Main Linac Cryomodule (MLC), the low energy splitter line, and a first prototype production permanent magnet girder featuring four cells of the FFA return loop (see Fig. 1). Besides hardware, the FAT commissioning involved testing and benchmarking of CEBTA-V, the CBETA online model. This paper describes the online modeling system and initial experience during machine running.

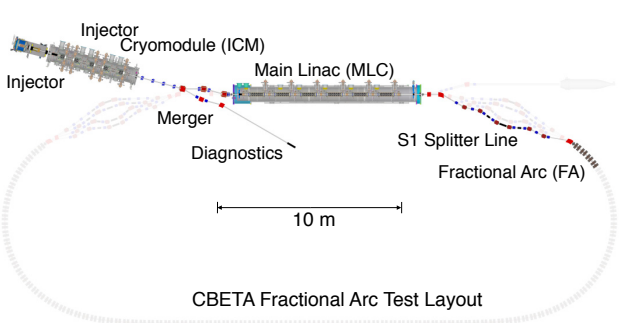

Figure 1: Schematic of the CBETA machine highlighting the components installed for Fractional Arc Test.

ONLINE SIMULATION ENVIRONMENT

The online single particle dynamics simulation model CBETA-V is based upon Bmad [6] and Tao [7]. Bmad is a modular, object-oriented subroutine library for simulating charged particle beams in high-energy accelerators and storage rings. Tao is a general purpose design and simulation program based upon Bmad and includes several optimization routines allowing the user to correct orbits, fit measured data, etc.

There were a number of advantages to basing CBETA-V on Bmad and Tao. For one, the majority of the CBETA lattice design was done using Bmad and Tao. This, and the fact that any Bmad based program is able to read Bmad lattice files, meant that offline and online simulations could be seamlessly interfaced. Additionally, the modular nature of both Bmad and Tao meant that CBETA-V development essentially consisted of creating a custom version of Tao which had the ability to communicate with the CBETA online EPICS database [8]. This was a relatively simple procedure requiring development of only about 1500 lines of code, and resulted in an online program which had all the capabilities of Tao. The ease of which CBETA-V was implemented is due in no small part to the fact that Bmad was originally developed for use with online modeling. Chan-

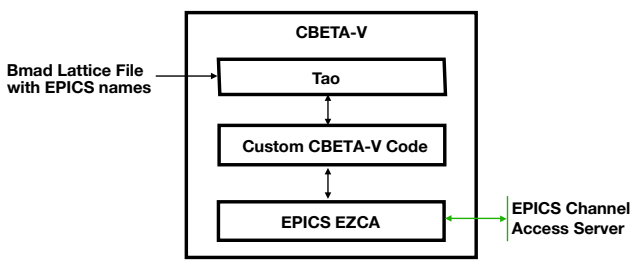

Figure 2: Schematic of the CBETA-V application showing the linking of the Tao with the EPICS EZCA library.

ISBN: 978-3-95450-200-4 doi:10.18429/JACoW-ICAP2018-TUPAF12

LONGITUDINAL BEAM DYNAMICS WITH A HIGHER-HARMONIC CAVITY FOR BUNCH LENGTHENING*

G. Bassi†, J. Tagger, Brookhaven National Laboratory, Upton, 11973 NY, USA

Abstract

We discuss the longitudinal beam dynamics in storage rings in the presence of a higher-harmonic cavity (HHC) system for bunch lengthening. We first review the general conditions for HHC operations, either in active or passive mode, assuming the stability of the system. For uniform filling patterns, a distinction is made between operations with a normal-conducting HHC, where optimal conditions for bunch lengthening can be satisfied, and operations with super-conducting HHC, where optimal conditions can be met only approximately. The option to operate the NSLS-II storage ring with a passive, super-conducting third harmonic cavity (3HC) system is discussed next. The stability and performance of the system in the presence of a gap in the uniform filling, which corresponds to the present mode of operation of the NSLS-II storage ring, is investigated with self-consistent Vlasov-Fokker-Planck simulations performed with the code SPACE [1].

INTRODUCTION

Higher-harmonic cavities (HHCs) play a crucial role for stable operations of present and future low- emittance storage rings. The primary benefic effect provided by the HHC is bunch lengthening without energy spread increase, with consequent beam lifetime improvement and reduction of the effect of intrabeam scattering on the transverse emittance [2]. Besides bunch lengthening, the highly nonlinear potential well distortion produced by the HHC introduces a strong dependence of the synchrotron tune on the amplitude of synchrotron oscillations. The induced anharmonic motion with enhanced synchrotron tune spread provides a powerful mechanism, known as Landau damping, for the suppression of collective instabilities. Moreover, the increase in bunch length and synchrotron tune spread can enhance the stabilizing effect of positive chromaticity on the transverse oscillations and help to stabilize higher-order head-tail modes [2]. The option considered for the NSLS-II storage ring is to operate with a passive superconducting 3HC [3, 4], a choice motivated by the successful development and operation of the superconducting 3HC system at the ELETTRA [5] and SLS [6] storage rings, a system that has been developed in the framework of the SUPER-3HC project [7]. The SUPER-3HC project represented the first superconducting application of a HHC system in storage rings, taking advantage of the very high quality factor of the superconducting cavity and the associated narrow bandwidth, allowing for the tuning of the 3HC very near to the third harmonic of the beam, without exciting longitudinal instabilities [5]. The success of the 3HC operation at the ELETTRA storage ring is substantiated by a beam lifetime improvement by more than a factor of three with respect to the nominal value, an improvement that has led to a change in the refilling frequency of the storage ring, allowing a refilling every 48 hr instead of every 24 hr, with benefit for the reliability and stability of user's operations and relevant benefit even for the machine thermal stability [5]. The success with the operation of a 3HC at the SLS storage ring is substantiated by a bunch lengthening up to a factor of three and a beam lifetime increase greater than a factor of two, achieved with stable conditions at the design current of 400 mA [6]. The success experienced at the ELETTRA and SLS storage rings has clearly shown that the very high quality factor of the superconducting HHC renders the performance of the HHC system less sensitive to high-order modes (HOMs) driven longitudinal coupled bunch instabilities, which is a major issue with normal conducting HHCs, where powerful longitudinal feedback systems are often needed for stable operations. Performance limiting factors, however, such as transients effects induced by non uniform filling patterns and the beam phase instability [8], can be detrimental for stable HHC operations, and need to be carefully investigated with detailed design studies. Accurate numerical simulations represent an essential part of the aforementioned design studies, with their goal to determine feasible conditions of operation and their range of applicability. To this end, the stability and performance of the passive superconducting 3HC system for the NSLSI-II storage ring is studied numerically with the parallel, particle tracking code SPACE [1], which allows to follow self-consistently the dynamics of h bunches, where h in the number of RF buckets, in arbitrary multi-bunch configurations. The specific goal of the numerical simulations is to determine stable HHC cavity settings and to study the performance limitation due to a gap in the uniform filling, which represents the nominal NSLS-II mode of operation.

OPERATIONS WITH HIGHER-HARMONIC CAVITIES

In the discussion of the theoretical conditions for optimal bunch lengthening, we assume a stable, beam loading compensated HHC system characterized by an equilibrium multi-bunch configuration. Radiation damping and quantum fluctuations are excluded from the analysis. The overall stability of the HHC system, including radiation damping and quantum fluctuations, together with the inclusion of a model for beam loading compensation, will be addressed in the next section with time-dependent Vlasov-Fokker-Planck simulations.

* Work supported by Brookhaven Science Associates, LLC under Contract No. DE-AC02-98CH10886 with the U.S. Department of Energy
† gbassi@bnl.gov

ISBN: 978-3-95450-200-4 doi:10.18429/JACoW-ICAP2018-TUPAF13

CALCULATION OF THE AGS OPTICS BASED ON 3D FIELDS DERIVED FROM EXPERIMENTALLY MEASURED FIELDS ON MEDIAN PLANE*

N. Tsoupas†, J. S. Berg, S. Brooks, F. Méot, V. Ptitsyn, D. Trbojevic
Brookhaven National Laboratory, Upton, NY, USA

Abstract

Closed orbit calculations of the Alternating Gradient Synchrotron (AGS) were performed and the beam parameters at the Fast Beam Extraction (FEB) point of the AGS [1] were calculated using a modified RAYTRACE computer code [2] to generate 3D fields from measured field maps on the median plane of the AGS combined function magnets. The algorithm which generates 3D fields from field maps on a plane is described in reference [3] which discusses the details of the mathematical foundation of this approach. In this paper we discuss results from studies reported in Refs. [1,4] that are based on the 3D fields generated from measured field components on a rectangular grid of a plane. A brief overview of the algorithm used will be given, and one of the two methods of calculating the required field derivatives on the plane will be discussed.

INTRODUCTION

The AGS is one of the pre-accelaration stages of the RHIC complex. Figure 1 is an aerial picture of the site with the green trace indicating the tunnel of the AGS. The 240 combined function main magnets of the AGS are placed inside the AGS tunnel whose schematic diagram is showing in Fig. 2. The AGS main magnets are separated in 12 superperiods of 20 magnets per superperiod spanning an arc of 30^o as shown in Fig. 2.

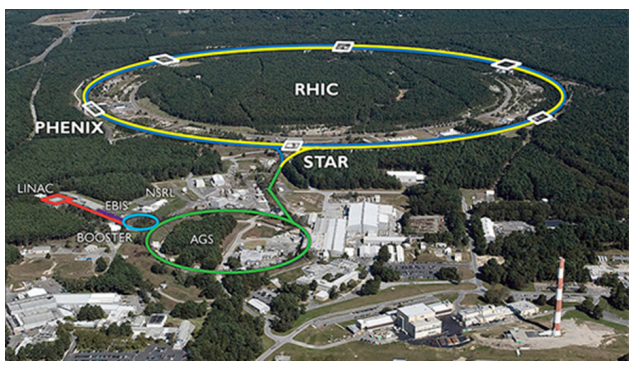

Figure 1: Area view of the RHIC complex. The green trace indicates the location of the AGS tunnel.

Figure 3 is a schematic diagram of the main magnets layout (small rectangles) in each superperiod. The "+" and "−" signs on each magnets indicate the focusing and defocusing quadrupole property of each combined function magnet for positive ions circulating in the synchrotron.

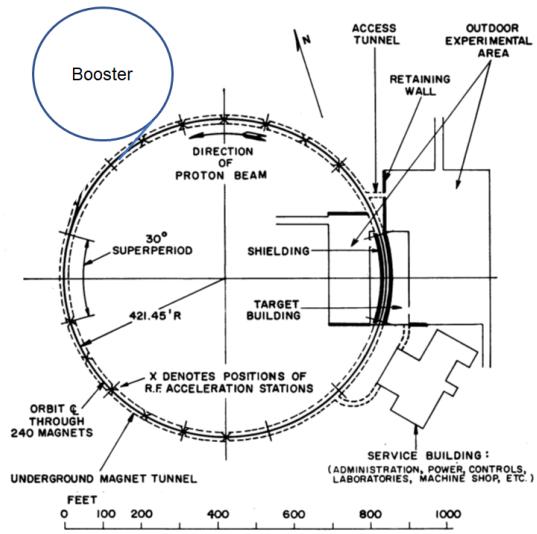

Figure 2: Schematic diagram of the AGS tunnel. The 240 main AGS magnets are separated in 12 superperiods with 20 magnets per superperiod wich spans an arc of 30^o

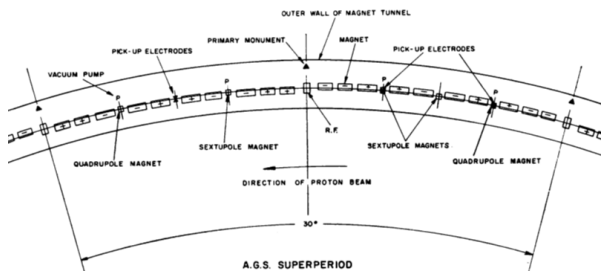

Figure 3: Drawing of the AGS superperiod which consist of 20 combined function main magnets. The "+" and "-" signs on each magnets indicate the focusing and defocusing quadrupole property of each combined function magnet for positive ions circulating in the synchrotron. There is one tune quadrupoles in each of the straight sections SS03,SS17 and one chromaticity sextupole in each of the straight sections SS07,SS13 of each superperiod.

There is one tune quadrupoles in each of the straight sections SS03,SS17 and one chromaticity sextupole in each of the straight sections SS07, SS13 of each superperiod. Three pickup electrodes are also located in the straight sections SS03, SS05, and SS13 respectively. Additional information on the AGS appears in Refs. [1,5].

BEAM OPTICS OF AGS

The beam optics of the AGS for a charged particle beam which is not subject to space charge forces depends on the

* Work supported by the US Department of Energy
† tsoupas@bnl.gov

ISBN: 978-3-95450-200-4 doi:10.18429/JACoW-ICAP2018-TUPAF14

ANALYTICAL CALCULATIONS FOR THOMSON BACKSCATTERING BASED LIGHT SOURCES

P. Volz*, A. Meseck, Helmholtz-Zentrums Berlin für Materialien und Energie, Berlin, Germany

Abstract

There is a rising interest in Thomson-backscattering based light sources, as scattering intense laser radiation on MeV electrons produces high energy photons that would require GeV or even TeV electron beams when using conventional undulators or dipoles. Particularly, medium energy high brightness beams delivered by LINACs or Energy Recovery LINACs, such as bERLinPro being built at Helmholtz-Zentrum Berlin, seem suitable for these sources. In order to study the merit of Thomson-backscattering-based light sources, we are developing an analytical code to simulate the characteristics of the Thomson scattered radiation. The code calculates the distribution of scattered radiation depending on the incident angle and polarization of the laser radiation. Also the impact of the incident laser polarization and the full 6D bunch profile, including microbunching, are incorporated. The Status of the code and first results will be presented.

INTRODUCTION

Shortly after the invention of the LASER the idea of Thomsaon-backscattering light sources emerged [1]. Only in recent years however did lasers become powerful enough to make these sources viable due to the small Thomson scattering cross section. In the case of Thomson backscattering a relativistic electron beam interacts with a counter-propagating laser field. The backscattered photons travel in the direction of the electron beam in a small cone with an opening angle proportional to $1/\gamma$. The scattered laser photons experience a Doppler shift according to the energy of the electrons they are scattered on. This allows Thomson backscattering sources to produce very high energy photons, from relatively low energy electron beams, that would otherwise require GeV electron energies. Thomson scattering is the low energy limit of Compton scattering. The Thomson limit is accurate if the photon energy in the particle's rest frame is significantly lower than its rest mass.

Nowadays the demand for beam time at hard X-ray synchrotron facilities heavily outweighs supply. Such facilities however are very cost prohibitive to build and operate. Thomson-backscattering light sources provide an alternative to conventional sources at a cost that would be manageable for smaller laboratories and universities. Furthermore, in recent years there have been advances in the development of high brightness electron beam sources in both classical linac, and energy recovery linac (ERL) configuration. These sources provide electron beams with very low energy spread and emittance which results in less quality degradation of the backscattered light. This has opened up new possibilities for high performance ERL based Thomson backscattering light sources. The design and development of such a source requires a fast code that takes into account the relevant properties of the electron beam and laser pulse to calculate the critical properties of the backscattered radiation field. The development of such a code is the goal of the presented work.

First we will present a short description of our code, followed by some test cases to validate its results. Then we will present our first results in simulating the radiation of microbunched beams. Finishing off with an outlook of what improvements are planned.

CODE DESCRIPTION

The goal of our code is to calculate the spatial and spectral radiation distribution for different Thomson scattering events. It has to include the laser polarization, the incident angle between the laser and the electron beam, and the coherent effects resulting from the full 6D bunch profile of the beam. As of now emittance cannot be fully incorporated by the code because evaluation of transverse momentum distribution is not yet implemented. The laser is treated as a flat top pulse with no rise time or fringe effects. The 6D particle configuration can be imported from ascii files in ASTRA [2] output format. The underlying calculations are based on an Evaluation of Liénard-Wiechert potentials. The derivation of the formulas is shown in detail in [3] and [4]. The code does not use numerical integration. The essential calculations are based on complex Bessel functions.

Our code can calculate the spatial intensity distribution of the radiation produced by electrons interacting with a circularly or linearly polarized laser. The incident angle between the laser and the electron beam as well as the detector size and position can be chosen freely. The detector is modeled as grid of pixels. The number of pixels together with the size of the detector dictates the resolution. The backscattered radiation generated by individual particles are added up at each pixel. For multiple particles either the intensities or the amplitude of the radiation generated by the individual particles can be added. As will be explained in the following sections, the addition of amplitudes is necessary for the correct calculation of coherent effects.

A simulation run with 200 k particles and a detector resolution of 80×80 pixels takes around 2000 s on a current workstation CPU (single core load). The computation time scales linearly with the number of particles.

CODE VALIDATION

To validate our code we simulated some simple scenarios for which we have a clear expectation of results.

* paul.volz@helmholtz-berlin.de

ISBN: 978-3-95450-200-4 doi:10.18429/JACoW-ICAP2018-TUPAF15

A HOLISTIC APPROACH TO SIMULATING BEAM LOSSES IN THE LARGE HADRON COLLIDER USING BDSIM

S. D. Walker*, A. Abramov, S. T. Boogert,
H. Garcia-Morales, S. M. Gibson, H. Pikhartova, W. Shields, L. J. Nevay
Royal Holloway, University of London, Egham, TW20 0EX, United Kingdom

Abstract

To fully understand the beam losses, subsequent radiation, energy deposition, backgrounds and activation in particle accelerators, a holistic approach combining a 3-D model, physics processes and accelerator tracking is required. Beam Delivery Simulation (BDSIM) is a program developed to simulate the passage of particles, both primary and secondary, in particle accelerators and calculate the energy deposited by these particles via material interactions using the Geant4 physics library. A Geant4 accelerator model is built from an optical description of a lattice by procedurally placing a set of predefined accelerator components. These generic components can be refined to an arbitrary degree of detail with the use of user-defined geometries, detectors, field maps, and more. A detailed model of the Large Hadron Collider has been created in BDSIM, validated with existing tracking codes and applied to study beam loss patterns.

INTRODUCTION

The Large Hadron Collider (LHC) at CERN is at the forefront of the accelerator energy frontier, with a design energy of 7 TeV and with a stored energy of 386 MJ per beam [1]. This extremely large stored energy presents a challenge to protect the experiments, and machine elements both from irradiation and prevent any superconducting magnets from quenching, where as little as 1 mJ cm^{-3} is sufficient to cause a quench [2]. Beam losses are inevitable in any machine and it is due to the aforementioned factors that a dedicated collimation system has been designed and built. It is primarily located in two insertion regions (IRs)—IR3 for momentum cleaning, and IR7, for betatron cleaning. Common to both is the concept of a collimation hierarchy, which consists of a sequence of collimators with increasing apertures, such that large amplitude particles will first hit the primary (smallest aperture) collimator, followed by the secondary collimators (wider aperture), and finally the absorbers (larger still). Added to this are tertiary collimators (TCTs) on either side of the experimental IRs, which protect the final focus magnets and reduce beam-induced backgrounds. This design has proven exceedingly successful in protecting the machine.

Detecting beam losses reliably in critical regions requires the presence of 3600 beam loss monitors (BLMs) placed around the ring [2]. These are used to detect abnormal beam conditions, and if one detects losses above a given threshold, a beam dump is triggered. In order to characterise the pattern of losses around the ring and study the effectiveness of the collimation system, special runs are performed where a low-intensity beam is blown up to produce losses and the signal from the BLMs is recorded. This is referred to as a loss map of the machine.

To ensure the collimation system works effectively both in normal-functioning as well as in adverse scenarios, such as an asynchronous beam dump, effective simulation tools are necessary. The tool of choice used at CERN for collimation studies is SixTrack, and is used to generate loss maps [3]. SixTrack is a fully symplectic 6-D thin lens tracking code which was originally used for dynamic aperture studies, but was extended for use in aiding the design and implementation of LHC collimation system [4]. SixTrack is often paired with another standard CERN code, FLUKA [5], for irradiation and beam background studies to study specific areas of interest. Together these have demonstrated themselves to be extremely effective in aiding the design and optimisation of the LHC collimation system.

SixTrack's approach to primary impacts on collimators is to call Monte Carlo scattering procedures, whereby the primary is either lost in an inelastic collision, or undergoes an elastic process and is reintroduced to the tracker. Elsewhere, if a primary particle exceeds the aperture at a given point, it is treated as lost immediately at that location. Secondary particles that would generally stem from these impacts are not treated.

Beam Delivery Simulation (BDSIM) is a novel code which seeks to track the passage of the primary particle as well as any resulting secondary particles [6]. As a result it is it will be more capable of capturing the details in LHC loss maps which are otherwise missing in existing tools, and present a more holistic method for simulating beam losses in particle accelerators.

In this paper, preliminary results comparing LHC loss maps from BDSIM, SixTrack, and BLM data from a recent run are presented.

BDSIM

BDSIM is a C++ particle tracking code based on a collection of high energy physics libraries, including Geant4 [7], CLHEP [8], and ROOT [9]. It automatically builds a Geant4 3-D accelerator model from a set of generic components which enables the seamless tracking of both primary and secondary particles throughout an accelerator or detector. In using Geant4 it has access to all of the standard particle physics processes, but is supplemented with accelerator tracking routines. Standard Geant4 numerical integrators are replaced with transfer matrices for elements such as drifts,

* stuart.walker@rhul.ac.uk

ISBN: 978-3-95450-200-4 doi:10.18429/JACoW-ICAP2018-TUPAF16

ANALYSIS OF THE BEAM LOSS MECHANISM DURING THE ENERGY RAMP-UP AT THE SAGA-LS

Y. Iwasaki†, SAGA Light Source, [841-0005] Tosu, Japan

Abstract

The accelerator of the SAGA Light Source consists of the 255 MeV injector linac and the 1.4 GeV storage ring. The accumulated electron beam current of the storage ring is about 300 mA. The energy of the electrons is raised up to 1.4 GeV in 4 minutes in the storage ring. At the moment of the beam acceleration, the electron beam is lost. The amount of beam loss is normally about 5 mA to 30 mA. All electrons are sometimes lost. We investigated the relationship between the beam loss and the betatron tune shifts. The tune shifts during the beam acceleration were analyzed from the measured data of the output currents of the magnets power supplies by using beam tracking code of TRACY2. It was found that the anomalous output of the power supply of bending magnets was one of the causes of the beam loss.

INTRODUCTION

The accelerator of the SAGA Light Source (SAGA-LS) consists of the 255 MeV injector linac and the 1.4 GeV storage ring [1, 2]. The accumulated electron beam current of the storage ring is about 300 mA. The energy of the electrons is raised up to 1.4 GeV in 4 minutes in the storage ring. At the moment of the beam acceleration (the beam energy is lower than 400 MeV), the electron beam is lost (see Figure 1). The amount of beam loss is normally about 5 mA to 30 mA. All electrons are sometimes lost. To understand the beam loss mechanism, which depends on the beam current, we developed high-speed logging system of 100 kHz for monitoring the beam current and the magnets power supplies using National Instruments PXI. We investigated the relationship between the beam loss and the betatron tune shifts. The tune shifts during the beam acceleration were analyzed from the measured data of the output currents of the magnets power supplies by using beam tracking code of TRACY2 [3]. To estimate the K-value of the quadrupole magnets, we used orbit response matrix analysis method [4]. By adopting the new high-speed logging system, the time structure of the beam loss process was clearly observed. In this paper, we describe the data acquisition and the data processing system, and the result of the analysis.

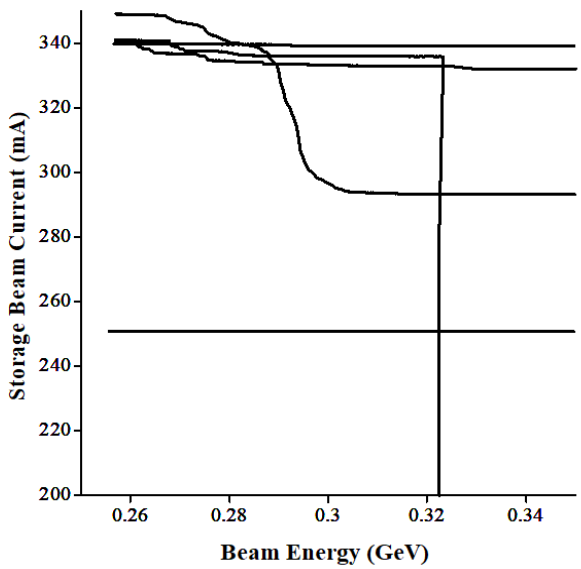

Figure 1: Beam loss at the energy ramp-up.

† iwasaki@saga-ls.jp

METHODS

Commonly we use N.I. Fieldpoints, PLCs and PCs system for controlling and monitoring the SAGA-LS accelerator [5]. The beam loss occurs at the moment of the energy ramp-up and it observed like a step function by using slow (1 Hz) monitoring system. Therefore, we developed high-speed logging system of 100 kHz for monitoring the beam current and the magnets power supplies using National Instruments PXI. Figure 2 shows the data acquisition and analysis system for investigation of the beam loss. Since the signals of output currents of the power supplies are highly noisy, the low-pass filter (100 Hz) was performed to the measured data. The data sets were thinning out to 1/100 to calculate tunes and Twiss parameters step by step. Orbit response matrix analysis method [4] was adopted to estimate effective K-value of quadrupole magnets from the measured output currents of the power supplies of the quadrupole magnets.

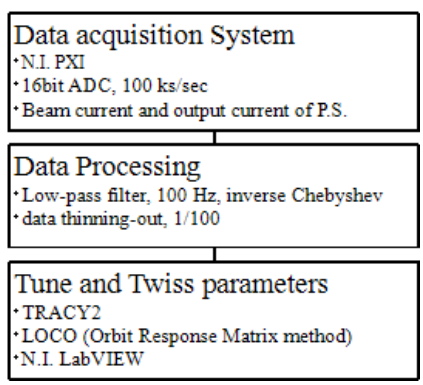

Figure 2: Data acquisition and analyses System.

The TRACY2 was used to calculate the tunes and Twiss parameters. The tracking code of TRACY2 was called from the National Instruments LabVIEW. The Data processing and the optics calculation were performed under the environment of LabVIEW for Microsoft Windows.

ISBN: 978-3-95450-200-4 doi:10.18429/JACoW-ICAP2018-TUPAF19

pyaopt OPTIMIZATION SUITE AND ITS APPLICATIONS TO AN SRF CAVITY DESIGN FOR UEMS*

Ao Liu†, Roman Kostin, Euclid Techlabs, Bolingbrook, IL, USA
C. Jing, Pavel Avrakhov, Euclid Beamlabs, Bolingbrook, IL, USA

Abstract

Designing and commissioning particle accelerators need great optimization efforts. This is particularly true for large accelerators with complex components that provide stable beam such as light sources and colliders, where nonlinearities of the beam play an important role. Currently, many design optimizations are provided by individual user-created automated problem-finding and solution-proposing algorithms, which requires an extensive amount of computing resources. Heuristic algorithms such as Genetic Algorithms (GA) and Simulated Annealing (SA) are commonly implemented. They are either created for individual tasks, or are implemented directly in simulation codes, such as OPAL or IMPACT3D. An optimization suite that is independent of the accelerator codes is needed for general application studies. Meanwhile, researchers now have access to the HPC resources, which can be utilized for parallelization of codes. We propose a Python-based optimization suite for general applications. In this paper, we introduce the pyaopt suite by giving some details of its applications, including a design of an SRF photogun for UEMs.

INTRODUCTION

Recently, there has been multiple new applications of heuristic algorithms in the particle accelerator community. The fields include secondary particle collection [1], DA optimizations [2, 3], and space charge calculations [4]. In most of these cases, algorithms were customized for specific physics problems, or built in a specific simulation program. In fact, the number of programs that include the Genetic Algorithm (GA) as the multi-objective optimizer is rapidly increasing [5, 6]. However, for many accelerator physicists and engineers, these algorithms are still inaccessible to some extent: there is no easy way to use them in a "plug and play" fashion.

The design of Python advanced optimization pyaopt suite aims at delivering a package that has an API for users to conveniently describe the optimization problem, select the optimization algorithm and start the job. It not only includes widely-accepted algorithms such as the GA, Simulated Annealing (SA) and the Particle Swarm Algorithm (PSA), but also gradient-based (deterministic) algorithms, such as the Gauss-Newton method, etc. The goal of the Python-based package is to let users run optimization jobs in any environments, including a personal computer, a small-scale cluster, or a HPC supercomputer. Users may select the mode such that the pyaopt job manager can handle the job submission, monitoring, and logging. The idea of running the jobs on an HPC is illustrated in Figure 1.

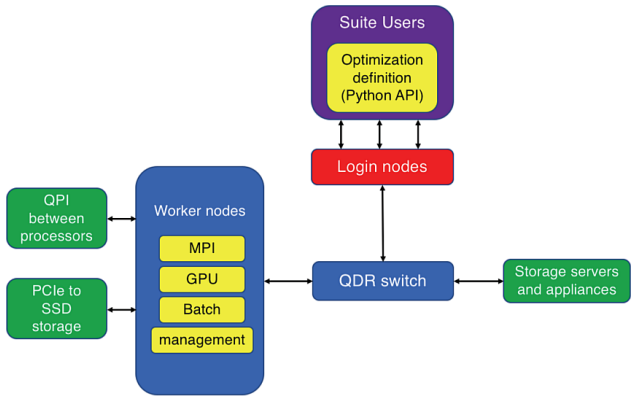

Figure 1: The flowchart of running optimization jobs on an HPC machine.

pyaopt includes a few customized metaheuristic algorithms and some deterministic algorithms. We introduce a selection of the metaheuristics below:

- pyaopt-GA, which is based on the NSGA-II [7] and can do both single-objective GA (SOGA) and multi-objective GA (MOGA). The customization is on the crowding distance (CD) of individuals, which represents the similarities of them, and the "rescue method": judgment day, which is used only when the whole population seizes improving prematurely. The algorithm is enhanced by MPI [8], such that calculations of dominance and CD are distributed on different ranks.

- pyaopt-SA, which is based on the standard annealing formula $P = e^{(f(x)-f(x')/T)}$ for $f(x) < f(x')$, where $f(x)$ is the fitness value for solution x, and T is the current temperature. The customization is on the adaptive cooling schedule, ΔT per iteration, and on the cooling range assignment for MPI implementation. Although it is already a common practice to normalize the fitness value to an expected one and implemented by many SA users, using an adaptive cooling schedule further helps to prevent the system to converge prematurely. As for the search range where multiple workers are present, users can choose how many slices each variable's range needs to be divided, based on the number of workers available. Then pyaopt allocates each combination of range slices evenly to the workers.

- pyaopt-ANN, which is based on multiple artificial neural network (ANN) algorithms. The parallelization is

* SRF cavity design work supported by DOE under contract DE-SC0018621
† a.liu@euclidtechlabs.com

ISBN: 978-3-95450-200-4 doi:10.18429/JACoW-ICAP2018-TUPAF20

MEAN-FIELD DENSITY EVOLUTION OF BUNCHED PARTICLES WITH NON-ZERO INITIAL VELOCITY

B. S. Zerbe*, P. M. Duxbury†
Department of Physics and Astronomy, Michigan State University, East Lansing, MI, USA

Abstract

Reed presented a 1D mean-field model of initially cold pancake-beam expansion demonstrating that the evolution of the entire spatial distribution can be solved for all time where the 1D assumption holds. This model is relevant to ultra-fast electron microscopy as it describes the evolution of the distribution within the photoelectron gun, and this model is similar to Anderson's sheet beam density time dependence except that Reed's theory applies to freely expanding beams instead of beams within a focussing channel. Our recent work generalized Reed's analysis to cylindrical and spherical geometries demonstrating the presence of a shock that is seen in the Coulomb explosion literature under these geometries and further discussed the absence of a shock in the 1D model. This work is relevant as it offers a mechanistic explanation of the ring-like density shock that arises in non-equilibrium pancake-beams within the photoelectron gun; moreover, this shock is coincident with a region of high-temperature electrons providing an explanation for why experimentally aperturing the electron bunch results in a greater than 10-fold improvement in beam emittance, possibly even resulting in bunch emittance below the intrinsic emittance of the cathode. However, this theory has been developed for cold-bunches, i.e. bunches of electrons with 0 initial momentum. Here, we briefly review this new theory and extend the cylindrical- and spherical- symmetric distribution to ensembles that have non-zero initial momentum distributions that are symmetric but otherwise unrestricted demonstrating how initial velocity distributions couple to the shocks seen in the less general formulation. Further, we derive and demonstrate how the laminar condition may be propagated through beam foci.

INTRODUCTION

Freely expanding ensembles of charged particles are fundamental to accelerator physics. Although continuous beams near the particle source are relatively diffuse, bunched beams can reach densities where space-charge effects dominate the expansion. In such a regime, the expansion dynamics are similar to the dynamics of Coulomb explosion that are well studied in the laser ablation field, where it is well established that shocks that form at the periphery of the distribution [1–6]. Our group recently found that in an ultrafast electron microscope experimentally aperturing a high density bunch of electrons after they exit the photocathode gun can result in a significant improvement to the brightness. Simulation results suggest that this effect is due to a density shock, akin to the shock seen in the Coulomb explosion literature, of high-temperature electrons that form at the longitudinal median of the bunch and migrate out to the transverse edge [7].

It has been known for decades that charge redistribution near the particle source is the origin of a major portion of the emittance seen in standard beams [8]. More than 30 years ago, Anderson presented 1D and cylindrical mean-field fluid models of beam dynamics for ensembles of particles with arbitrary initial distributions relevant while the beam remains laminar [9]. These models describe the transverse density and emittance evolution in the presence of a focussing force, and specifically they provide insight into emittance oscillation that is important for emittance compensation [10, 11]. While it is reasonable to make an analogy between that mechanism and the freely expanding charge redistribution we see during Coulomb explosion, Anderson's models are inappropriate for a freely expanding bunch as they assume the focussing force is non-zero and radially inward. Therefore, other models are needed to describe the freely expanding case.

Within the ultrafast electron microscopy (UEM) literature, numerous works postulated 1D models for non-relativistic longitudinal free expansion [12–14], and Reed eventually settled upon the same mean-field fluid approach used by Anderson but without any external fields [15]. Again this model was to describe the longitudinal density evolution of initially dense "pancake" bunches — named so as they have much shorter longitudinal widths than transverse radius — that can be assumed to be planar symmetric instead of Anderson's description of a cylindrical symmetric beam's transverse density evolution. Reed's mean-field model accurately describes the longitudinal expansion while planar symmetry can be assumed [15]. However, Reed was concerned that no Coulomb explosion-like shock was seen in the model even when non-uniform initial conditions were assumed, in stark disagreement to what had been previously found within the Coulomb explosion literature. We recently demonstrated that such a shock cannot occur in the non-relativistic 1D model without careful tuning of the initial velocity distribution [16]. In contrast, we showed that these shocks spontaneously occur in higher dimensions for non-uniform distributions [16], so that the theoretical results found in the UEM community are consistent with the shocks found in the Coulomb explosion literature.

To demonstrate these results, we generalized Reed's model to higher dimension by deriving closed form analytic expressions that describe arbitrary density evolution under cylindrical and spherical symmetries. We discovered that the shocks arise due to relative bunching of particles

* zerbe@pa.msu.edu
† duxbury@pa.msu.edu

ISBN: 978-3-95450-200-4 doi:10.18429/JACoW-ICAP2018-TUPAF22

FEL SIMULATION USING THE LIE METHOD*

Kilean Hwang†, Ji Qiang, Lawrence Berkeley National Laboratory, Berkeley, USA

Abstract

Advances in numerical methods for free-electron-laser (FEL) simulation under wiggler period averaging (WPA) are presented. First, WPA is generalized using perturbation Lie map method. The conventional WPA is identified as the leading order contribution. Next, a widely used shot-noise modeling method is improved along with a particle migration scheme across the numerical mesh. The artificial shot noise arising from particle migration is suppressed. The improved model also allows using arbitrary mesh size, slippage resolution, and integration step size. These advances will improve modeling of longitudinal beam profile evolution for fast FEL simulation.

INTRODUCTION

FEL design optimization often involve multiple times of numerical simulations with different system parameters. Such a study requires highly efficient simulation code. The WPA is the one of the best options. Indeed, most of the start-to-end design codes choose to incorporate the WPA FEL simulation code [1–5]. In this proceeding, we review the advances in numerical methods within the WPA framework presented in our previous work [6].

First, we generalize the WPA using the perturbation Lie map method. The conventional WPA is identified as the leading order contribution. The next order corrections we includes are coupling between betatron and wiggling motion, transverse field gradient, and longitudinal field envelope variation.

Second, we present an improved shot-noise model within WPA framework. Unless particle migration across the numerical mesh is artificially suppressed, as in many old WPA codes [7], there can be large artificial shot noise due to the nature of the shot-noise modeling method [8]. We solve this problem by re-interpreting and combining the two widely used shot-noise modeling methods of Refs. [8] and [9]. The improved modeling can further benefit smoothness of numerical mesh through arbitrary weight and shape functions. Here, the weight function refers to the integral kernel used for particle deposition on numerical mesh points. The shape function refers to the shape of the field representation at numerical mesh points used for field interpolation from mesh points to particles' coordinates. This, in turn, allows arbitrary mesh size, integration step size and slippage resolution. Especially, the arbitrary slippage resolution comes with many other benefits. It can naturally simulate correct slippage through non-resonant transport line other than wiggler and allows applying the operator split-composition method [10] on field solver for better accuracy. Last but the least, the particle loading method can naturally accept the particle data from upstream simulation enabling start-to-end simulation seamless.

* Work supported by the Director of the Office of Science of the US Department of Energy under Contract no. DEAC02-05CH11231
† kilean@lbl.gov

GENERALIZATION OF WIGGLER PERIOD AVERAGING

In general, when a Hamiltonian can be decomposed into integrable part and a small parametric potential, one can build a perturbation map in order of the small parameters. In an undulator, if a map is constructed over a undulator period, the lowest order of the wiggling motion average out leaving the small coupling effects between the fast wiggling and slow betatron motion.

Magnus Series

We split the Hamiltonian into $H = S + F(z) + V(z)$ where S is the wiggler period averaged Hamiltonian representing slow motion, V is the radiation field potential, F is the rest representing the fast wiggling motion. Accordingly, we factor the Lie map as the following [11]:

$$\begin{aligned}\mathcal{H}(\lambda_u) &= \mathcal{S}(\lambda_u)\mathcal{F}(\lambda_u)\mathcal{V}(\lambda_u), \\ \mathcal{S}(\lambda_u) &= e^{\mathcal{G}_S(\lambda_u)}, \quad (1)\\ \mathcal{F}(\lambda_u) &= e^{\mathcal{G}_F(\lambda_u)}, \quad (2)\\ \mathcal{V}(\lambda_u) &= e^{\mathcal{G}_V(\lambda_u)},\end{aligned}$$

where λ_u is the wiggler period. The generators can be written in terms of the Magnus's series

$$\begin{aligned}\mathcal{G}_F(z) &= -\int_0^z dz_1 :F_1^{\rm int}: + \frac{1}{2!}\int_0^z dz_1\int_0^{z_1} dz_2 :[2,1]: \quad (3)\\ &\quad + \frac{1}{3!}\int_0^z dz_1\int_0^{z_1} dz_2\int_0^{z_2} dz_3 :[3,[2,1]] + [[3,2],1]: \\ \mathcal{G}_V(z) &= -\int_0^z dz :V^{\rm int}(z): \quad (4)\end{aligned}$$

where the pair of colons is Dragt's notation [11] of the Poisson bracket, i.e., $:A:B = [A,B]$, and the numbers in the Poisson bracket is an abbreviation of $i \equiv F_i^{\rm int}$ with $F_i^{\rm int} \equiv \mathcal{S}(z_i)F(z_i)$. Since the raidaiton field strength is much weaker than external field strength only the 1st sequence is taken for $\mathcal{G}_V$ [6].

Hamiltonian

Starting from the following Hamiltonian,

$$H(\boldsymbol{x},\boldsymbol{p},ct,-\gamma;z) = -\sqrt{\gamma^2 - 1 - (p_x - a_x)^2 - (p_y - a_y)^2},$$

where ct is the time multiplied by the speed of light and it's canonical momentum pair is negative of the normalized

ISBN: 978-3-95450-200-4 doi:10.18429/JACoW-ICAP2018-TUPAF23

START-TO-END SIMULATIONS OF THz SASE FEL PROOF-OF-PRINCIPLE EXPERIMENT AT PITZ

M. Krasilnikov*, P. Boonpornprasert, F. Stephan, DESY, Zeuthen, Germany
E.A. Schneidmiller, M.V. Yurkov, DESY, Hamburg, Germany
H.-D. Nuhn, SLAC, Menlo Park, California, USA

Abstract

The Photo Injector Test facility at DESY in Zeuthen (PITZ) develops high brightness electron sources for modern linac-based Free Electron Lasers (FELs). The PITZ accelerator has been proposed as a prototype for a tunable, high power THz source for pump and probe experiments at the European XFEL. A Self-Amplified Spontaneous Emission (SASE) FEL is considered to generate the THz pulses. High radiation power can be achieved by utilizing high charge (4 nC) shaped electron bunches from the PITZ photo injector. THz pulse energy of up to several mJ is expected from preliminary simulations for 100 μm radiation wavelength. For the proof-of-principle experiments a re-usage of LCLS-I undulators at the end of the PITZ beamline is under studies. One of the challenges for this setup is transport and matching of the space charge dominated electron beam through the narrow vacuum chamber. Start-to-end simulations for the entire experimental setup - from the photocathode to the SASE THz generation in the undulator section - have been performed by combination of several codes: ASTRA, SCO and GENESIS 1.3. The space charge effect and its impact onto the output THz radiation have been studied. The results of these simulations will be presented and discussed.

INTRODUCTION

The Photo Injector Test facility at DESY in Zeuthen (PITZ) has been suggested as a prototype for developments on an accelerator based high power tunable THz source for pump and probe experiments at the European XFEL [1]. The SASE FEL is considered as main option to generate THz pulses at PITZ using a high bunch charge (4 nC) operation mode of the photo injector. In order to prepare a proof-of-principle experiment start-to-end beam dynamics simulations have been performed. They include generation of electron bunches in the RF photogun, further acceleration by the booster cavity, further transport (~25 m) of the space charge dominated electron beam and its matching into the undulator section. A measured field profile of a typical LCLS-I undulator has been used to reconstruct a 3D magnetic field map used for the beam transport through the undulator section. Best obtained matching solution was used to simulate THz SASE FEL with a centre radiation wavelength of ~100 μm.

* mikhail.krasilnikov@desy.de

RF GUN AND BOOSTER

The PITZ RF photogun with a peak cathode field of 60 MV/m operated at the launch phase of maximum mean momentum gain (MMMG) is used to generate 4 nC electron bunches by applying photocathode laser pulses with a flattop temporal profile (21.5 ps FWHM) and with a radially homogeneous transverse distribution. Preliminary emittance optimization yielded the optimum photocathode laser spot size which is larger than the whole cathode size. In order to be closer to the practical case a 5 mm diameter of the photocathode laser spot (coinciding with the size of the photocathode) has been used for further optimizations. Beam mean longitudinal momentum of ~16.7 MeV/c required for generating THz radiation with ~100 μm radiation wavelength is achieved using a booster cavity. For each booster gradient (peak electric field) the booster phase (w.r.t. MMMG) was tuned in order to yield the required final mean momentum of electron beam. Corresponding curve is shown in Fig. 1a. Besides the mean beam momentum booster cavity gradient and phase were tuned in order to yield a small correlated energy spread ($\langle zE \rangle \rightarrow 0$) of the electron beam close to the undulator (z=29 m). This two-fold optimization resulted in a peak booster field of 12.85 MV/m and a phase of -26 deg. w.r.t. MMMG (Fig. 1a). The main gun solenoid was tuned to control electron beam size and emittance. Beam dynamics simulations were performed using the ASTRA code [2] with 200000 macroparticles. Simulated rms normalized emittance at the location of the first emittance measurement station (EMSY1 at z=5.277 m) is shown in Fig. 1b for the booster MMMG phase and for the optimized correlated energy spread (working point, WP). The chosen absolute value of the gun solenoid peak field of the main solenoid (212.85 mT) is by ~5% lower than that delivering the minimum emittance for the booster in on-crest operation. Corresponding curves of the beam projected transverse emittance and correlated energy spread along the beam line are shown in Fig. 1c. The WP setup corresponds to a more flat emittance along the beamline, whereas a significant increase of the emittance after the minimum is clearly seen for the case of the MMMG booster phase.

Transverse and longitudinal phase spaces of the optimized electron beam (WP) at the EMSY1 location are shown in Fig. 2. This beam setup was used as a starting point for studies on the space charge dominated beam transport towards the undulator section.

ISBN: 978-3-95450-200-4 doi:10.18429/JACoW-ICAP2018-TUPAG01

COMPUTATION OF EIGENMODES IN THE BESSY VSR CAVITY CHAIN BY MEANS OF CONCATENATION STRATEGIES*

Thomas Flisgen†, Adolfo Vélez
Helmholtz-Zentrum Berlin für Materialien und Energie GmbH (HZB), 12489 Berlin, Germany
Johann Heller, Shahnam Gorgi Zadeh, and Ursula van Rienen
Institute of General Electrical Engineering, University of Rostock, 18059 Rostock, Germany

Abstract

The computation of eigenmodes in chains of superconducting cavities with asymmetric couplers is a demanding problem. This problem typically requires the use of high-performance computers in combination with dedicated software packages. Alternatively, the eigenmodes of chains of superconducting cavities can be determined by the so-called State-Space Concatenation (SSC) approach that has been developed at the University of Rostock. SSC is based on the decomposition of the full chain into individual segments. Subsequently, the RF properties of every segment are described by reduced-order models. These reduced-order models are concatenated to a reduced-order model of the entire chain by means of algebraic side constraints arising from continuity conditions of the fields across the decomposition planes. The constructed reduced-order model describes the RF properties of the complete structure so that the field distributions, the coupling impedances and the external quality factors of the eigenmodes of the full cavity chain are available. In contrast to direct methods, SSC allows for the computation of the eigenmodes of cavity chains using desktop computers. The current contribution revises the scheme using the BESSY VSR cavity chain as an example. In addition, a comparison between a direct computation of a specific localized mode is described.

INTRODUCTION

The computation of eigemodes of superconducting RF resonators used for the acceleration of charged particles is a standard task in computational accelerator physics. Complementary to the characterization of the accelerating mode, higher-order modes are of special interest as they can interact with the beam as well and may lead to additional cryogenic load or beam instabilities. Often eigenmode computations are restricted to single cavities with couplers to reduce computational efforts, despite the fact that the cavities are arranged in chains and are connected via the beam pipes. These chains are accommodated in cryomodules providing the cryogenic infrastructure to cool the resonators so that their surfaces become superconducting.

The consideration of single cavities with couplers is a reasonable approximation for characterizing the accelerating mode as the field distribution of this mode is on purpose confined in the cavity. However, the restriction to a single cavity often becomes invalid for higher-order modes, in particular if mode resonant frequencies are larger than the fundamental cutoff frequency of the beam pipe connecting the adjacent cavities. The field distributions of higher-order modes in cavity chains are much more complex than in single cavities as the fields can be distributed along the entire cavity chain or along parts of it.

Direct approaches to determine the eigenmode spectrum of cavity chains require high-performance computers [1–4]. Alternatively, the State-Space Concatenation (SSC) [5–9] approach allows for computing the eigenmodes in complex chains of cavities with asymmetric couplers using desktop computers. The scheme is based on decomposing the complex cavity chain into segments. The electromagnetic fields of the segments are described using state-space equations (coupled systems of ordinary differential equations) obtained from analytical calculations or from numerical discretization techniques such as the Finite-Integration Technique [10, 11]. Typically, the aforementioned state-space equations have many degrees of freedom to account for the distributed nature of the underlying partial differential equations. Fortunately, the number of degrees of freedom for each state-space model can be significantly reduced using model-order reduction (MOR) approaches [12–14]. Subsequently, all reduced-order models are concatenated by means of algebraic side constraints, which ensure that the tangential electric and magnetic fields are continuous across the surfaces of the decomposition planes. This concatenation delivers a very compact description of the complex structure in terms of its electromagnetic properties and allows for the determination of its eigenmodes by computing the eigenvalues and eigenvectors of comparably small matrices.

In this paper, the SSC scheme is revised using the BESSY VSR chain of superconducting cavities as an application example. The presented work has been conducted in the framework of a collaboration between the University of Rostock and the Helmholtz-Zentrum Berlin. Predominantly, this article is based on the internal report [15], which comprises all details of the computations. The field patterns and properties of the computed eigenmodes are listed in a compendium attached to [15]. All computations for the internal report have been conducted by J. Heller. In addition to the results provided by the internal report, this article presents a comparison between results from SSC and a direct computation using CST Studio Suite® (CST) [16]. Note that

* The research leading to these results was supported by the German Bundesministerium für Bildung und Forschung, Land Berlin and grants of Helmholtz Association.
† thomas.flisgen@helmholtz-berlin.de

ISBN: 978-3-95450-200-4 doi:10.18429/JACoW-ICAP2018-TUPAG02

FIRST STEPS TOWARDS A NEW FINITE ELEMENT SOLVER FOR MOEVE PIC TRACKING*

Ursula van Rienen[1†], Dawei Zheng, Johann Heller, Christian Bahls
Institute of General Electrical Engineering, University of Rostock, 18059 Rostock, Germany
[1]also at Department Life, Light & Matter, University of Rostock, 18051 Rostock, Germany

Abstract

A relevant task in designing high-brilliance light sources based on high-current linear accelerators (e.g. Energy Recovery Linacs (ERLs)) consists in systematic investigations of ion dynamics in the vacuum chamber of such machines. This is of high importance since the parasitic ions generated by the electron beam turned out to be a current-limiting factor for many synchrotron radiation sources. In particular, the planned high current operation at ERL facilities requires a precise analysis and an accurate development of appropriate measures for the suppression of ion-induced beam instabilities. The longitudinal transport of ions through the whole accelerator plays a key role for the establishment of the ion concentration in the machine. Using the Particle-in-Cell (PIC) method, we started redesigning our code MOEVE PIC Tracking in order to allow for the fast estimation of the effects of ions on the beam dynamics. For that, we exchanged the previously used Finite Difference (FD) method for the solution of Poisson's equation within the PIC solver by a solver based on the Finite Element Method (FEM). Employing higher order FEM, we expect to gain improved convergence rates and thus lower computational times. We chose the Open Source Framework FEniCS for our new implementation.

INTRODUCTION

MOEVE was developed as a Particle-in-Cell (PIC) solver at the University Rostock. It is an abbreviation and stands for **M**ultigrid for n**o**n-**e**quidistant grids to sol**v**e Poisson's **e**quation. The software was originally developed in C by G. Pöplau et al. [1] and employs the Finite-Difference Technique (FD) to numerically discretize Poisson's equation. The discretized system of linear equations is solved iteratively by a geometric multigrid method.

MOEVE has been used successfully to simulate the interaction of electron beams with ionized residual gas [2, 3], several investigations for the clearing of ions with clearing electrodes and/or clearing gaps [4] and the simulation of transverse wake functions [5]. MOEVE has also been implemented in the tracking code GPT [6] and ASTRA [7].

Ion Clearing

Any residual gas in the vacuum chamber of an accelerator can be ionized rapidly by the electron beam. The resulting ion distribution is denoted as ion cloud. For many synchrotron radiation sources, these parasitic ions generated by the electron beam are a current-limiting factor. They often lead to beam instabilities, beam loss and they prevent a continuous filling of electron bunches into the ring shape machine.

In the existing synchrotron accelerators, mainly two strategies are used to ensure a minimum stability in standard operational regimes: clearing gaps and special electrodes for removing and neutralizing the ions. In certain high-current operating conditions ion effects are important, as they lead to beam instabilities. In particular, the planned high-current operation at ERL facilities requires a precise analysis and an accurate development of appropriate measures for the suppression of ion-induced beam instabilities [8].

The longitudinal transport of ions through the whole accelerator plays a key role for the establishment of the ion concentration in the machine. This aspect of the dynamics has implications on both the beam dynamics and the ion clearing efficiency but it has not been deeply studied up to now. In particular, the extent to which the accelerating resonators contribute to the transport is largely unclear. Thus, we are targeting a fast, systematic investigation of ion dynamics in the vacuum chamber of the machines involving the impact on the beam and and its application to reduce the effects related to ionized residual gas in high-current electron machines. This study follows our previous investigations on ion trapping in high-current storage rings and linear accelerators [2–4, 9, 10].

Prior Limitations of MOEVE Due to Finite Differences

Any PIC software consists of five different main modules. These are

1. Charge weighting
2. Discretization of Poisson's equation
3. Solver for Poisson's equation
4. Field interpolation at particles position
5. Update scheme of the particle distribution

MOEVE's current limitations, caused by the underlying FD discretization, affect the discretization and solution of Poisson's equation. A comparably large number of degrees of freedom (DOFs) are required for the accurate solution, especially because the tensor product grid in the FD method

* Work supported by the German Federal Ministry for Research and Education BMBF under contract 015K16HRA.
† ursula.van-rienen@uni-rostock.de

ISBN: 978-3-95450-200-4 doi:10.18429/JACoW-ICAP2018-TUPAG04

STATISTICAL ANALYSIS OF THE EIGENMODE SPECTRUM IN THE SRF CAVITIES WITH MECHANICAL IMPERFECTIONS*

A. Lunin†, T. Khabiboulline, N. Solyak, A. Sukhanov, V. Yakovlev, Fermilab, 60510 Batavia, USA

Abstract

The superconducting radio frequency (SRF) technology is progressing rapidly over the last decades toward high accelerating gradients and low surface resistance making feasible the particle accelerators operation with high beam currents and long duty factors. However, the coherent RF losses due to high order modes (HOMs) excitation becomes a limiting factor for these regimes. In spite of the operating mode, which is tuned separately, the parameters of HOMs vary from one cavity to another due to finite mechanical tolerances during cavities fabrication. It is vital to know in advance the spread of HOM parameters in order to predict unexpected cryogenic losses, overheating of beam line components and to keep stable beam dynamics. In this paper we present the method of generating the unique cavity geometry with imperfections while preserving operating mode frequency and field flatness. Based on the eigenmode spectrum calculation of a series of randomly generated cavities, we can accumulate the data for the evaluation of the HOM statistics. Finally, we describe the procedure for the estimation of the probability of the resonant HOM losses in the SRF resonators. The study of these effects leads to specifications of SRF cavity and cryomodule and can significantly impact the efficiency and reliability of the machine operation.

INTRODUCTION

Over recent decades the progress in SRF technology has made it feasible for a number of applications of the particle accelerators to operate in the continuous wave (CW) regime with a high beam current. There is an active demand on such machines based on multiple projects in the industry, high energy physics and material science, such as developing subcritical fission reactors based on an accelerator driven system (ADS), next generations of neutrino facilities and neutron spallation sources (PIP-II, ESS), radioactive ion beam facilities (RIBs) and free electron lasers (FELs) [1-6]. Variety of experimental programs often require a complex beam pattern and an ultra-short bunch length. Figure 1 shows typical examples of the dense beam frequencies spectrum in the PIP-II proton linac and the broadband power spectrum of wake fields generated by a series of 25 μm rms bunches in the LCLS-II cryomodule. Evidently a combination of a large average beam current, a high bunch repetition rate and a broadband generated wake fields might result in significant cavity rf losses. The most danger comes out of the trapped HOMs in a case of their coherent excitation by the beam. The later causes excessive cryogenic loads, overheating of beam line components and beam emittance dilution.

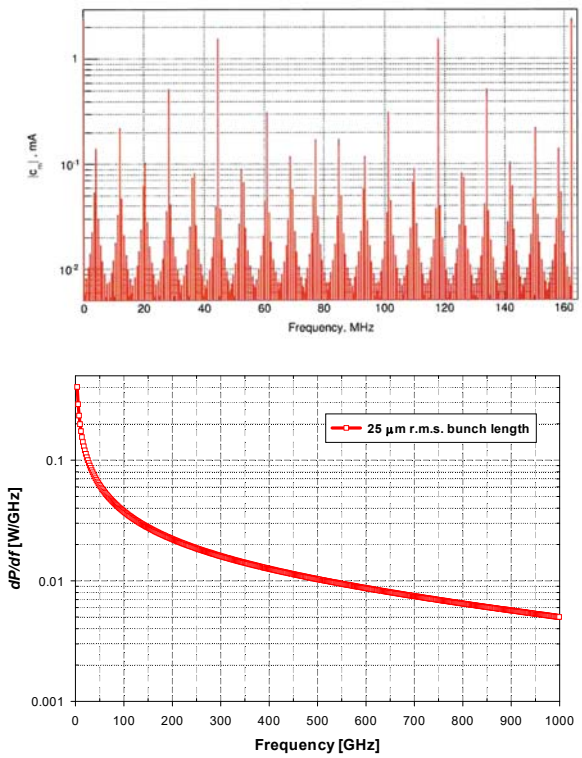

Figure 1: Beam frequency spectrum in the PIP-II linac (up) and power spectrum of wake fields generated by a series of ultra-short bunches in the LCLS-II cryomodule (down)

Due to a nature of SRF cavities they are very good resonance systems with multiple low loss eigenmodes with high intrinsic quality factors. For the coherent excitation one of the beam harmonics must coincide or be close to HOM frequencies. At the same time the HOM spectra in actual cavities will have significant frequency spreads comparing to the cavity with ideal geometry due to mechanical errors. Because of a randomness of mechanical errors, the resonant HOM excitation by the beam is inherently the probabilistic issue. The idea is illustrated on Figure 2, where the left sketch shows overlapping of the beam spectrum line and the HOM frequency spread with a high probability of coherent HOM excitation. The problem is complicated if we consider the propagating HOMs with frequencies above the beam pipe cut off. In this case the probability of mode trapping depends on the frequencies of neighbour cavities and, thus, taking into account the stochastic behaviour of cavity HOMs spectrum is essential for a proper analysis of the HOMs excitation.

* Work supported by Fermi Research Alliance, LLC, under Contract DE-AC02-07CH11359 with the U.S. DOE
† lunin@fnal.gov

ISBN: 978-3-95450-200-4 doi:10.18429/JACoW-ICAP2018-TUPAG07

EFFICIENT COMPUTATION OF LOSSY HIGHER ORDER MODES IN COMPLEX SRF CAVITIES USING REDUCED ORDER MODELS AND NONLINEAR EIGENVALUE PROBLEM ALGORITHMS*

H. W. Pommerenke†, J. D. Heller, U. van Rienen[1]
Institute of General Electrical Engineering, University of Rostock, Germany
[1]also at Department Life, Light & Matter, University of Rostock, Germany

Abstract

Superconducting radio frequency (SRF) cavities meet the demanding performance requirements of modern accelerators and high-brilliance light sources. For the operation and design of such resonators, a very precise knowledge of their electromagnetic resonances is required. The non-trivial cavity shape demands a numerical solution of Maxwell's equations to compute the resonant eigenfrequencies, eigenmodes, and their losses. For large and complex structures this is hardly possible on conventional hardware due to the high number of degrees of freedom required to obtain an accurate solution. In previous work it has been shown that the considered problems can be solved on workstation computers without extensive simplification of the structure itself by a combination of State-Space Concatenation (SSC) and Newton iteration to solve the arising nonlinear eigenvalue problem (NLEVP).

First, SSC is applied to the complex, closed and thus lossless RF structure. SSC employs a combination of model order reduction and domain decomposition, greatly reducing the computational effort by effectively limiting the considered frequency domain. Next, a perturbation approach based on SSC is used to describe the resonances of the same geometry subject to external losses. This results in a NLEVP which can be solved efficiently by Newton's method. In this paper, we expand the NLEVP solution algorithm by a contour integral technique, which increases the completeness of the solution set.

INTRODUCTION

Superconducting radio frequency (SRF) cavities are essential components of modern particle accelerators, as they provide the radio frequency (RF) electromagnetic fields used to accelerate charged particles to high energies. The design of RF cavities requires a precise knowledge of their resonant frequencies f, field distributions, and power losses P. This usually requires solving an eigenvalue problem, where the eigenvalues and eigenvectors correspond to the frequencies and field distributions, respectively. In this context, the eigenvectors are also denoted as eigenmodes of the cavity.

A dimensionless measure for power losses in general is the quality factor

$$Q = 2\pi f W/P, \tag{1}$$

which is the ratio between the energy loss per oscillation and the total energy W stored in the electromagnetic field. Generally, there are dielectric, magnetic, surface and external losses. The latter occur when energy is propagating out of the cavity through its openings, e.g. a coupler or the beam pipe. For an SRF cavity, the external losses are several orders of magnitude larger than other loss mechanisms, since the structure is both superconducting and evacuated [1]. Therefore, the external quality factor Q_{ext} is often equivalent to the total Q (and in the following denoted as such). External losses are of significant importance for eigenmodes, whose resonant frequencies are larger than that of the operating mode used for acceleration. They are denoted as higher order modes (HOM). These usually unwanted modes are excited by the current of the passing beam and may influence the beam in an unwanted manner, e.g. by deviation from its optimum trajectory or emittance growth [2, 3]. One usually designs cavities such that HOM energy is dissipated quickly and the mode is practically completely damped before the next particle bunch arrives. The structures must thus feature low Q factors regarding the HOMs. Besides available openings like the beam pipe or the power coupler, HOM couplers are utilized. Nevertheless, there exist additional HOMs whose interaction with the couplers is almost non-existent and which therefore have very high Q factors. Identification and computation of these trapped modes is particularly important in SRF cavity design [1, 4, 5].

Even for comparatively simple structures, an analytical solution of Maxwell's equations [6] is not available. Numerical methods such as the Finite Element Method (FEM) [7] or Finite Integration Technique (FIT) [8, 9] are therefore employed. If one solely considers closed lossless cavities, this leads to a linear eigenvalue problem (LEVP), whose solution can be acquired by a variety of methods. However, the precise computation of external losses is accomplished by applying suitable boundary conditions to the cavity's openings leading to a complex-valued, nonlinear eigenvalue problem (NLEVP), whose solution requires significantly more effort.

The above-mentioned numerical methods show disadvantageous scaling behavior regarding size and complexity of the structure. Especially large and complex structures, e.g. a sequence of cavities and couplers like in Fig. 1, require many degrees of freedom (DOF) for an accurate solution. In a direct approach, these problems can only be solved on powerful computational infrastructure which is costly and rarely available. Another possibility is to only con-

* This work has been supported by the German Federal Ministry of Education and Research (grant no. 05K13HR1).
† Currently also at CERN, Geneva, Switzerland.
Email: hermann.pommerenke@uni-rostock.de

ISBN: 978-3-95450-200-4 doi:10.18429/JACoW-ICAP2018-TUPAG10

NONLINEAR OPTICS AT UMER: LESSONS LEARNED IN SIMULATION

K. Ruisard*, Oak Ridge National Laboratory, Oak Ridge, Tennessee
B. Beaudoin, I. Haber, D. Matthew, and T. Koeth,
Institute for Research in Electronics and Applied Physics, College Park, Maryland

Abstract

Design of accelerator lattices with nonlinear optics to suppress transverse resonances is a novel approach and may be crucial for enabling low-loss high-intensity beam transport. Large amplitude-dependent tune spreads, driven by nonlinear field inserts, damp resonant response to driving terms. This presentation will focus on simulations of the UMER lattice operated as a quasi-integrable system (one invariant of transverse motion) with a single strong octupole insert. We will discuss the evolution of simulation models, including the observation of losses associated with the original operating point near a fourth-order resonance. Other operating points farther from this resonance are considered and shown to be more promising.

INTRODUCTION

Nonlinear integrable optics (NLIO) is a novel implementation of focusing optics for accelerator rings. Proposed by Danilov and Nagaitsev [1], this technique is expected to mitigate resonant beam losses in circular machines. This is of particular interest at the "intensity frontier," where even low-level losses can threaten machine components and personnel safety.

Nonlinear terms in the transverse focusing potential have long been known to counteract resonant interactions in rings. In the presence of nonlinear forces, the coupling of regular driving terms to particle orbits is reduced and collective motions such as envelope modes decohere. The most well-known example is octupole-induced Landau damping, in which an octupole-induced tune shift in the particle distribution can damp transverse collective instability [2]. Simulation studies of NLIO systems shows fast decoherence of envelope modes, which are a known mechanism for halo formation [3].

In general, introducing nonlinearities reduces dynamic aperture due to chaotic orbits near resonance overlap, which has previously restricted the use of nonlinear correctors to weak perturbations of the linear Hamiltonian. The breakthrough of NLIO is the identification of a family of highly nonlinear, physically-realizable magnetic potentials in which transverse particle orbits conserve coupled, quadratic invariants of motion that are distinct from the Courant-Snyder invariants.

This paper describes progress towards an experimental demonstration of quasi-integrable optics (QIO) at the University of Maryland Electron Ring (UMER). This variation on the NLIO theory utilizes an octupole potential (rather than the fully-integrable fields discussed in reference [1]) that allows one invariant of transverse motion: the Hamiltonian in normalized coordinates[1]:

$$H_N = \frac{1}{2}\left(p_{x,N}^2 + p_{y,N}^2 + x_N^2 + y_N^2\right) + \frac{\kappa}{4}\left(x_N^4 + y_N^4 - 6y_N^2 x_N^2\right). \quad (1)$$

Although motion is not fully integrable (only one invariant for 2D motion), the invariant corresponds with particle amplitude resulting in chaotic but bounded motion [3].

This proceedings discusses simulation results for the QIO as designed for UMER. We probe dynamics within the octupole insert "as designed" and show clear improvement for one insert configuration over another. We also compare transport properties across a range of tune operating points while seeking to maximize octupole-induced tune spread and preserve stable particle orbits.

NONLINEAR OPTICS PROGRAM AT UMER

UMER is a scaled, 10 keV ($\beta = 0.195$) electron ring designed for the study of high-intensity beam dynamics relevant to higher-energy ion rings. Different space charge densities are selected by aperturing the beam near the source, in the range $\nu/\nu_0 = 0.85 \rightarrow 0.14$ for nominal UMER tune 6.7 (incoherent shifts $\Delta\nu = 0.3 \rightarrow 5.7$) [4, 5].

A proof-of-principle QIO experiment has been designed for UMER. The experiment layout, shown in Figure 1, includse a single octupole insert element. This effort uses existing UMER quadrupole optics to meet requirements for linear lattice focusing, which are outlined below. The RMS envelope solution for the linear optics as designed is shown in Figure 2. Details of implementing this solution in the UMER ring are discussed in references [6, 7]. A custom-designed octupole insertion, consisting of seven independently-wired octupole PCBs, has been fabricated and is capable of meeting requirement 2 to within RMS error of 2%. Design of the octupole element is covered in reference [8].

For initial tests of the QIO concept, we desire beams with lower space-charge tune shift than the typical UMER range, as the NLIO/QIO theory is based on single-particle dynamics. An ultra-low-current, high emittance beam was characterized for use in initial experiments. A beam with current 10 to 100 μA is generated by operating the UMER triode electron gun in voltage amplification mode. This beam has low tune shift due to its large emittance; quadrupole scan emittance measurement at 40 μA output current returns

* ruisardkj@ornl.gov

[1] $x_N \equiv \frac{x}{\sqrt{\beta_x(s)}}$, $p_{x,N} \equiv p_x\sqrt{\beta_x(s)} + \frac{\alpha_x x}{\sqrt{\beta_x(s)}}$

ISBN: 978-3-95450-200-4 doi:10.18429/JACoW-ICAP2018-TUPAG11

ESS ACCELERATOR LATTICE DESIGN STUDIES AND AUTOMATIC SYNOPTIC DEPLOYMENT

Y. Levinsen, M. Eshraqi, T. Grandsaert, A. Jansson, H. Kocevar, Ø. Midttun, N. Milas,
R. Miyamoto, C. Plostinar, A. Ponton, R. de Prisco, T. Shea, ESS, Lund, Sweden
H. D. Thomsen, Aarhus University, Aarhus, Denmark

Abstract

The European Spallation Source is currently under construction in the south of Sweden. A highly brilliant neutron source with a 5 MW proton driver will provide state of the art experimental facilities for neutron science. A peak proton beam power in the accelerator of 125 MW means that excellent control over the beam losses becomes essential. The beam physics design of the ESS accelerator is in a TraceWin format, for which we have developed revision control setup, automated regression analysis and deployment of synoptic viewer and tabulated spreadsheets. This allows for an integrated representation of the data that are always kept synchronized and available to other engineering disciplines. The design of the accelerator lattice has gone through several major and minor iterations which are all carefully analysed. In this contribution we present the status of the latest studies, which includes the first complete end-to-end study beginning from the ion source.

INTRODUCTION

The construction of the European Spallation Source (ESS) is currently ongoing at full force [1], with the first part of the accelerator under commissioning now in the second half of 2018. The ESS is designed to provide the neutron instruments with the world brightest neutron source, coming from the spallation process of a 5 MW proton beam hitting a rotating tungsten target [2]. ESS is built outside of Lund, Sweden, and is a European Infrastructure Research Consortium (ERIC) [3], with 12 founding member countries. A large fraction of the contributions from the member states to the ESS project is done in form of in-kind contracts, and there are currently 38 in-kind partners involved in the ESS project. The ESS user programme is planned to start in 2023.

The ESS accelerator layout is shown in Fig. 1. A microwave discharge ion source is producing approximately 3 ms of stable proton beam pulse of 75 keV at around 70 mA, which is accelerated through an RFQ and DTL, together with two transport sections that make up the normal-conducting front end. After that there are three families of superconducting cavities that bring the beam energy up from around 90 MeV to the final 2 GeV beam energy that is painted onto the rotating tungsten target.

To maintain control over the changes in the beam physics design lattice, and to try to keep the beam physics simulations as close to reality as possible, we have developed a deployment procedure for changing the beam physics lattice files. This procedure involves the use of modern revision control systems, continuous integration, and scripting languages for automated deployment on an interactive web page. Tools which will be familiar to any programmer, but might be a less obvious use case for physicists.

In the second part of this paper, we will go through our recent progress with the large scale integrated error studies of the entire machine, starting from the ion source and up to the target. These studies are essential to confirm that the design can deliver a performance according to specifications, while keeping the losses low enough to not cause problems in the machine.

AUTOMATED LATTICE DEPLOYMENT SETUP

A challenge most accelerator projects face is how to translate beam physics design to accurate locations for all machine elements. Further, during the transition from a pure design phase to an installation and commissioning phase, the physics design might still change, which one wants to make sure to propagate to the appropriate databases when it involves changing physical locations and/or dimensions, or changes such as polarity switches which involves cable routing changes. In the end, most projects end up with some discrepancies between the files used for beam physics studies, and the actual machine installed. This complicates the work for beam physicists, who then need to evaluate which differences may have a relevant impact to beam physics studies, and need to go hunting for errors whenever there is a discrepancy betwen the machine behaviour and what is expected from simulations.

For the ESS, we have predominantly been using TraceWin [4, 5] to simulate the machine, so the beam physics files are stored in TraceWin format. In the beginning these were manually updated and kept in a synchronised folder, with one person being the main responsible for collecting the files for the different sections of the machine and combining to an integrated lattice description. An improvement on this procedure was to store all lattice files in a revision control system (git), so that all changes were authored and could be tracked properly. We extended this with a slightly stricter change control process for what we define as the baseline branch, in order to make sure that all involved parties are aware of and agree to changes to the official machine description.

This quickly ended up being the most accurate and up to date description of element locations, which typically means engineers and other non-physicists started being interested in the data. These users do not know the structure of the TraceWin format, and further, the TraceWin files are not

ISBN: 978-3-95450-200-4 doi:10.18429/JACoW-ICAP2018-TUPAG13

S-BASED MACRO-PARTICLE SPECTRAL ALGORITHM FOR AN ELECTRON GUN

Paul M. Jung, Thomas Planche, TRIUMF, Vancouver, Canada

Abstract

We derive a Hamiltonian description of a continuous particle distribution and its electrostatic potential from the Low Lagrangian. The self consistent space charge potential is discretized according to the spectral Galerkin approximation. The particle distribution is discretized using macro-particles. We choose a set of initial and boundary conditions to model the TRIUMF 300keV thermionic DC electron gun. The field modes and macro-particle coordinates are integrated self-consistently. The current status of the implementation is discussed.

INTRODUCTION

The section of beamline we are trying to model includes the electron gun (Fig. 1) and one solenoid, a total length of 57 cm up to the first view screen. The electrons are emitted from a hot cathode. An RF grid is placed a fraction of a millimetre downstream from the cathode. It is used to modulate the emission of electrons at 650 MHz. Electrons are accelerated to 300 keV using a DC field. The distance between the cathode and the ground electrode is 12 cm. The emitting surface of the cathode has a radius of 4 mm. The nominal bunch charge is 15 pC with a bunch length of 130 ps, see [1]. The solenoid enables us to adjust the phase advance between the cathode and the view screen. At a particular phase advance, we can use the electron beam to create an image of the RF grid on the view screen see Fig. 2. Scanning the phase advance enables us to measure the transverse phase space distribution using tomography [2]. Our objective is to reproduce these measurements using an algorithm derived from the least action principle like in [3–5]. The description of thermionic emission and effects from the grid are outside the scope of this model.

Following classical field theory conventions, let an over dot '$\cdot$' represent an explicit derivative with respect to time, and similarly a prime '$\prime$' denotes a partial derivative with respect to z. We write the vectors that lie in the transverse xy plane with a lower '$\perp$'. For example: $\mathbf{x}_\perp$ is the vector $(x, y, 0)$.

CONTINUOUS MODEL

We start from the Low Lagrangian [6] which is a sum of two integrals:

$$L = \int \mathrm{d}^3\mathbf{x}_0 \mathrm{d}^3\dot{\mathbf{x}}_0 \, \mathcal{L}_p(\mathbf{x}(\mathbf{x}_0, \dot{\mathbf{x}}_0, t), \dot{\mathbf{x}}(\mathbf{x}_0, \dot{\mathbf{x}}_0, t); \mathbf{x}_0, \dot{\mathbf{x}}_0, t) + \int \mathrm{d}^3\bar{\mathbf{x}} \, \mathcal{L}_f(\phi, \mathbf{A}; \bar{\mathbf{x}}, t), \tag{1}$$

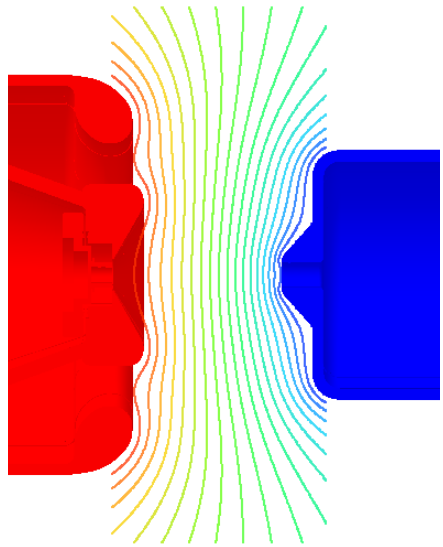

Figure 1: OPERA Model of the 300 keV TRIUMF electron gun with equipotential lines of the electric potential.

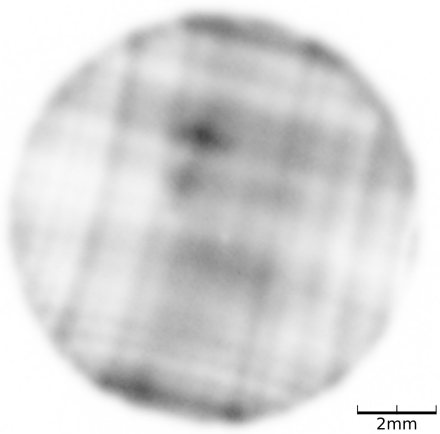

Figure 2: The view screen image, after the first solenoid.

where the Lagrangian densities are:

$$\mathcal{L}_p(\mathbf{x}, \dot{\mathbf{x}}; \mathbf{x}_0, \dot{\mathbf{x}}_0, t) = f(\mathbf{x}_0, \dot{\mathbf{x}}_0) \left(-mc^2 \sqrt{1 - |\dot{\mathbf{x}}|^2/c^2} - q\phi(\mathbf{x}, t) + q\dot{\mathbf{x}} \cdot \mathbf{A}(\mathbf{x}, t) \right), \tag{2}$$

$$\mathcal{L}_f(\phi, \mathbf{A}; \mathbf{x}, t) = \frac{\epsilon_0}{2} \left(\left| \nabla\phi(\mathbf{x}, t) + \dot{\mathbf{A}}(\mathbf{x}, t) \right|^2 - c^2 \left| \nabla \times \mathbf{A}(\mathbf{x}, t) \right|^2 \right). \tag{3}$$

and $\bar{x}$ is a dummy variable of integration.

To describe the self field we make the assumption that in the centre of mass frame the self field is completely described by the scalar potential $\varphi(\mathbf{x}, t)$, and the vector potential is zero. We assume that the beam is travelling in the positive z-direction, with unit vector $\hat{z}$. Now, by applying an active

ISBN: 978-3-95450-200-4 doi:10.18429/JACoW-ICAP2018-TUPAG14

CONSTRAINED MULTI-OBJECTIVE SHAPE OPTIMIZATION OF SUPERCONDUCTING RF CAVITIES TO COUNTERACT DANGEROUS HIGHER ORDER MODES

M. Kranjčević*, P. Arbenz, Computer Science Department, ETH Zurich, 8092 Zürich, Switzerland
A. Adelmann, Paul Scherrer Institut (PSI), 5232 Villigen, Switzerland
S. Gorgi Zadeh, U. van Rienen, University of Rostock, 18059 Rostock, Germany

Abstract

High current storage rings, such as the Z operating mode of the FCC-ee (FCC-ee-Z), require superconducting radio frequency (RF) cavities that are optimized with respect to both the fundamental mode and the dangerous higher order modes (HOMs). In this paper, in order to optimize the shape of the RF cavity, a constrained multi-objective optimization problem is solved using a massively parallel implementation of an evolutionary algorithm. Additionally, a frequency-fixing scheme is employed to deal with the constraint on the frequency of the fundamental mode. Finally, the computed Pareto front approximation and an RF cavity shape with desired properties are shown.

INTRODUCTION

Superconducting RF cavities are mainly optimized with respect to the properties of the fundamental mode [1]. However, in high current machines, such as the FCC-ee-Z [2], monopole and dipole modes are major sources of beam instability. The first monopole HOM band can be untrapped by enlarging the beam pipe radius, but the first dipole band remains trapped in the cavity and requires a special damping mechanism. In order to ease the HOM damping of the first dipole band, in this paper, a multi-objective shape optimization of a single-cell cavity that takes into account both the fundamental mode and the first dipole band is performed. The optimization algorithm is described on the concrete problem of optimizing the shape of the axisymmetric cavity for the FCC-ee-Z, but the same method can be used with other objectives and parameterizations.

MULTI-OBJECTIVE OPTIMIZATION

In this paper four objective functions have to be optimized simultaneously. First, the distance between the frequency of the first dipole mode, f_1, which is typically the TE_{111} mode, and the frequency of the fundamental mode, f_0, has to be maximized. Second, the distance between f_1 and the frequency of the second dipole mode, f_2, which is typically the TM_{110} mode, has be minimized. These two objectives simplify the design of the HOM couplers for damping the first dipole band. Third, the sum of the transverse shunt impedances of the dipole modes has to be minimized. The following definition of the transverse shunt impedance for the dipole modes is used [3]

$$\frac{R}{Q}_{\perp} = \frac{\left(V_{||(r=r_0)} - V_{||(r=0)}\right)^2}{k^2 r_0^2 \omega U},$$

where k is the wave number, r_0 the offset from the axis, ω the angular frequency, and U the stored energy. Fourth, $G_0 \cdot R/Q_0$ (G_0 is the geometry factor) of the fundamental mode has to be maximized, since it is inversely related to the dissipated power on the surface of the cavity [4]. In addition to these four objectives, f_0 has to be fixed to the operating frequency of 400.79 MHz.

Seven variables (R_{eq}, R_i, L, A, B, a and b) uniquely describe the shape of an elliptical cavity as shown in Fig. 1. The wall slope angle α can be computed from these design variables and, in order to avoid re-entrant shape cavities, it must be at least 90°.

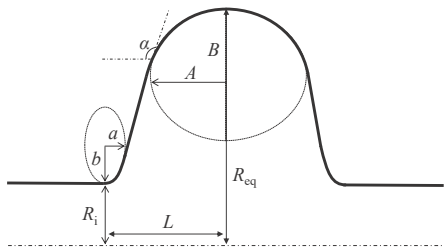

Figure 1: Parameterization of a single-cell elliptical cavity.

This can be formulated as the constrained multi-objective optimization problem

$$\min_{R_i, L, A, B, a, b} \quad (\overbrace{f_0 - f_1}^{F_1}, \overbrace{|f_1 - f_2|}^{F_2}, \overbrace{\frac{R}{Q}_{\perp 1} + \frac{R}{Q}_{\perp 2}}^{F_3}, \overbrace{-G_0 \cdot \frac{R}{Q}_0}^{F_4}),$$
$$\text{subject to} \quad f_0 = 400.79\ \text{MHz} \ \text{ and } \ \alpha \geq 90°. \qquad (1)$$

Since in a single-cell cavity there is no restriction on the length $2L$ of the cell (because the particle only passes through one cell), and since this length highly affects f_1, L is also taken to be a design variable. On the other hand, the variable R_{eq} has the highest influence on the value of f_0, so it is not considered to be a design variable in the optimization, but rather used to tune f_0 to the desired value.

As part of the field leaks into the beam pipe, the cell and the beam pipe are simulated together and f_0 is tuned to 400.79 MHz taking the beam pipe effect into account. In this paper, the beam pipe length is set to the value of the wave length $\lambda = 748$ mm.

* marija.kranjcevic@inf.ethz.ch

ISBN: 978-3-95450-200-4 doi:10.18429/JACoW-ICAP2018-TUPAG17

BEAMLINE MAP COMPUTATION FOR PARAXIAL OPTICS

B. Nash*, N. Goldring, J. P. Edelen, S. Webb
RadiaSoft LLC, Boulder, CO, USA

Abstract

Modeling of radiation transport is an important topic tightly coupled to many charged particle dynamics simulations for synchrotron light sources and FEL facilities. The radiation results from the electron dynamics and then passes through beamlines, either directly to an experiment or may be recirculated back to interact with the electron beam in the case of an FEL oscillator. The Wigner function representation of these wavefronts have been described in the literature, and is the closest relation to the phase space description of charged particle dynamics. We describe this formalism and the computation of phase space maps using the code SRW, applying this to the case of a 4 crystal FELO 1:1 imaging beamline, resulting in a substantial speed-up in computation time.

INTRODUCTION

Optical beamlines for radiation transport are crucial components of many scientific facilities. They may be used to transport radiation from the electron beam source in a synchrotron light source, or in recirculation optics in a free electron laser oscillator (FELO) to improve longitudinal coherence of the radiation. Numerous codes exist to model the radiation transport through the beamline elements typically either using a ray tracing, geometrical optics approach (e.g. SHADOW [1]), or a physical optics wavefront propagation approach (e.g. SRW [2]). The wavefront propagation captures more of the optical physics, but can be highly intensive computationally.

For FELO and synchrotron light source modeling, one requires many passes of radiation through a beamline, while varying either the initial conditions, or some beamline parameters. A more compact representation of a beamline is desired for such calculations.

In this paper, we consider a map based approach to beamline modeling that, once computed, allows a large range of initial conditions to be rapidly transported through the beamline. The formalism we use for representing the wavefront is based on the Wigner function, pioneered in x-ray optics by K. J. Kim [3]. Although the general non-linear map applied to the Wigner function may be quite complex, in the case of linear transport (so-called ABCD matrix, in the optics literature), the transformation is quite straight forward.

We provide a proof of principle for this method, applied to an FELO recirculation optics beamline, with radiation transport of increasing complexity. The beamline is shown in Fig. 1. The radiation transport starts at the end of the undulator and diffracts off the crystals in Bragg geometry. A single ideal lens is used for focussing the radiation back to the beginning of the undulator for the next pass. We first consider Gaussian wavefronts, in which case, only transport of second moments is necessary. We set up the beamline in SRW and propagate the initial wavefront. We also compute the transfer matrix for the beamline to transport the Wigner function. For the Gaussian case, only the moments need be transported, but we also apply the method to the numerical Gaussian to check our calculation of the Wigner function. Finally, we consider a non-Gaussian case of an $m_x = 2$ Hermite Gaussian mode, to show the generality of the method. In each case, we compare the SRW simulation to the linear transport of the Wigner function, to confirm that the method is sound. One important difference between our Wigner function transport and the wavefront propagation, is the absorption effect in the crystals. However, since ideal crystals don't affect the wavefront distribution, only the intensity, the two effects can be treated separately.

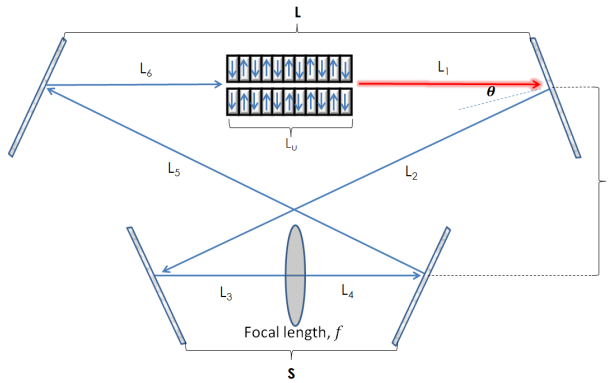

Figure 1: Four crystal FELO beamline schematic as described in reference [4].

LINEAR PARAXIAL OPTICS PROPAGATION

We start by briefly reviewing the evolution equations for a wavefront with wavelength λ propagating through empty space. By this means we will set our notation, and clarify the issue of separability, which we will be assuming. We consider one component of an electric field travelling in the z direction, which we write as

$$E(x, y, z; t) = \bar{E}(x, y, z)e^{i(kz-\omega t)}, \quad (1)$$

where $k = \frac{2\pi}{\lambda}$ and $\omega = ck$. The paraxial Helmholtz equation for the evolution of the electric field in free space is given by

$$\nabla_\perp^2 E + 2ik\frac{\partial E}{\partial z} = 0, \quad (2)$$

where

$$\nabla_\perp^2 = \frac{\partial^2}{\partial x^2} + \frac{\partial^2}{\partial y^2} \quad (3)$$

* bnash@radiasoft.net

ISBN: 978-3-95450-200-4 doi:10.18429/JACoW-ICAP2018-TUPAG20

COMPUTATIONAL BEAM DYNAMICS REQUIREMENTS FOR FRIB*

P. N. Ostroumov†, Y. Hao, T. Maruta, A. Plastun, T. Yoshimoto, T. Zhang, Q. Zhao
Facility for Rare Isotope Beams, Michigan State University, East Lansing, MI, USA

Abstract

The Facility for Rare Isotope Beams (FRIB) being built at Michigan State University moved to the commissioned stage in the summer of 2017. There were extensive beam dynamics simulations in the FRIB driver linac during the design stage. Recently, we have used TRACK and IMPACT simulation codes to study dynamics of ion beam contaminants extracted from the ECR together with main ion beam. The contaminant ion species can produce significant uncontrolled losses after the stripping. These studies resulted in development of beam collimation system at relatively low energy of 17 MeV/u and room temperature bunchers instead of originally planned SC cavities. Commissioning of the Front End and the first 3 cryomodules enabled detailed beam dynamics studies experimentally which were accompanied with the simulations using above-mentioned beam dynamics codes and envelope code FLAME with optimizers. There are significant challenges in understanding of beam dynamics in the FRIB linac. The most computational challenges are in the following areas: (1) Simulation of the ion beam formation and extraction from the ECR; (2) Development of the virtual accelerator model available on-line both for optimization and multi-particle simulations. The virtual model should include realistic accelerator parameters including device misalignments; (3) Large scale simulations to support high-power ramp up of the linac with minimized beam losses; (4) Extension of the existing codes for large scale simulations to support tuning of fragment separators for selected isotopes.

INTRODUCTION

The Facility for Rare Isotope Beams (FRIB) currently being built at Michigan State University (MSU) is the next generation facility for rare isotope science. The FRIB includes a high-power driver accelerator, a target, and fragment separators. The FRIB driver linac will provide stable nuclei accelerated to 200 MeV/u for the heaviest uranium ions and higher energies for lighter ions with 400 kW power on the target [1]. FRIB features a continuous wave (CW) linac with a room-temperature 0.5 MeV/u front-end followed by a superconducting radiofrequency (SRF) linac consisting of 4 types of niobium cavities. The first SRF section includes quarter-wave resonators (QWR) with β_{OPT}=0.041 and β_{OPT}=0.085 which accelerate ion beams from 0.5 MeV/u to ~20 MeV/u at the charge stripper. The optimal beta is defined as relative velocity, β_{OPT}, where the maximum transit time factor T is achieved. The ion beams are further accelerated with the half-wave resonators (HWR) of β_{OPT} =0.29 and β_{OPT} =0.53. Total 316 SRF cavities are used for acceleration to the design energy of 200 MeV/u for heaviest uranium ions. 400 kW accelerated ion beams will be delivered to the target which is followed by a large acceptance high resolution fragment separator. While many isotopes will be studied in the in-flight experiments, FRIB will use upgraded National Superconducting Cyclotron Laboratory (NSCL) facilities to prepare and re-accelerate stopped isotopes up to 12 MeV/u. Currently, the re-accelerator (ReA3), consisting of a radiofrequency quadrupole (RFQ) and a superconducting radio-frequency (SRF) linac provides 3 MeV/u rare isotope beams for experiments.

The layout of the FRIB is shown in Fig. 1.

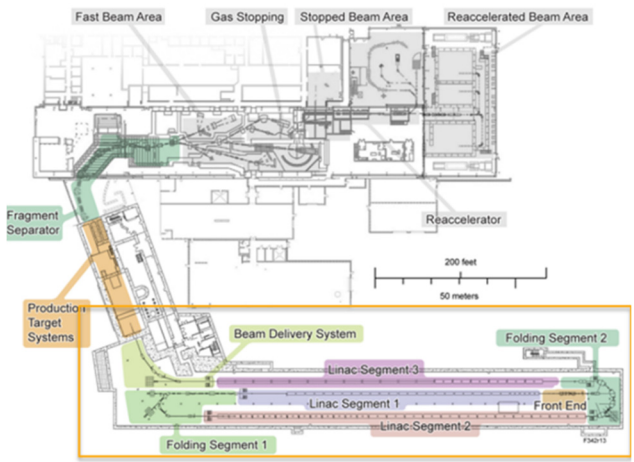

Figure 1: Layout of the FRIB driver accelerator, target, fragment separator, re-accelerator and existing infrastructure. The driver linac consist of three straight segments, LS1, LS2, LS3 and two folding segments FS1 and FS2.

DRIVER LINAC

Due to CW mode of the FRIB driver linac, the final beam power of 400 kW can be achieved with a low beam current which is below 1 emA for all ion species. The space charge effects are mostly negligible over the entire linac except in the ion source and low energy beam transport (LEBT). FRIB linac will be equipped with the state-of-the art high intensity superconducting ECR ion source capable to produce required intensity of heaviest ions in a single charge state. However, to operate the SC ECR with a large margin the linac was designed to accelerate two charge states of heaviest ions (e.g. U^{33+} and U^{34+}) up to the stripper [2]. To meet power requirement, a multiple charge state acceleration for the most ions heavier than argon is foreseen after the stripping at ~17 MeV/u [3].

In the FRIB design stage we have evaluated beam dynamics of the most critical beam of uranium with high statistics simulations in realistic conditions with all types of

* Work supported by the U.S. Department of Energy Office of Science under Cooperative Agreement DE-SC0000661 and the National Science Foundation under Cooperative Agreement PHY-1102511, the State of Michigan and Michigan State University.
† ostroumov@frib.msu.edu

ISBN: 978-3-95450-200-4 doi:10.18429/JACoW-ICAP2018-TUPAG21

NOVEL, FAST, OPEN-SOURCE CODE FOR SYNCHROTRON RADIATION COMPUTATION ON ARBITRARY 3D GEOMETRIES

Dean Andrew Hidas*, Brookhaven National Laboratory, Upton, NY, USA

Abstract

Open Source Code for Advanced Radiation Simulation (OSCARS) is an open-source project (https://oscars.bnl.gov) developed at Brookhaven National Laboratory for the computation of synchrotron radiation from arbitrary charged particle beams in arbitrary and time-dependent magnetic and electric fields on arbitrary geometries in 3D. Computational speed is significantly increased with the use of built-in multi-GPU and multi-threaded techniques which are suitable for both small scale and large scale computing infrastructures. OSCARS is capable of computing spectra, flux, and power densities on simple surfaces as well as on objects imported from common CAD software. It is additionally applicable in the regime of high-field acceleration. The methodology behind OSCARS calculations will be discussed along with practical examples and applications to modern accelerators and light sources.

INTRODUCTION

OSCARS [1] is an open source software developed at Brookhaven National Laboratory (BNL). OSCARS is a general purpose code for the calculation of radiation from charged particles in motion. Primary uses are for synchrotron and accelerator facilities where photon density distributions and heat loads on accelerator and beam-line equipment is of interest. This software allows for the calculation of these properties on arbitrary shaped surfaces in 3 dimensions. Recently added features include the ability to import surface models directly in the common Computer Aided Design (CAD) STL format and the implementation of of time dependent magnetic and electric source fields.

The core code is written in modern C++ for speed and has a python extension which serves as the main application programming interface (API). The API was written in python for ease of use and integrability by the larger scientific community. Currently OSCARS is available for Python 2.7 and Python 3+, for Linux, OS X, and Windows operating systems.

Throughout this paper the 2 example undulators referred to (U49 and EPU49) have a period of 49 mm, 55 periods plus terminating fields, and a peak magnetic field of 1 Tesla. U49 is a planar undulator with the only non-zero component of the magnetic field $\vec{B}$ being a sinusoidally varying B_v (vertical component). EPU49 is an elliptically polarizing undulator where B_h (horizontal component) and B_v are sinusoidally varying with the same peak magnitude, but phase shifted by $\pi/2$ relative to each other while B_l (longitudinal component) remains zero. The beam parameters used in these simulations are that of the NSLS-II 6.6 m straight sections with a beam energy $E = 3$ GeV, energy spread $\Delta E/E = 0.001$, emittance $\epsilon_{\mathrm{h,v}} = [0.9, 0.008]$ nm rad, and beta function in the center $\beta_{\mathrm{h,v}} = [1.5, 0.8]$ m.

* dhidas@bnl.gov

PARTICLE BEAMS

Particle beams in OSCARS are defined by particle mass, energy, current, and their position and direction. Optionally one can include the emittance ($\epsilon_{\mathrm{h,v}}$), beta function ($\beta_{\mathrm{h,v}}$), and energy spread ($\Delta E/E$). In multi-particle simulations the energy, initial position, and initial momentum are sampled accordingly assuming a Gaussian distribution of the position (σ) and momentum (σ'). OSCARS also allows for the definition of multiple beams which are sampled randomly according to their relative weights given. Any beam direction is valid in OSCARS. For convenience several predefined beams exist in OSCARS, for example in this case "NSLSII-ShortStraight".

MAGNETIC AND ELECTRIC FIELDS

Several field types (applicable to both magnetic and electric fields) are available in OSCARS. These source fields may be time dependent, static, or any combination therein. Simple parameters exist for configuring any static field as a time-dependent sinusoidal resonant field with a phase offset. Some common built-in fields include uniform fields in a given range, Gaussian fields, sinusoidal undulator (wiggler) fields with terminating fields, user input python functions, and 1D, 2D, and 3D discrete field data. In the case of the 1D discrete field data, the field points do not need to be uniformly distributed in space as OSCARS will regularize it by interpolation for internal use and fast internal field lookup. OSCARS also has an interpolating tool (using a cubic spline method) in the case that you have field data measured at several parameter points (such as undulator gap, but not restricted to this) but wish to use the field at an intermediate point. Several input data formats are implemented for convenience.

CALCULATION OF ELECTRIC FIELD

Particle trajectories are calculated in 3D according to the relativistic Lorentz equation given in Eq. (1) using a fourth-order Runge-Kutta (RK4) algorithm or an optional adaptive step RK4 method. Care is taken in the RK4 method implementation to avoid $\beta \geq 1$ by an iterative step-halving method until the criteria $\beta < 1$ is satisfied in for the trajectory propagation of Eq. (1):

$$\frac{\mathrm{d}\vec{p}}{\mathrm{d}t} = q(\vec{E} + c\vec{\beta} \times \vec{B}). \quad (1)$$

ISBN: 978-3-95450-200-4 doi:10.18429/JACoW-ICAP2018-TUPAG22

MAIN AND FRINGE FIELD COMPUTATIONS FOR THE ELECTROSTATIC QUADRUPOLES OF THE MUON *g*-2 EXPERIMENT STORAGE RING*

Eremey Valetov[1†] and Martin Berz[‡], Michigan State University, East Lansing, MI 48824, USA
[1]also at Lancaster University and the Cockcroft Institute, UK

Abstract

We consider semi-infinite electrostatic deflectors with plates of different thickness, including plates with rounded edges, and we calculate their electrostatic potential and field using conformal mappings. To validate the calculations, we compare the fringe fields of these electrostatic deflectors with fringe fields of finite electrostatic capacitors, and we extend the study to fringe fields of adjacent electrostatic deflectors with consideration of electrostatic induction, where field falloffs of semi-infinite electrostatic deflectors are slower than exponential and thus behave differently from most magnetic fringe fields. Building on the success with electrostatic deflectors, we develop a highly accurate and fully Maxwellian conformal mappings method for calculation of main fields of electrostatic particle optical elements. A remarkable advantage of this method is the possibility of rapid recalculations with geometric asymmetries and mispowered plates. We use this conformal mappings method to calculate the multipole terms of the high voltage quadrupole used in the storage ring of the Muon *g*-2 Experiment (FNAL-E-0989). Completing the methodological framework, we present a method for extracting multipole strength falloffs of a particle optical element from a set of Fourier mode falloffs. We calculate the quadrupole strength falloff and its effective field boundary (EFB) for the Muon *g*-2 quadrupole, which has explained the experimentally measured tunes, while simple estimates based on a linear model exhibited discrepancies up to 2%.

INTRODUCTION

Methods for measurement of anomalous magnetic dipole moment (MDM) and electric dipole moment (EDM) using a storage ring rely on electrostatic particle optical elements, including the Muon *g*-2 Experiment's storage ring at FNAL, which uses electrostatic quadrupoles with a curved reference orbit. Accordingly, it is necessary to accurately model main and fringe fields of electrostatic elements. In particular, inaccurate treatment of fringe fields of electrostatic elements provides a mechanism for energy conservation violation.

In this research, we address the problem of accurate representation for fringe fields of electrostatic deflectors, as well as for main and fringe fields of electrostatic quadrupoles with the specific case of the Muon *g*-2 quadrupole [1] considered. Our model of the main field of the Muon *g*-2 quadrupole allows rapid recalculations with geometric asymmetries and mispowered plates, the latter being useful, *inter alia*, for simulations of RF scraping and the effects of damaged quadrupole resistors. For the fringe field of the Muon *g*-2 quadrupole, we calculated the field map and extracted the falloff of the quadrupole strength, which was a basis for achieving a good agreement of calculated tunes with experimentally measured tunes.

CONFORMAL MAPPING METHODS

We used conformal mappings for calculation of fringe fields of electrostatic deflectors and the main field on the Muon *g*-2 quadrupole [2, App. A]. A conformal mapping (or conformal map) is a transformation $f : \mathbb{C} \to \mathbb{C}$ that is locally angle preserving. A conformal mapping satisfies Cauchy–Riemann equations and, therefore, its real and imaginary parts satisfy Laplace's equation: $\Delta\Re(f) = 0$ and $\Delta\Im(f) = 0$. Conformal mappings automatically provide the electrostatic potential in cases where the electrostatic element's geometry can be represented by a polygon, possibly with some vertices at the infinity. The domain of a conformal mapping is called the canonical domain, and the image of a conformal mapping is called the physical domain. A Schwarz–Christoffel mapping is a conformal mapping from the upper half-plane as the canonical domain to the interior of a polygon as the physical domain.

The electrostatic potential for a cross section or a longitudinal section modeled by a generalized polygon may be found by obtaining a conformal mapping f from a suitable canonical domain to the polygon. A bi-infinite strip is a suitable canonical domain if the polygon comprises two groups of consecutive sides characterized by the same constant Dirichlet boundary condition, with two constant values in total. A rectangular part of a bi-infinite strip is a suitable canonical domain when the physical domain is a logical (or generalized) quadrilateral.

If the solution of the Laplace equation in the canonical domain is ϕ, the solution of the Laplace equation in the physical domain is $\varphi = \phi \circ f^{-1}$. In practice, the electrostatic potential is usually the appropriately selected, shifted, and scaled real or imaginary part of f^{-1}.

The solution for the electrostatic potential obtained this way is fully Maxwellian in the sense that the analytic formula for f or f' results in the solution for the potential satisfying the Laplace equation.

As described in [3,4], inverse conformal mapping $g = f^{-1}$ may be obtained by

* Fermilab report FERMILAB-CONF-18-571-PPD.
† Email: evaletov@fnal.gov. ORCID: 0000-0003-4341-0379.
‡ ORCID: 0000-0001-6141-8230.

ISBN: 978-3-95450-200-4 doi:10.18429/JACoW-ICAP2018-WEPAF01

A COMPACT PERMANENT MAGNET SPECTROMETER FOR CILEX

M. Khojoyan†, A. Cauchois, J. Prudent, A. Specka
LLR (Laboratoire Leprince-Ringuet), CNRS and Ecole Polytechnique, Palaiseau UMR7638, France

Abstract

Laser Wakefield acceleration experiments make extensive use of small permanent magnets or magnet assemblies for analyzing and focusing electron beams produced in plasma accelerators. Besides being compact, these magnets have to have a large angular acceptance for the divergent laser and electron beams which imposes constraint of the gap size. We will present the optimized design and characterization of a 100 mm long, 2.1 Tesla permanent magnet dipole. Furthermore, we will present the performance of such a magnet as a spectrometer in the CILEX/APOLLON 10 PW laser facility in France.

INTRODUCTION

CILEX (Centre Interdisciplinaire de la Lumiere Extrême / Interdisciplinary Center for Extreme Light) is a research center which aims at using the Apollon-10P laser for exploring laser-matter interaction at extremely high laser intensities (~10^{22} W/cm^2). The long focal length area of CILEX will be used to investigate plasma acceleration and radiation generation. It will be equipped with two interaction chambers able to accommodate laser focal lengths ranging from 3 m to 30 m. The spectrometer magnet presented here is designed to be compatible with the mentioned laser parameters. Sketch of the laser-plasma interaction chamber is shown in Fig. 1. The total volume of interaction chamber is about 3 m^3 and it is practical to use permanent magnets for characterization of electron beam. Permanent magnets, as compared to electromagnets, do not need power supplies (and consequently cooling system) and can be more compact due to smaller apertures. In our case, the apertures of the magnets will be limited by the envelope of the laser, which according to our requirements, should pass through the magnets unobstructed. The paper

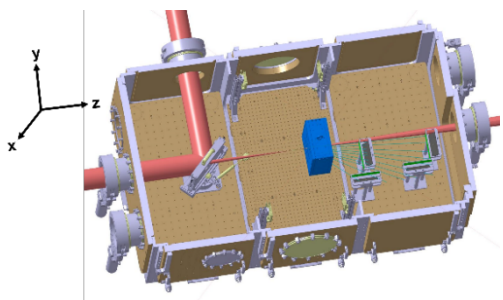

Figure 1: Schematic of interaction chamber at CILEX with laser envelope shown in purple and dipole magnet in blue colors. Measurement screens and reference electron trajectories (green) are shown as well.

is organized as follows. First, the design considerations of a permanent magnetic dipole are introduced together with analytical and computational field estimations. Next, construction of a magnet and field measurements are presented. Finally, the result of beam dynamics simulations implementing 3D magnetic field data are presented by applying the magnet as a spectrometer inside the interaction chamber of the CILEX facility.

† martin.khojoyan@llr.in2p3.fr

MOTIVATION

Let us consider a simple C shaped dipole (Fig. 2). The field in the gap of height h_g is driven by a permanent magnet of the same height $h_{pm} = h_g$ and of width w_{pm}. Assuming constant field in the gap (no horizontal field component) it is straightforward to calculate the magnetic flux density using Ampere's and flux conservation laws:

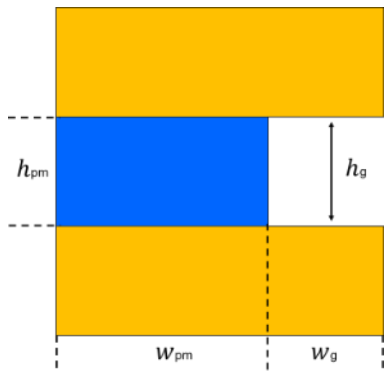

Figure 2: 2D view of a C shaped dipole with a permanent magnet shown in blue and steel/iron in yellow colors.

$$B_g = -\frac{B_r w_{pm}}{w_g + \frac{\mu_r h_g w_{pm}}{h_{pm}}} \quad (1)$$

with B_r and μ_r being the remnant field and relative permeability of the permanent magnet. From Eq. (1) it follows that the maximum achievable field in the gap cannot exceed the remnant induction field of the magnet independent of how small the gap height (h_g) is for reasonably large magnet width (w_g). It becomes clear that for a permanent magnet (PM) dipole, to reach fields higher than remnant field of an individual magnet, a special arrangement of magnetic sub-materials is necessary. Common structures for generating very strong fields are Halbach [1] and Stelter [2] configurations. Nowadays, permanent magnet dipoles are widely used in magnetic resonance imaging applications [3], in facilities such as third [4] and next [5] generation light sources. Neodymium iron Boron (Nd-Fe-B) magnets are the desired candidates for generating strong fields due to their high remnant induction and the highest up to date BH energy product [6]. Moreover, almost linear behaviour of the demagnetization curve [7] and relative permeability close to unity makes the analytical design of such systems relatively straight forward.

ISBN: 978-3-95450-200-4 doi:10.18429/JACoW-ICAP2018-WEPAF02

SIMULATIONS OF BEAM CHOPPING FOR POTENTIAL UPGRADES OF THE SNS LEBT CHOPPER*

B. X. Han†, V. V. Peplov, R.F. Welton, R. B. Saethre, S.N. Murray Jr., T. R. Pennisi, C.M. Stinson, M. P. Stockli, SNS, Oak Ridge National Laboratory, Oak Ridge, TN 37831, USA

Abstract

The LEBT chopper is a critical element of the SNS accelerator system. In this work, the benefit of increasing the chopping voltage amplitude for the present chopping pattern is shown with beam simulations, and an ongoing hardware upgrade of the chopper pulser units is discussed. In addition, with the prospect of higher voltage capability of the new pulser design, two alternative chopping patterns which reduce the switching frequency of the chopper pulsers down to ½ or ¼ of the present chopping pattern, are also explored with beam simulations.

INTRODUCTION

The Spallation Neutron Source (SNS) accelerator system consists of a 65 keV H^- injector, a 2.5 MeV RFQ, a 1 GeV linac chain (DTL-CCL-SCL), and a proton accumulator ring. The H^- injector is made of a RF-driven, Cs enhanced H^- ion source and a two-lens electrostatic low energy beam transport (LEBT). The injector feeds the RFQ accelerator with 1 ms long H^- beam pulses at 60 Hz. Figure 1 shows a cross-section view of the SNS H^- injector.

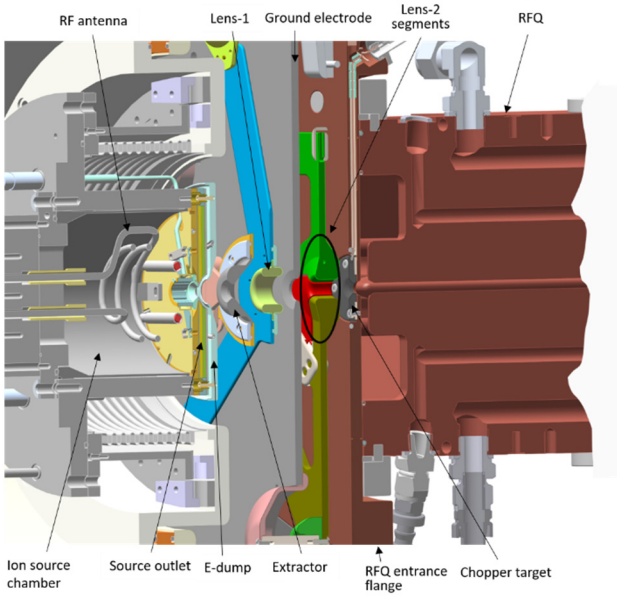

Figure 1: A cross-section view of the SNS H^- injector.

To facilitate the multi-turn beam stacking in the accumulator ring and to create gaps for clean beam extraction from the ring, the 1 ms H^- pulses are chopped ~300 ns at the ring revolution frequency (~1 MHz) in the LEBT in front of the RFQ. The second lens electrode of the LEBT is azimuthally split into four segments to allow applications of various transverse electric fields on top of the lens voltage for beam steering (misalignment correction), chopping or blanking. A donut-shape TZM plate surrounding the RFQ entrance aperture serves as chopper target as shown in Figure 1 [1, 2].

* This work was performed at Oak Ridge National Laboratory, which is managed by UT-Battelle, LLC, under contract number DE-AC05-00OR22725 for the United States Department of Energy.
† hanb@ornl.gov

THE PRESENT CHOPPING PATTERN AND BEAM SIMULATION

The Present Chopping Pattern

The four segments of the lens-2 are driven independently by four bipolar high voltage pulsers for beam chopping. With the present chopping pattern, a pair of neighbouring two segments are driven to negative potential and the other two are driven to positive potential, i.e. the lens-2 segments are driven as two opposing pairs with opposite potentials, to generate the transverse field needed for beam chopping. The waveforms of the four pulsers are configured in a manner as shown in Figure 2 so that the beam deflection is sequentially rotated to four different directions to avoid sputtering and heat loading at a single spot on the chopper target. The lens-2 is oriented in a way that the beam deflection directions coincide with the gaps between the neighbouring vanes of the RFQ to minimize ions impacting the vanes if the beam is not completely intercepted at the chopper target during beam chopping [3].

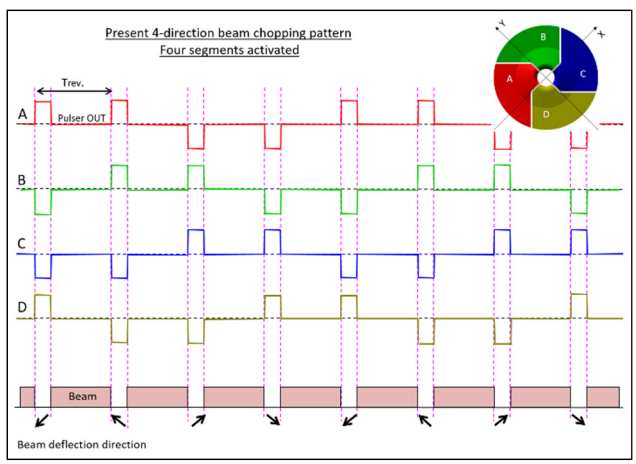

Figure 2: Bipolar chopping voltages applied sequentially on opposing pairs of the lens-2 segments.

Beam Simulations

The SIMION 8.1 code [4] was used to track the ions starting from the ion source outlet aperture to the RFQ vanes. A total of 10000 H^- ion macro-particles were launched with a total charge of 1.5×10^{-8} coulomb over 0.25 μs to simulate the space charge effect of a 60 mA

ISBN: 978-3-95450-200-4 doi:10.18429/JACoW-ICAP2018-WEPAF04

LONGITUDINAL BEAM DYNAMICS IN FRIB AND REA LINACS

A. S. Plastun†, P. N. Ostroumov, A. C. C. Villari, Q. Zhao
Facility for Rare Isotope Beams, Michigan State University, 48824, East Lansing, Michigan, USA

Abstract

The Front-End and first three cryomodules of the Facility for Rare Isotope Beam (FRIB) at Michigan State University (MSU) commissioned in July, 2018. The paper describes the online tuning procedures of the longitudinal beam dynamics through the FRIB linac. These procedures include tuning of the accelerating field phases and amplitudes in the cavities. We developed an automated simulation-based tuning procedure for the multi-harmonic buncher. In order to tune the radio-frequency quadrupole (RFQ) we measured and calculated its threshold voltage and scanned its longitudinal acceptance. Tuning of the rebunchers and superconducting accelerating cavities is performed by means of the phase scans and Time-Of-Flight (TOF) beam energy measurements with beam position and phase monitors.

While FRIB is being commissioned, the re-accelerator (ReA3) for rare isotope beams (RIBs) is being upgraded. We redesigned the ReA3 RFQ to improve its cooling system and provide reliable operation with 16.1 MHz prebunched ion beams with A/Q = 5. In order to provide matching of any ReA3 beam both to the following upgrade cryomodules and physics experiments' requirements, room temperature rebuncher/debuncher is being designed. The design procedure includes the beam dynamics, electromagnetic, thermal and mechanical simulations and optimizations.

INTRODUCTION

The Facility for Rare Isotope Beams (FRIB) [1] is being built to provide 400 kW ion beams up to uranium for the rare isotope production. The beam will be accelerated by the RFQ and 316 superconducting RF (SRF) cavities to the energy of 200 MeV/u.

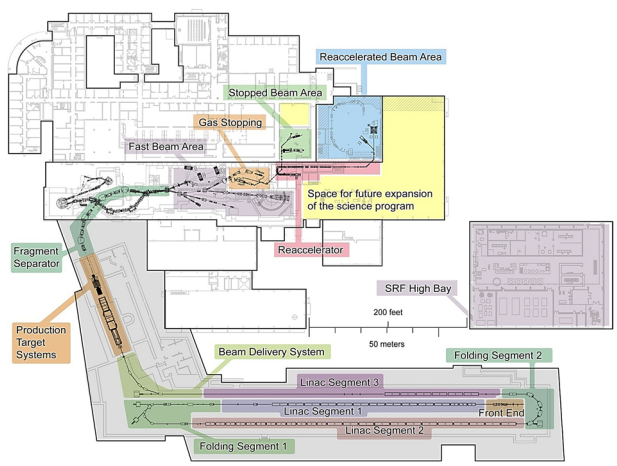

Figure 1: FRIB Layout.

† email address: plastun@frib.msu.edu

The FRIB linac consists of the Front-end and three linac segments (see Fig. 1). The DC beam, created in the ECR ion sources is accelerated to 500 keV/u and injected into the cryomodules of the linac segment 1 (LS1) as shown in Fig. 2 [2]. The 12 keV/u DC beam is pre-bunched by a multi-harmonic buncher to form a small longitudinal emittance. The RFQ is followed by medium energy beam transport (MEBT) to the cryomodules. The MEBT has two room-temperature quarter-wave (QWR) rebunchers to match the beam to the following SRF cavities in the longitudinal phase space.

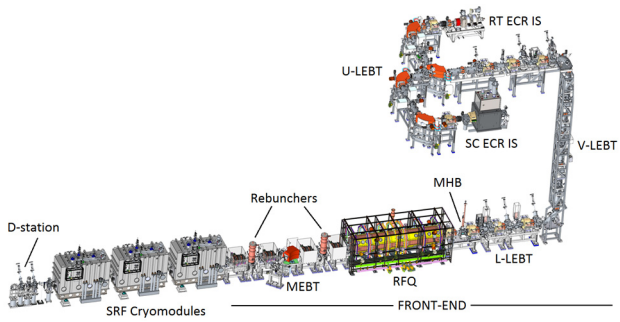

Figure 2: FRIB Front-end and first three cryomodules.

The detailed description of the FRIB linac components is given elsewhere [3-6].

FRIB is designed to accelerate two uranium charge states (33+ and 34+) in LS1 simultaneously, strip them in the liquid lithium stripper and continue acceleration of all five charge states (76+ through 80+) in one RF bucket [4, 5]. Proper tune of field amplitudes and phases of all FRIB cavities, including the bunching ones, is an essential procedure required to provide low losses and low emittance growth of the multi-charge-state beam [6].

MULTI-HARMONIC BUNCHER

The main purpose of the multi-harmonic buncher (MHB) is to form bunches with a small longitudinal emittance, which is required to maintain low particle losses in the SRF part of FRIB in multi-charge acceleration mode [6]. Also, MHB provides the longitudinal matching of the beam with the RFQ acceptance to maintain small emittance along the RFQ.

The FRIB MHB consists of two resonant quarter-wave lines attached to a pair of conical drift tubes [7]. The long line resonates at frequencies of 40.25 MHz and 120.75 MHz. The short line resonates at 80.5 MHz. Tuning of the MHB is an optimal choice of harmonics amplitudes and phases to provide small longitudinal beam emittance, proper matching with the RFQ and ~80% transmission of the accelerated beam.

ISBN: 978-3-95450-200-4 doi:10.18429/JACoW-ICAP2018-WEPLG01

ANALYSIS OF EMITTANCE GROWTH IN A GRIDLESS SPECTRAL POISSON SOLVER FOR FULLY SYMPLECTIC MULTIPARTICLE TRACKING

C. E. Mitchell*, Ji Qiang, Lawrence Berkeley National Laboratory, Berkeley, CA 94720, USA

Abstract

Gridless spectral methods for self-consistent symplectic space charge modeling possess several advantages over traditional momentum-conserving particle-in-cell methods, including the absence of numerical grid heating and the presence of an underlying multi-particle Hamiltonian. Nevertheless, evidence of collisional particle noise remains. For a class of such 1D and 2D algorithms, we provide analytical models of the numerical field error, the optimal choice of spectral modes, and the numerical emittance growth per time step. We compare these results with the emittance growth models of Struckmeier, Hoffman, Kesting, and others.

INTRODUCTION

Distinguishing between physical and numerical emittance growth observed in long-term tracking of beams with space charge is critical to understanding beam performance in high-intensity proton rings. Numerical emittance growth has been modeled as a collisional increase of the beam phase space volume driven by random noise caused by the use of a small number of macroparticles [1–4]. Recently, several authors have developed methods for multiparticle tracking (in plasmas or beams) using variational or explicitly symplectic algorithms designed to preserve the geometric properties of the self-consistent equations of motion [5–7]. In this paper, we address the problem of numerical emittance growth generated by the multi-particle symplectic algorithm described in [7]. Due to its relative simplicity, this algorithm can be used as a test-bed for explicit probabilistic models of numerical errors in the computed field and numerical emittance growth.

SYMPLECTIC SPECTRAL ALGORITHM

We apply the algorithm described in Section III of [7] to treat the Poisson equation in a general bounded domain $\Omega \subset \mathbb{R}^d$ $(d \leq 2)$ with conducting boundary $\partial\Omega$. The symplectic map describing a numerical step in the path length coordinate s is performed by applying second-order operator splitting to the following multi-particle Hamiltonian:

$$H = \sum_{j=1}^{N_p} H_{\text{ext}}(\vec{r}_j, \vec{p}_j, s) - \frac{n}{N_p}\frac{1}{2}\sum_{j=1}^{N_p}\sum_{k=1}^{N_p}\sum_{l=1}^{N_l}\frac{1}{\lambda_l}e_l(\vec{r}_j)e_l(\vec{r}_k).$$

Here H_{ext} is the single-particle Hamiltonian in the external applied fields, N_p denotes the number of simulation particles, N_l denotes the number of computed modes, and n is a space charge intensity parameter. The smooth functions e_l form an orthonormal basis for the space of square-integrable functions on the domain Ω, and satisfy

$$\nabla^2 e_l = \lambda_l e_l, \quad e_l|_{\partial\Omega} = 0, \quad (\lambda_l < 0). \tag{1}$$

It follows from H that each particle moves in response to the smooth space charge force $\vec{F} = -\nabla U$, where

$$U(\vec{r}) = -\frac{n}{N_p}\sum_{l=1}^{N_l}\sum_{j=1}^{N_p}\frac{1}{\lambda_l}e_l(\vec{r}_j)e_l(\vec{r}). \tag{2}$$

The space charge potential U satisfies the Poisson equation $\nabla^2 U = -\rho$ and $U|_{\partial\Omega} = 0$, where ρ is a particle-based approximation to the beam density, given in terms of the modes e_l $(l = 1, 2, \ldots)$ by:

$$\rho = \sum_{l=1}^{N_l}\rho^l e_l, \quad \rho^l = \frac{n}{N_p}\sum_{j=1}^{N_p}e_l(\vec{r}_j). \tag{3}$$

The set of functions

$$\vec{e}_l = \frac{1}{\sqrt{-\lambda_l}}\nabla e_l \quad (l = 1, 2, \ldots) \tag{4}$$

is orthonormal and can be extended to an orthonormal basis for the space of square-integrable vector-valued functions on Ω. The relationships between the corresponding modes of ρ, U, and $\vec{F}$ are then given simply by:

$$U^l = \rho^l/\lambda_l, \quad F^l = -\sqrt{-\lambda_l}U^l. \tag{5}$$

By appropriately grouping the sums appearing in the space charge kick, the complexity of a single numerical step using the Hamiltonian H scales as $O(N_p N_l)$ [7].

PROBABILISTIC MODEL

Assume that particle coordinates $(\vec{r}_j, \vec{p}_j)$, $j = 1, \ldots, N_p$ are sampled from the joint probability density P_N given by:

$$P_N(\vec{r}_1, \vec{p}_1, \ldots, \vec{r}_{N_p}, \vec{p}_{N_p}) = \prod_{j=1}^{N_p} P(\vec{r}_j, \vec{p}_j), \tag{6}$$

where P is the probability density on the single-particle phase space describing an ideal (smooth) beam distribution. If a denotes any function on the single-particle phase space, we denote its beam-based average by

$$\langle a \rangle = \frac{1}{N_p}\sum_{j=1}^{N_p} a(\vec{r}_j, \vec{p}_j), \quad \Delta a = a - \langle a \rangle. \tag{7}$$

* ChadMitchell@lbl.gov

ISBN: 978-3-95450-200-4 doi:10.18429/JACoW-ICAP2018-WEPLG03

THEORETICAL AND COMPUTATIONAL MODELING OF A PLASMA WAKEFIELD BBU INSTABILITY*

S. D. Webb†, N. M. Cook, D. L. Bruhwiler
RadiaSoft, LLC, Boulder, CO 80301
A. Burov, V. Lebedev, S. Nagaitsev
Fermi National Accelerator Laboratory, Batavia, IL 60510

Abstract

Plasma wakefield accelerators achieve accelerating gradients on the order of the wave-breaking limit, mc^2k_p/e, so that higher accelerating gradients correspond to shorter plasma wavelengths. Small-scale accelerating structures, such as plasma and dielectric wakefields, are susceptible to the beam break-up instability (BBU), which can be understood from the Panofsky-Wenzel theorem: if the fundamental accelerating mode scales as b^{-1} for a structure radius b, then the dipole mode must scale as b^{-4}, meaning that high accelerating gradients necessarily come with strong dipole wake fields. Because of this relationship, any plasma-accelerator-based future collider will require detailed study of the trade-offs between extracting the maximum energy from the driver and mitigating the beam break-up instability. Recent theoretical work predicts the tradeoff between the witness bunch stability and the amount of energy that can be extracted from the drive bunch, a so-called efficiency-instability relation. We will discuss the beam break-up instability and the efficiency-instability relation and the theoretical assumptions made in reaching this conclusion. We will also present preliminary particle-in-cell simulations of a beam-driven plasma wakefield accelerator used to test the domain of validity for the assumptions made in this model.

INTRODUCTION

A future lepton collider will have to operate at center of mass energies near 10 TeV. Conventional warm copper or superconducting rf structures are limited to around 50 MeV m^{-1} accelerating gradients, meaning that a conventional rf linac would require hundreds of kilometers of accelerating structures. Smaller scale millimeter or THz structures can achieve gradients closer to 300 MeV m^{-1} bring the length of the linac to the scale of ten kilometers. The gradients in both of these structures are primarily limited by breakdown phenomena. Much higher accelerating gradients are possible in accelerating structures that are already broken down, that is to say plasmas. The accelerating gradients available to plasma-based accelerators – beam-driven plasma wakefield accelerators (PWFAs) or laser-driven laser plasma accelerators (LPAs) – have accelerating gradients limited by the wave-breaking limit of the plasma $E_{WB} = mc^2k_p/e \approx 96.\sqrt{n_{pe}[\mathrm{cm}^{-3}]}[\mathrm{V/m}]$ which, for laboratory plasma densities around 1×10^{16} cm^{-3} corresponds to accelerating gradients near 10 GV m^{-1}.

This accelerating gradient comes at the cost of small-scale structures, since decreasing the plasma wavelength $\lambda_p = 2\pi/k_p$ increases the wave-breaking limit. At the same time, this shrinks the size of the accelerating plasma wave, which makes the witness bunch more prone to various transverse instabilities, such as the hosing instability [1], which is similar to the transverse beam break-up (BBU) instability [2] in traditional linear accelerators. In the case of conventional accelerator, BBU is dictated by the transverse size of the beam pipe, while the accelerating gradient depends on the longitudinal length scales of the accelerating cavity, two independent parameters. In plasma accelerators, the "beam pipe" and "accelerating cavity" are both the plasma wave, and the scales are not independent.

Because these scales are related, there exists an *efficiency-instability relationship* [3] predicted to limit how much energy can be extracted from the driver of a plasma accelerator before the BBU instability makes the witness bunch unusable for collider applications. Our ongoing work is to study the domain of validity of this theory, and ways to avoid this limit, to design a high-efficiency plasma accelerator based TeV lepton collider.

BEAM BREAK-UP AND HOSING INSTABILITIES

The dipole beam break-up instability occurs when a beam is off-center from the beam pipe. This excites a transverse dipole field, where betatron oscillations of the head of the bunch can drive the tail of the bunch to larger betatron amplitudes. A description of this instability in conventional linear accelerators is discussed in detail in Chapter 3 of Chao [4], and is illustrated in Fig. 1.

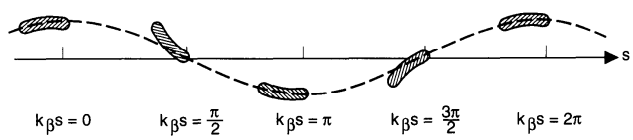

Figure 1: Illustration of the beam break-up instability in Chao [4].

In the beam break-up instability, the head of the bunch begins with some transverse offset. This excites a dipole wake field, which oscillates at the betatron wavelength. The oscillating dipole wake acts as a resonant driving term for the

* Work supported by Department of Energy Office of Science, Office of High Energy Physics under award no. DE-SC0018718
† swebb@radiasoft.net

ISBN: 978-3-95450-200-4 doi:10.18429/JACoW-ICAP2018-WEPLG05

REVIEW OF SPECTRAL MAXWELL SOLVERS FOR ELECTROMAGNETIC PARTICLE-IN-CELL: ALGORITHMS AND ADVANTAGES

R. Lehe*, J.-L. Vay, Lawrence Berkeley National Laboratory, CA 94720 Berkeley, U.S.A

Abstract

Electromagnetic Particle-In-Cell codes have been used to simulate both radio-frequency accelerators and plasma-based accelerators. In this context, the Particle-In-Cell algorithm often uses the finite-difference method in order to solve Maxwell's equations. However, while this method is simple to implement and scales well to multiple processors, it is liable to a number of numerical artifacts that can be particularly serious for simulations of accelerators.

An alternative to the finite-difference method is the use of spectral solvers, which are typically less prone to numerical artifacts. The present article reviews recent progress in the use of spectral solvers for simulations of plasma-based accelerators. This includes techniques to scale those solvers to large number of processors, extensions to cylindrical geometry, and adaptations to specific problems such as boosted-frame simulations.

INTRODUCTION

Particle-In-Cell (PIC) codes [1, 2] are widely used in various fields of physics, and in particular in accelerator physics. For many accelerator-related problems, electrostatic PIC codes are usually sufficient to capture the physics at stake. However, some applications do require full electromagnetic PIC codes. This includes for instance accelerators based on laser-plasma interactions [3–7], where e.g. the self-consistent evolution of the laser driver needs to be captured by the PIC algorithm.

For these applications that require an electromagnetic Particle-In-Cell code, the Finite-Difference-Time-Domain (FDTD) method (e.g. [8]) has been the most commonly-used approach for solving Maxwell's equations. However, due to some of the limitations of the FDTD method, other methods are increasingly being used—and this includes spectral solvers.

This paper focuses on spectral solvers for PIC codes and their advantages—with an emphasis on their application to laser-plasma interactions. Note that, for the sake of conciseness, the present paper is restricted to Particle-In-Cell codes that do solve Maxwell's equations on a grid (in which case spectral solvers are sometimes referred to as *pseudo-spectral*), and does not discuss the set of *gridless* spectral electromagnetic algorithms that have been recently developed, in the context of accelerator simulations (e.g. [9–11]).

* rlehe@lbl.gov

SPECTRAL SOLVERS, AND DIFFERENCE WITH FDTD SOLVERS

In order to summarize the principle of the spectral solvers, let us contrast them with the FDTD algorithm. In the standard Yee FDTD algorithm [8], Maxwell's equations

$$\frac{\partial \boldsymbol{B}}{\partial t} = -\boldsymbol{\nabla}\times\boldsymbol{E}, \quad (1)$$

$$\frac{1}{c^2}\frac{\partial \boldsymbol{E}}{\partial t} = \boldsymbol{\nabla}\times\boldsymbol{B} - \mu_0\boldsymbol{j} \quad (2)$$

are discretized in two ways:

- Spatial derivatives are approximated by a finite difference between neighboring points on a staggered grid. For instance,

$$\partial_x E_x|^n_{i,j,k} = \frac{E_x|^n_{i+1/2,j,k} - E_x|^n_{i-1/2,j,k}}{\Delta x}.$$

- Time derivatives are approximated by a finite difference between consecutive time steps. For instance,

$$\partial_t E_x|^{n+1/2}_{i+1/2,j,k} = \frac{E_x|^{n+1}_{i+1/2,j,k} - E_x|^n_{i+1/2,j,k}}{\Delta t}.$$

where we adopted standard notations whereby superscripts represent the index of the time step whereas subscripts represent positions on a staggered grid. As a consequence of the above simple space and time discretizations, the discretized Maxwell equations can easily be rewritten as a set of explicit update equations for the $\boldsymbol{E}$ and $\boldsymbol{B}$ fields.

While the above approximations allow fast execution and efficient parallelization, they also introduce numerical artifacts. One of these numerical artifacts is *spurious numerical dispersion*, i.e. the fact that the phase velocity of simulated electromagnetic waves (in vacuum) differs from the speed of light c, and depends on their wavelength and propagation angle. Spurious numerical dispersion can have a very serious impact in realistic simulations, and can lead to unphysical results. For instance, in the context of laser-plasma interactions, numerical dispersion can lead to spurious early dephasing in laser-driven accelerator [12], unphysical growth of emittance [13], and erroneous angle-frequency correlations in high-harmonics generation [14].

One of the main motivation for spectral solvers is to mitigate numerical dispersion. This is done by overcoming the approximations of FDTD schemes in two ways:

- Spatial derivatives are approximated by a high-order expression involving many grid points. These derivatives are typically evaluated in Fourier space for efficiency. Algorithms that use this feature but retain a